Contents lists available at ScienceDirect

Earth-Science Reviews

journal homepage: www.elsevier.com/locate/earscirev

Invited Review

Continental rifts and mantle convection

Laurent Jolivet [a,b,*], Claudio Faccenna [b,c], Thorsten Becker [d,e,f], Anne Davaille [g], Eric Lasseur [h], Justine Briais [h], Alexander Koptev [i,b], Pietro Sternai [j], Laetitia Le Pourhiet [a,k]

[a] ISTeP, Sorbonne Université, CNRS UMR 7193, 4 Place Jussieu, 75252, Paris cedex 05, France
[b] Lithosphere Dynamics, Helmholtz Centre Potsdam, German Research Centre for Geosciences (GFZ), Potsdam, Germany
[c] Dipartimento di Scienze, University of "Roma TRE", Rome, Italy
[d] Institute for Geophysics, Jackson School of Geosciences, The University of Texas at Austin, Austin, 78758, TX, USA
[e] Department of Earth and Planetary Sciences, Jackson School of Geosciences, The University of Texas at Austin, Austin 78712, TX, USA
[f] Oden Institute for Computational Engineering & Sciences, The University of Texas at Austin, Austin 78712, TX, USA
[g] Laboratoire FAST - Bat. 502, Campus Universitaire, 91405 Orsay, France
[h] BRGM, Orléans, France
[i] HUN-REN Institute of Earth Physics and Space Science, Sopron, Hungary
[j] Dipartimento di Scienze dell'Ambiente e della Terra, Universita di Milano Bicocca, Italy
[k] Institut Universitaire de, France

ARTICLE INFO

Keywords:
Rifting
East African Rift
European Cenozoic Rift System
ECRIS
Convection
Low-velocity finger
A-type rift
B-type rift
Plate fragmentation

ABSTRACT

Continental rifting is an important component of the Wilson cycle, and a process-level description requires integration of constraints from seismic tomography, seismic anisotropy, and non-isostatic topography in addition to geological observations. We discuss the evolution of the East African Rift (EAR) and the European Cenozoic Rift System (ECRIS) and define two end members. 1) *a-type rifts*, such as the EAR and ECRIS, form parallel to mantle flow above elongated, asthenospheric anomalies of low-seismic velocity, "fingers" (LVF) and stay at embryonic stage with slow extension mostly driven by gravitational potential energy. 2) *b-type rifts*, such as the Menderes and Corinth Rifts, form perpendicular to mantle flow and lead to oceanisation; the Gulf of Aden, Red Sea and Baikal are intermediate. We then propose a new model for the evolution of the short-lived ECRIS (~44–33 Ma) in the magma-poor period of transition between the Pyrenean orogeny and Mediterranean back-arc extension. The propagation of a LVF toward the north emanating from the Canaries hotspot, all the way to the Massif Central and the upper and lower Rhine region formed the rift on top of a positive anomaly of non-isostatic topography. Fast slab retreat from the end of the Eocene modified asthenospheric mantle flow, initiating the recent Mediterranean subduction regime with back-arc basin opening and dispersal of the asthenospheric anomaly. From ~8 Ma, slab retreat successively ceased in the central and western Mediterranean, giving way to compression and resumption of volcanism, possibly related to the reestablishment of a mantle LVF. We conclude speculating on the respective roles of *a-type* and *b-type rifts* for plate tectonics more general, including for the Mesozoic fragmentation of Pangea.

Contents

* Corresponding author at: ISTeP, Sorbonne Université, CNRS UMR 7193, 4 Place Jussieu, 75252, Paris cedex 05, France.
E-mail address: laurent.jolivet@sorbonne-universite.fr (L. Jolivet).

https://doi.org/10.1016/j.earscirev.2025.105243
Received 28 February 2025; Received in revised form 30 July 2025; Accepted 4 August 2025

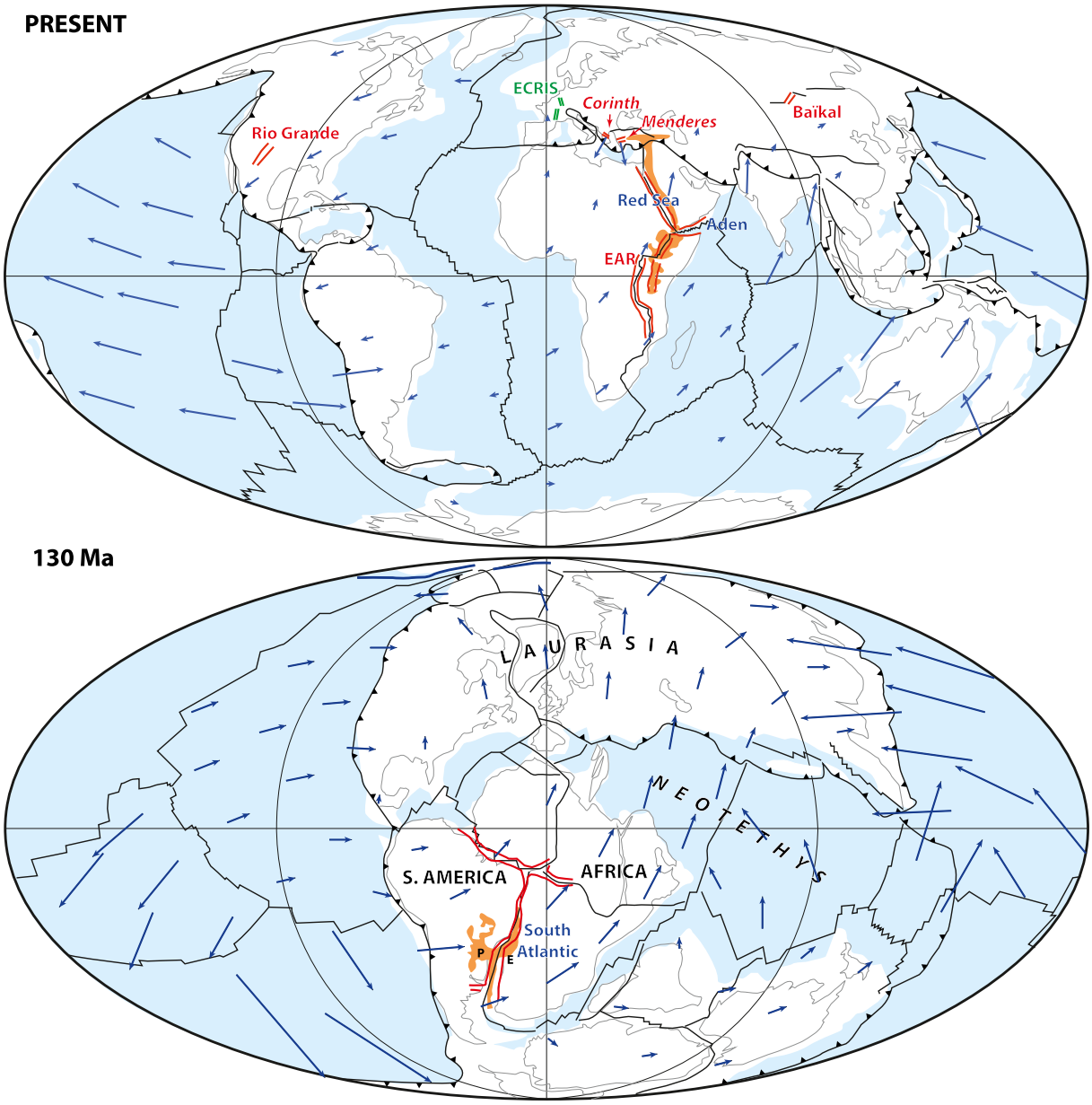

Fig. 1. Map of the main rifts systems discussed in the paper for the present-day and Early Cretaceous geodynamic frameworks simplified from Seton et al. (2012) and Torsvik and Cocks (2016). Maps show the disposition of continents and oceans, plate boundaries and absolute motions (blue arrows). The European Cenozoic Rift System (ECRIS) is shown in green. Intra-continental rifts are in red with red labels (Rio Grande, Baikal, East African Rift), in italic when in back-arc regions (Corinth and Menderes rifts). Rifts that evolved into oceanic spreading systems are shown in red with blue labels (Red Sea, Gulf of Aden, South Atlantic rift). Orange areas are the Paraña-Etendeka and Afar LIPs. (For interpretation of the references to colour in this figure legend, the reader is referred to the web version of this article.)

1. Introduction

The common fate of an intracontinental rift is to evolve into a mid-oceanic ridge, but the geological record shows a number of examples of aborted rifts. Africa hosts several such aborted rifts dating back to the Mesozoic; their evolution stopped at an embryonic stage before the main Atlantic rift successfully reached full breakup and oceanisation, before the Gulf of Aden and Red Sea. Comparing the different inactive or active rifts at the surface of continents shows a diversity of behavior. Extension velocities vary from a few mm to 1–2 cm/yr. Some rifts are associated with volcanism while others are amagmatic. Rifting is often localized along a single main graben (narrow rift), but it can also be distributed across a series of parallel rifts like in the Basin and Range Province (wide rift; e.g. Buck, 1991). Wide rifts correspond to collapsed orogens (Dewey, 1988). The kinematic contexts of rift formation are likewise diverse (Fig. 1). Considered in an absolute plate kinematic framework, some rifts such as the East African Rift strike parallel to the absolute motion of their carrier plate, when others, such as the Gulf of Aden are highly oblique to the absolute motion. This 3-D context questions the origin of forces controlling rifting, including: what are the respective roles of far-field forces transmitted through the rigid lithosphere vs. the forces transmitted from the convective mantle underneath?

The dynamics of continental breakup has indeed often been discussed by contrasting passive *v.s* active rifting modes (Sengör and Burke, 1978; Turcotte and Emerman, 1983; Keen, 1985; Huismans et al., 2001; Frizon de Lamotte et al., 2015; Ivanov et al., 2015; Issachar et al., 2024). In active rifts (Fig. 2), extension results from lateral gradients of gravitational potential energy (GPE) built from the arrival of a mantle plume underneath, while passive rifting is caused by edge forces exerted on continental lithosphere due to plate interactions and slab pull (Larvet et al., 2022). Active rifts may thus be associated with intense volcanism and long-wavelength uplift before extension, while extension in passive rifts extension starts before, or is coeval with, relatively short wavelength uplift limited to the rift shoulders. Another major difference is that active and passive rifts evolve into volcanic and non-volcanic passive margins, respectively. The two end-member types of margins are also characterized by different deformation patterns with faults and ductile shear zones dipping toward the continent in active systems and oceanward-dipping normal faults in passive systems (Manatschal, 2004; Lavier and Manatschal, 2006; McDermott et al., 2015; Clerc et al., 2017; Manatschal et al., 2021). The distinction between passive and active rifts systems is however not always straightforward, as the deep mantle component may increase with time as an intrinsic consequence of the rifting process (Huismans et al., 2001; Ivanov et al., 2015; Issachar et al., 2024) and/or the action of mantle plumes may extinguish before full continental breakup (e.g., Ziegler, 1992a; Ziegler and Cloetingh, 2004). Long wavelength topography undulations can be used as a good indicator of the presence of a plume underneath a continental lithosphere (Koptev et al., 2018). However, rift regions also react to changes in stress regime along plate boundaries (Janssen et al., 1995), along with the complexities of lithospheric rheology (e.g., Burov and Guillou-Frottier, 2005), this may render the differentiation between the two passive and active endmembers difficult.

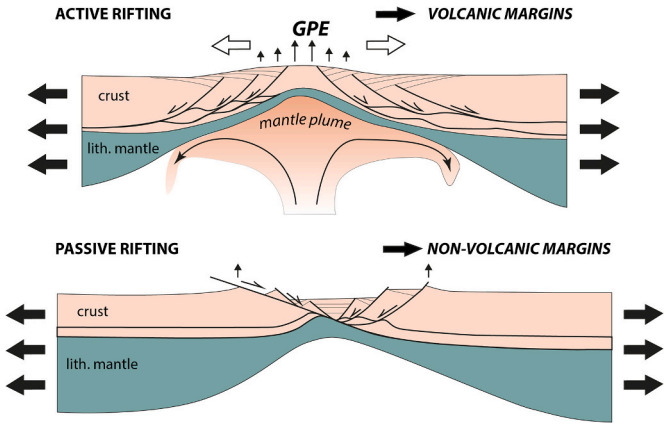

Fig. 2. Active vs passive rifting, a schematic view based on the original idea of Sengör and Burke (1978) and later works (Turcotte and Emerman, 1983; Keen, 1985; Huismans et al., 2001; Ziegler and Cloetingh, 2004) with their evolution toward oceans with volcanic or non-volcanic passive margins (Manatschal, 2004; Ivanov et al., 2015; Clerc et al., 2017; Manatschal et al., 2021). Active rifts form above active mantle plumes and are associated with large magmatic production expresses as massive development of SDRs; the main normal faults are low-angle and dip toward the continent. The gravitational potential energy built up by a mantle upwelling provides a regional force and may interact with far-field extensional stresses due to plate motions. Passive rifts form as the passive response of the lithosphere predominantly to the far-field extensional stresses due to plate motions, e.g. driven by subduction elsewhere. They evolve into oceanic lithosphere with non-volcanic passive margins; the main normal faults dip toward the ocean and they may be controlled by lithospheric-scale low-angle detachments.

Crustal thickness variations due to rifting and post-rift lithospheric due to compression are also efficient mechanisms for producing anomalous topography without the need of a plume underneath the lithosphere (Kooi and Cloetingh, 1992; Kooi et al., 1992; Cloetingh et al., 1999). Another difficulty arises when considering rifting in more realistic, 3-D settings (e.g., Burov and Gerya, 2014; Koptev et al., 2017a), because of the presence of inherited heterogeneities in the continental lithosphere (Koptev et al., 2017a) and the 3-D stress field imposed by surrounding plate interactions (Le Pourhiet et al., 2017; Jourdon et al., 2020) and their interraction with mantle plumes (Burov and Gerya, 2014). Driving forces from oceanic and continental GPE are typically considered insufficient to explain large-scale plate motions (Lithgow-Bertelloni and Richards, 1998; Becker and O'Connell, 2001; Ghosh et al., 2008) and the effects of mantle tractions play an important role in cratonic areas (Humphreys and Coblentz, 2007). However, GPE does affect regional, intraplate stress, including for rifted continental domains (Koptev and Ershov, 2010; Naliboff et al., 2012; Stamps et al., 2014).

Opening of the Atlantic Ocean offers a good illustration of the interaction between far-field forcing inherited weakness zones such as ancient sutures for continental rifting (Argand, 1924; Wilson, 1966) and mantle plumes (Buiter and Torsvik, 2014). Break-up and the formation of the first oceanic crust is often coeval with or shortly follows the emplacement of large igneous provinces (LIPs),), i.e. large volumes of predominantly mafic rocks characterized by a high rate of magma accumulation and formed far from plate boundaries within intraplate tectonic environments (Bryan and Ernst, 2008; Bryan and Ferrari, 2013). For example, the North Atlantic Ocean opened shortly after the eruption of the North Atlantic Igneous Province, NAIP) in the Paleocene, the Central Atlantic shortly after the Central Atlantic Magmatic Province (CAMP) in the Early Jurassic, and the South Atlantic in the Early Cretaceous right after the Paraña-Etendeka LIP, leading to the conclusion of a direct causal link between emplacement of large mantle plumes—manifested as corresponding LIPs—and rupture of the continent

(Courtillot et al., 1999). However, as shown in the recent review by Koptev and Cloetingh (2024), the relative role of LIPs in the breakup of different segments of the last supercontinent, Pangea, **can vary widely** depending on the tectonic and geodynamic conditions in each specific case.

Moreover, a systematic analysis of pairs of conjugate margins located on former suture zones—where this close temporal succession between LIPs and continental rupture is observed—has demonstrated that rifting occurs preferentially along inherited suture zones of different ages, in the Atlantic and Indian Oceans (Buiter and Torsvik, 2014). No correlation is observed with the age of the suture, which can be much older, suggesting that even very old suture zones can remain weak and preferentially localize extensional or strike-slip deformation. The reason why LIPs form close to rifts is questioned and Buiter and Torsvik (2014) propose that rifting is controlled by far-field forces (passive rifting), localized by lithospheric weak zones, and that the plume material is then guided toward zones of thinned lithosphere. The punctuated distribution of LIPs then explains the coeval formation of magmatic and amagmatic margins (Franke, 2013). The Atlantic rift would then be typically passive, plumes reaching upward where a rift has already formed. The case of East Africa however questions this last conclusion as alkaline volcanism has started at ~45 Ma (George et al., 1998), thus 15 Ma before the main rifting and emplacement of the Ethiopian traps (Ershov and Nikishin, 2004).

Mantle flow can exert a propelling pull or a resisting force on the lithosphere, depending on the setting, and can affect lithospheric deformation. A propelling effect of mantle flow in deforming the overlying lithosphere has been suggested by several lines of evidence and numerical models (Bird, 1998; Steinberger et al., 2001; Tikoff et al., 2004; Alvarez, 2010; Hoïnk et al., 2011; Sternai et al., 2014; Menant et al., 2016; Sternai et al., 2016; Jolivet et al., 2018a, 2018b).

Another source of 3-D complexity of rifting is that the flow of mantle underneath may be parallel to the rift instead of perpendicular as usually assumed in 2-D models. The case of the East African Rift is the best example of this situation. Stamps et al. (2014) have proposed that extension across the EAR is mainly driven by GPE rather than by lateral or mantle traction underneath and, interestingly, the SKS-splitting derived fast azimuthal anisotropy orientations are aligned with the rift and not perpendicular. This may indicate shear in the asthenosphere due to rift-parallel mantle flow (Bagley and Nyblade, 2013). Alternative interpretation is that this alignment results from the presence of melt underneath the rift (Bastow et al., 2010; Holtzman and Kendall, 2010), an effect that may act in conjunction with mantle flow (Ebinger et al., 2024).

Here, we address the question of the drivers of intracontinental rifting with the examples of two partly contemporaneous rifts with similar N-S strikes, both characterized by slow (~5 mm/yr), limited extension and alkaline volcanism, the East African Rift (EAR) and the European Cenozoic Rift System (ECRIS) (Figs. 3 and 4) and we explore the behavior of other rifts systems for comparison.

The ECRIS, no longer active since the Middle Miocene, has been associated with different causes in the literature, from a mantle plume to the lateral effects of the Alpine collision or a lithospheric crack parallel to the convergence of Africa and Eurasia (Illies, 1975; Tapponnier, 1977;

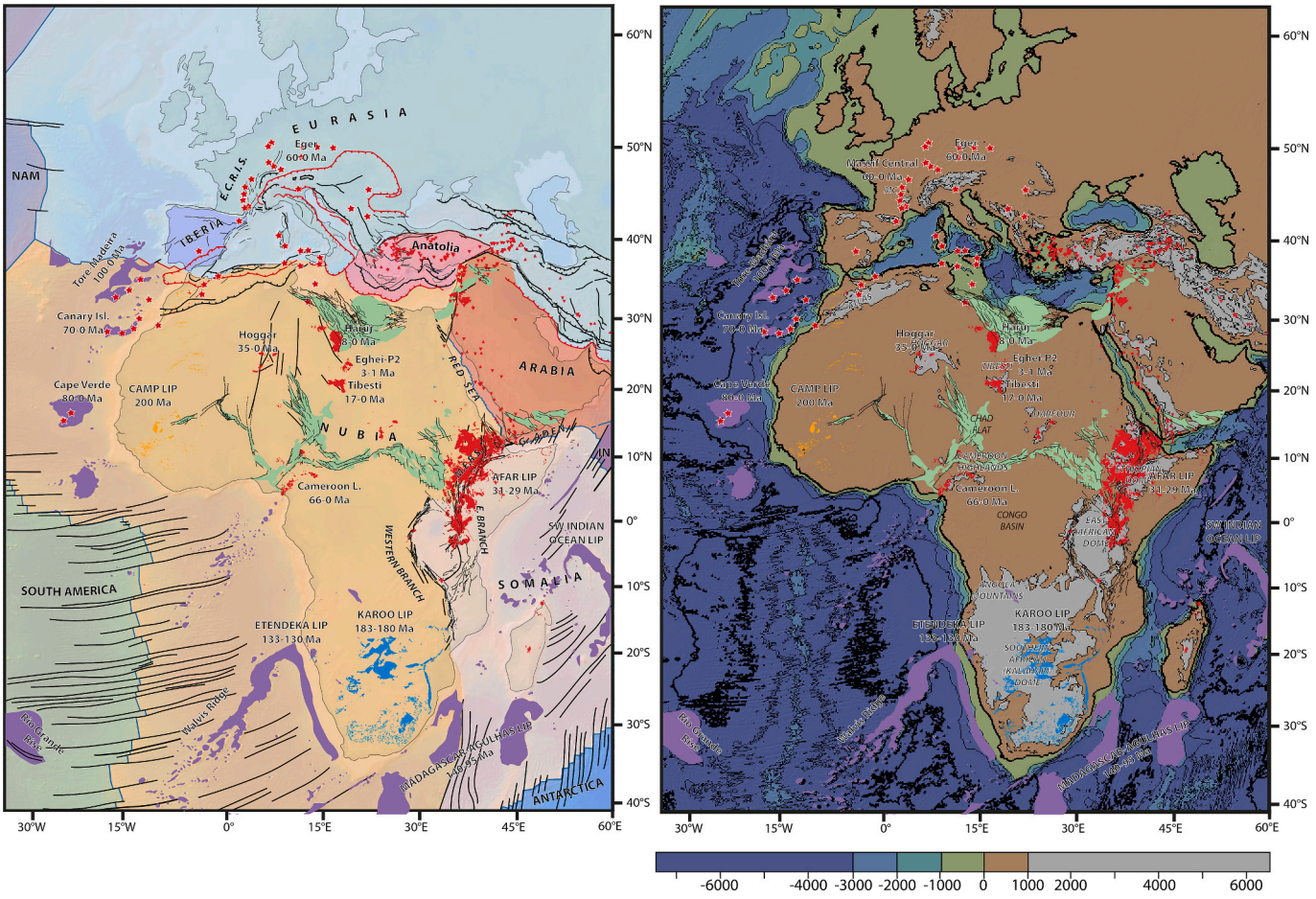

Fig. 3. Large-scale tectonic context of the East African Rift and ECRIS, displaying the alkaline magmatic provinces onshore and offshore. Green areas are the Early Cretaceous rifts in Africa. A: main tectonic features and the main plates, B: Topography. (For interpretation of the references to colour in this figure legend, the reader is referred to the web version of this article.)

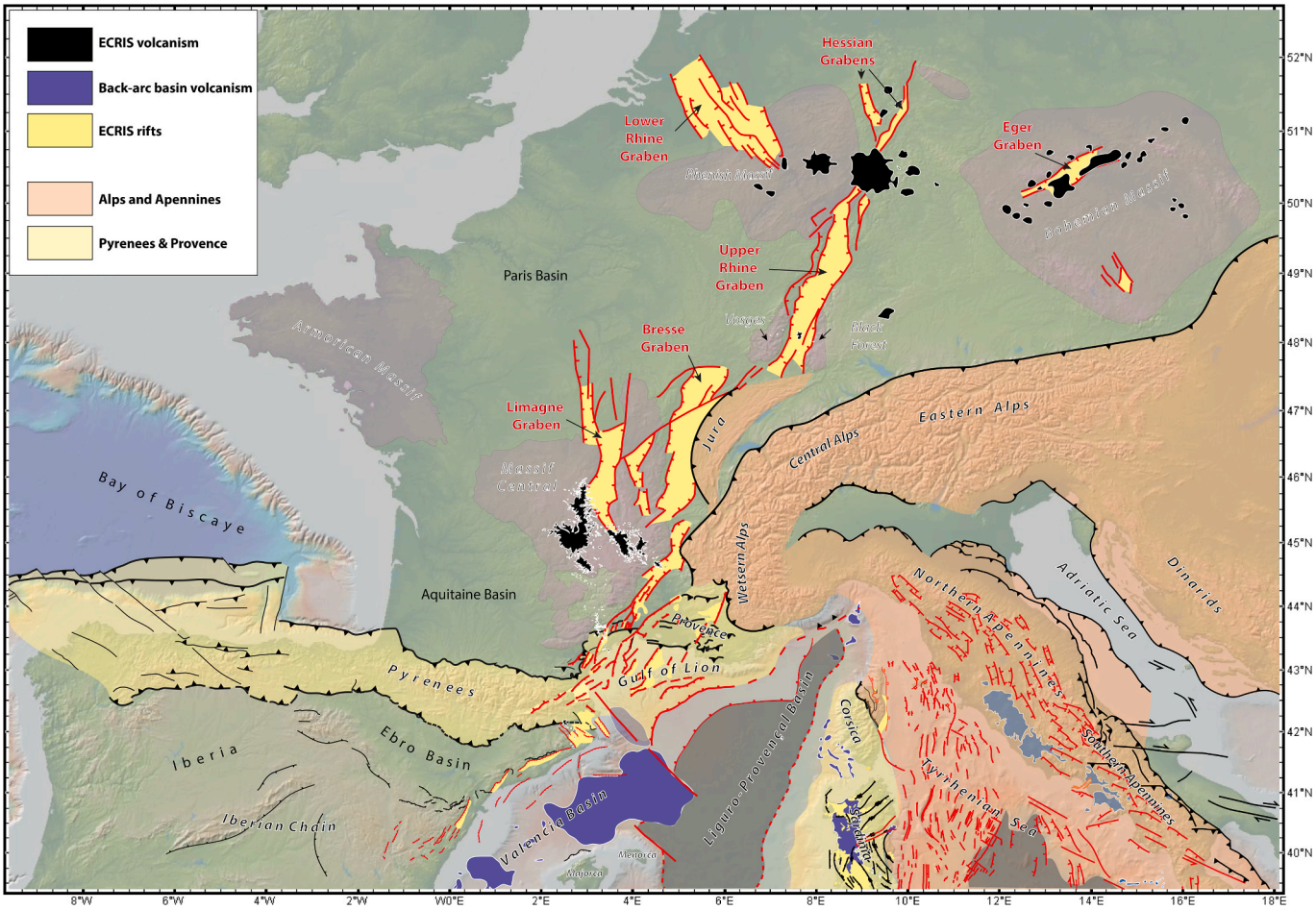

Fig. 4. Tectonic context of the European Cenozoic Rift system (ECRIS), the Pyrenees, the Alps and the Western Mediterranean.

Merle and Michon, 2001; Ziegler and Dèzes, 2005). The ECRIS developed during a short period of transition from the collision of Africa, Iberia and Eurasia, forming the Pyrenees, to the fast slab retreat forming the Mediterranean back-arc basins (Séranne, 1999; Ziegler and Dèzes, 2005; Ziegler and Dèzes, 2007; Mouthereau et al., 2021; Séranne et al., 2021).

Based on a synthesis of available tomographic models, seismic anisotropy data and estimates of the residual, non-isostatic topography, compared to their tectonic evolution, we show that these two emblematic rift systems, EAR and ECRIS, are parallel to positive residual topography anomalies and to the absolute motion of Africa and Europe. Moreover, they formed above horizontal low-velocity fingers (LVFs) of presumably hot asthenospheric mantle flowing parallel to the strike of the rift. We define such rifts as *a-type* rifts, in contrast to *b-type* rifts where the rift axis is perpendicular or highly oblique to the direction of the large-scale mantle flow underneath. In *a-type* rifts, GPE-induced forces create slow extension along the rift axis within a lithosphere weakened by early volcanic activity. The elevated residual topography generates outward-directed gravitational forces, which in turn cause extension perpendicular to the rift axis. We discuss the situations of some of the main Cenozoic continental rifts systems (EAR, ECRIS, Rio Grande, Red Sea, Aden, Baikal) in terms of (1) the *a-type* vs. *b-type* and (2) *active* vs. *passive* endmembers. We thus offer an alternative explanation for localized extension in the ECRIS in the Oligocene. We then discuss the competition of the large-scale convection on the scale of the whole mantle with the smaller scale, but faster, asthenospheric flow due to slab retreat in the Western Mediterranean region. Finally, we look back to the past and speculate about the role played by LVFs and *a-type* rifts in the fragmentation of Pangea.

2. A diversity of rifting contexts

Before focusing on the EAR and ECRIS, we first introduce the first order characteristics of all selected intracontinental rifts that will be referenced in the final discussion.

2.1. East Africa

The EAR separates the Somalia plate from Nubia plate (Fig. 3), once parts of the African plate. It strikes north to northeast and is divided in two branches separated by the Tanzania craton. Its northern part, the Main Ethiopian Rift, connects with the Aden and Red Sea oceanized rifts. Rifting started in the area at ~30 Ma ago during the time of eruption of the Ethiopian traps (Bosworth et al., 2005). Oceanic spreading, controlled by NNE-striking transform faults, started along most of the Aden Rift length at ~20 Ma and reached the Afar domain some 2 Myr ago (Leroy et al., 2012; Leroy et al., 2013). The western margins are associated with magmatism in the vicinity of the Afar hot-spot and are amagmatic east of longitude 46°E. Ultra-slow oceanic spreading started at around 13 Ma all along the axis of the Red Sea (Bosworth et al., 2005; Augustin et al., 2021). The rift ends to the north in the Gulf of Suez where no oceanic accretion is observed (Colletta et al., 1987; Moretti and Colletta, 1987) and the oceanic domain is limited by the southernmost extent of the left-lateral Dead Sea Fault in the Gulf of Aqaba (Ribot et al., 2021). Rifting in the EAR region also started at ~30 Ma but remained disconnected from the Aden-Red Sea system. The connection did not happen before the earliest Late Miocene at around 11 Ma the northern segment of the Main Ethiopian Rift formed (Bonini et al., 2005; Corti, 2009; Corti et al., 2019) resulting in the establishment of the Afar

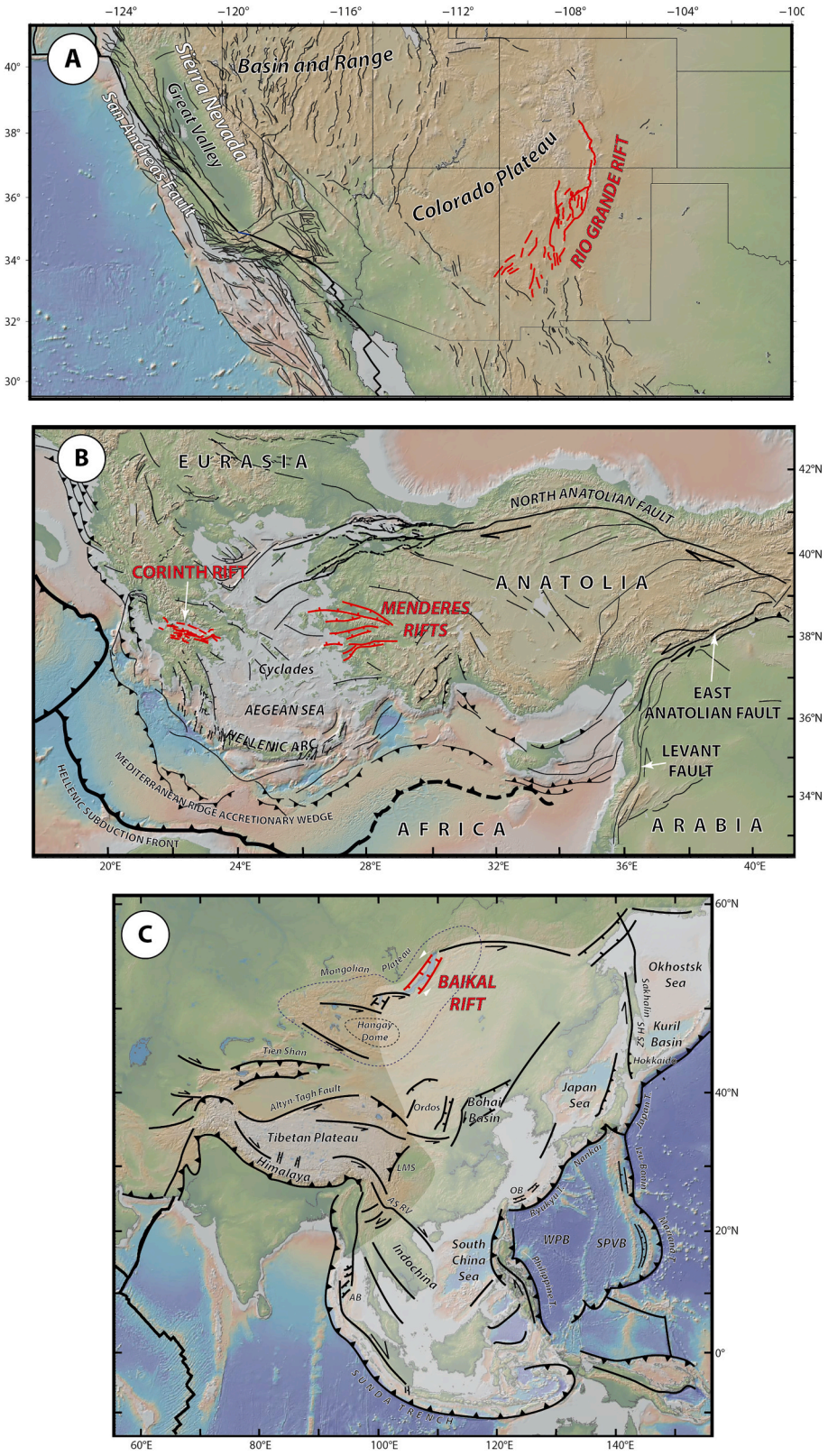

Fig. 5. Tectonic context of four active or recent continental rifts (in red). A: Rio Grande Rift, B: Corinth Rift and Menderes Rifts system, C: Baikal Rift. (For interpretation of the references to colour in this figure legend, the reader is referred to the web version of this article.)

rift-rift-rift triple junction. The strike of the EAR is NNE, parallel to the absolute motion of the African plate (see below) while the Gulf of Aden and Red Sea strike obliquely.

Jolivet and Faccenna (2000) and Bellahsen et al. (2003) suggested that the collision between the Afro-Arabian and Eurasian plates and the associated slowing down of the northward motion of the African continent were the main triggers for the rifting of the Gulf of Aden and Red Sea, as well as the drastic change in subduction dynamics in the

Mediterranean. The asymmetric conditions imposed by the transition from collision north of Arabia to subduction underneath the Aegean region led to the counterclockwise rotation of Arabia and the development of the Red Sea and Gulf of Aden rifts. The Arabian plate was then separated from the main body of the African plate carried by the northward mantle flow of the plume below East Africa (Faccenna et al., 2013; Hua et al., 2023; Issachar et al., 2024). Through numerical modelling, Koptev et al. (2018) showed that this configuration leads to the genesis of a triple junction of rifts, the EAR becoming the boundary between Nubia and Somalia (Chorowicz, 2005; Ebinger, 2012; Rooney, 2020b).

2.2. Rio Grande Rift

The NE-SW striking Rio Grande Rift extends along more than 1000 km on the eastern side of the Colorado Plateau (Figs. 1 and 5). It merges to the south with the southern Basin and Range extensional province (see the review by Olsen et al. (1987). It was active during two main periods, an early phase (30–18 Ma) characterized by the activity of low-angle normal faults and a later phase (10–3 Ma) with the development of high-angle normal faults. The crust is moderately thinned, with thickness decreasing from 45 to 33 km toward the center of the rift and low seismic velocities suggest abnormally high temperature below the rift axis. Volcanism is mostly younger than 5 Ma and the volumes of magma are small. Olsen et al. (1987) conclude that this rift "does not fit either passive or active endmember models" and that the observed thermal anomaly in the mantle is "not uniquely associated with rifting" and likely inherited from the earlier compressional event of the Laramide orogeny. The orientation of the Rio Grande rift is grossly parallel to the absolute motion of North America.

2.3. Baïkal Rift

The Baïkal rift system (Fig. 5) belongs to the long deformation zone resulting from the India-Asia collision, running from the Tien Shan to the Stanovoy mountains (Molnar and Tapponnier, 1975; Tapponnier and Molnar, 1977). It is limited to the south and the north by WNW-ESE striking left-lateral strike faults guiding the eastward escape of the North China Block. Set on a moderately thinned continental lithosphere (80–90 km) (Petit and Deverchère, 2006; Fullea et al., 2012), the Baïkal rift is slowly extending (~4 mm/yr) perpendicular to NNE-striking high-angle normal faults (Calais et al., 1998, 2003) and is associated to an alkaline magmatic province covering part of Mongolia and active since the Late Cretaceous, the Hangai dome (Windley and Allen, 1993; Ivanov et al., 2015). Petit and Deverchère (2006) see an evolution along strike of the support of topography with deep crustal root or an anomalous mantle under the southern part of the rift, while Fullea et al. (2012) conclude that the present-day topography is in isostatic equilibrium. The deep structure of the rift is asymmetric, which Petit and Deverchère (2006) interpret as a consequence of a reactivation of a suture zone limiting the Siberian craton. Rifting proceeded in two main stages, first in the Early Cretaceous and then from the Late Cretaceous to the Present (Ivanov et al., 2015). Active dynamics dates back to the Late Miocene or the Pliocene, however (Petit and Deverchère, 2006).

The ultimate causes of rifting are debated (Ivanov et al., 2015). Two main mechanisms have been proposed. Molnar and Tapponnier (1975) and Tapponnier and Molnar (1977) relate it to the India-Asia collision, as a far-field effects of the indentation. In this hypothesis the Baikal rift would be classified as a passive rift, the alkaline volcanism of the region being a consequence of extension. Alternatively, rifting may be a consequence of the presence of a high temperature anomaly in the mantle. In this case the rift would be considered as active. The high temperature anomaly has been interpreted as a consequence of mantle diapirs controlled by the Pacific subduction (Ivanov et al., 2015), where slab-induced effects were discussed by Faccenna et al. (2010).

2.4. Aegean region, Corinth and Menderes rifts

Active back-arc extension in the Aegean region (Fig. 5) is accommodated by two fast rifts, the Corinth Rift and several rifts within the Menderes Massif (King et al., 1985; Armijo et al., 1996; Aktug et al., 2009; Pérouse et al., 2012). Extension in the broader Aegean region and western Anatolia started some 30–35 Myr ago when the Hellenic slab started to retreat southward (Jolivet and Brun, 2010; Ring et al., 2010; Jolivet et al., 2013).

Between 30 Ma and ~ 6–5 Ma, extension was distributed over a wide domain covering most of the Aegean Sea and surrounding regions. Both the Corinth and Menderes rifts are amagmatic although a low seismic velocity anomaly underlies the eastern Aegean and Western Anatolian domain producing high heat flow actively exploited for geothermal energy (de Boorder et al., 1998; Gessner et al., 2018; Roche et al., 2018). Extension was accommodated by large low-angle normal faults exhuming metamorphic core complexes (Lister et al., 1984; Jolivet and Brun, 2010; Jolivet et al., 2010; Le Pourhiet et al., 2012). Retreat accelerated significantly at ~15 Ma at the time of slab tearing underneath the eastern Aegean (van Hinsbergen et al., 2005; Jolivet et al., 2015; Menant et al., 2016a). A further acceleration occurred in the Latest Miocene when the North Anatolian Fault propagated into the Aegean Sea, thanks to a second slab tear in formation underneath the Peloponnese (Royden and Papanikolaou, 2011; Sternai et al., 2014). Extension then localized to focus on the Corinth Rift and several grabens in the Menderes massif, from north to south, the Simav graben, the Gediz-Alasehir graben and the Büyük Menderes graben (Bozkurt, 2001; Bozkurt and Sözbilir, 2004; Bozkurt et al., 2011). The velocity of N-S extension across these active grabens, amounting to ~2 cm/yr (Briole et al., 2000; Avallone et al., 2004; Aktug et al., 2009), adds to the ~2.5 cm/yr westward motion of the Anatolian rigid plate with respect to Eurasia, following the fast retreat (>4 cm/yr) of the Hellenic slab (Reilinger et al., 1997; McClusky et al., 2000; Pérouse et al., 2010; Reilinger et al., 2010; Serpelloni et al., 2007), which exceeds by far the Africa/Eurasia convergence and the absolute velocity of these two large plates. The two rifts thus strike almost perpendicular to the slab retreat direction.

2.5. South Atlantic Rift

The Early Cretaceous rifting of the South Atlantic (Figs. 1 and 3) interacted with the activity of the Tristan-Gough mantle plume, giving rise to the Paraña-Etendeka LIP and the Walvis and Rio Grande volcanic ridges (Wilson, 1963; Morgan, 1971; Wilson, 1973; Beniest et al., 2017; Hoyer et al., 2022), the active part of those hot spots being located close to the mid-Atlantic ridge. Relative motion between South America and Africa is almost perpendicular to the strike of the rift, and strongly oblique on the absolute motion of both plates, producing the two most visible bathymetric features of the South Atlantic (Fig. 3). Coeval rifting and LIP development led to the formation of two conjugate magmatic margins, the Uruguay and Namibia margins, where large-scale low-angle extensional shear zones have thinned the crust during the emplacement of a thick pile of volcanic rocks seen as seaward dipping reflectors on seismic profiles (Clerc et al., 2015; McDermott et al., 2015; Clerc et al., 2017). Besides the presence or absence of magmatism, the main difference between magmatic and amagmatic margins is the polarity of normal faults. In amagmatic margins, normal faults mostly dip toward the ocean, while they dip toward the continent in magmatic margins and are associated with intense simple shear ductile deformation of the deep crust (Clerc et al., 2015; Geoffroy et al., 2015; Clerc et al., 2017) suggesting that the presence of the plume modifies the stress regime and the coupling between crust and mantle during rifting (Jolivet et al., 2018b).

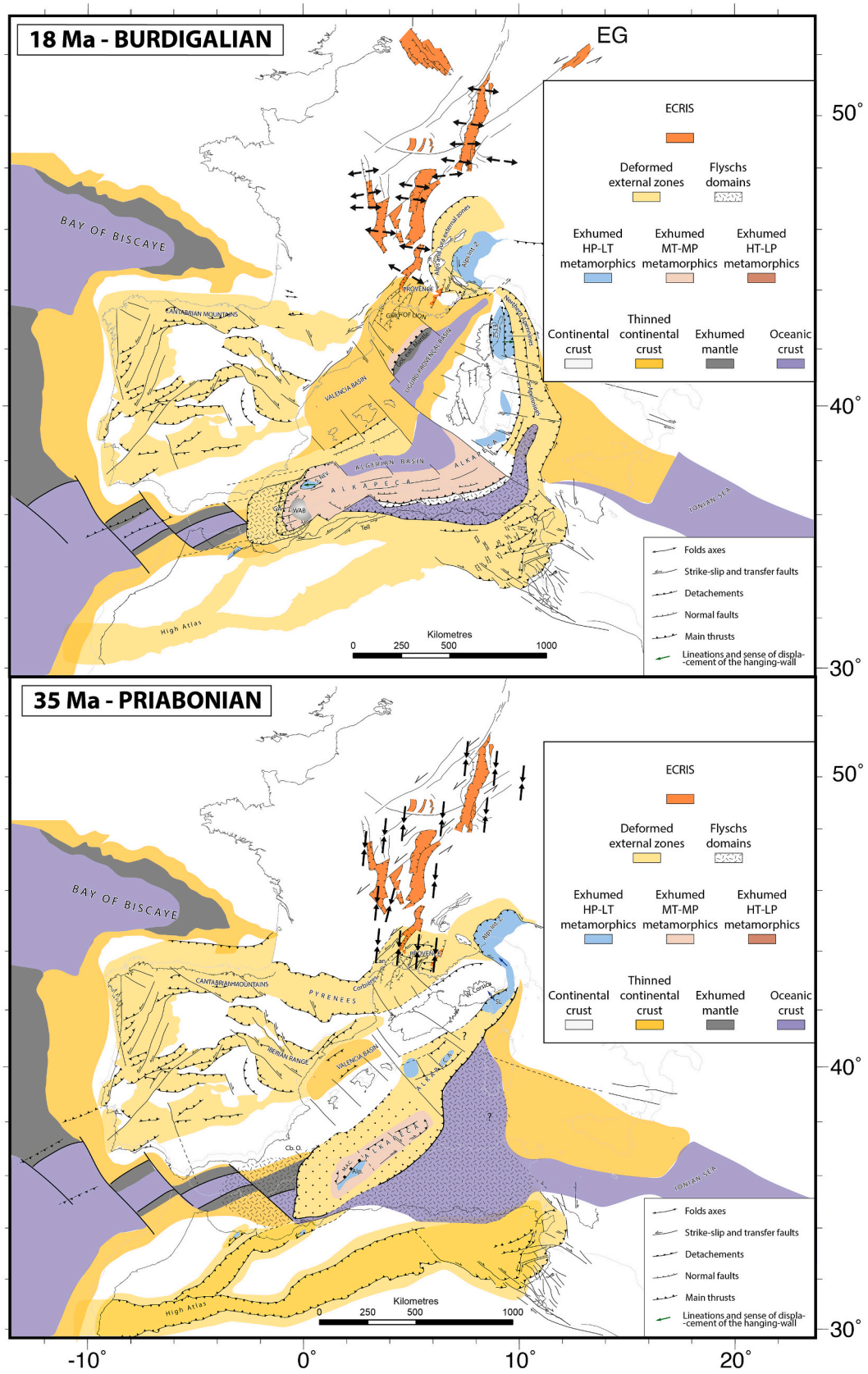

Fig. 6. Two reconstructions of the Western Mediterranean region after Romagny et al. (2020). The ECRIS rifts are shown with an orange filling. Black arrows indicate the direction of extension in the Burdigalian reconstruction when the rift system was purely extensional, and the direction of compression in the Priabonian when it was transtensional. The ECRIS started to form at the time of the climax of shortening in the Pyrenees at ~37 Ma ago and before the inception of slab retreat in the Mediterranean domain.

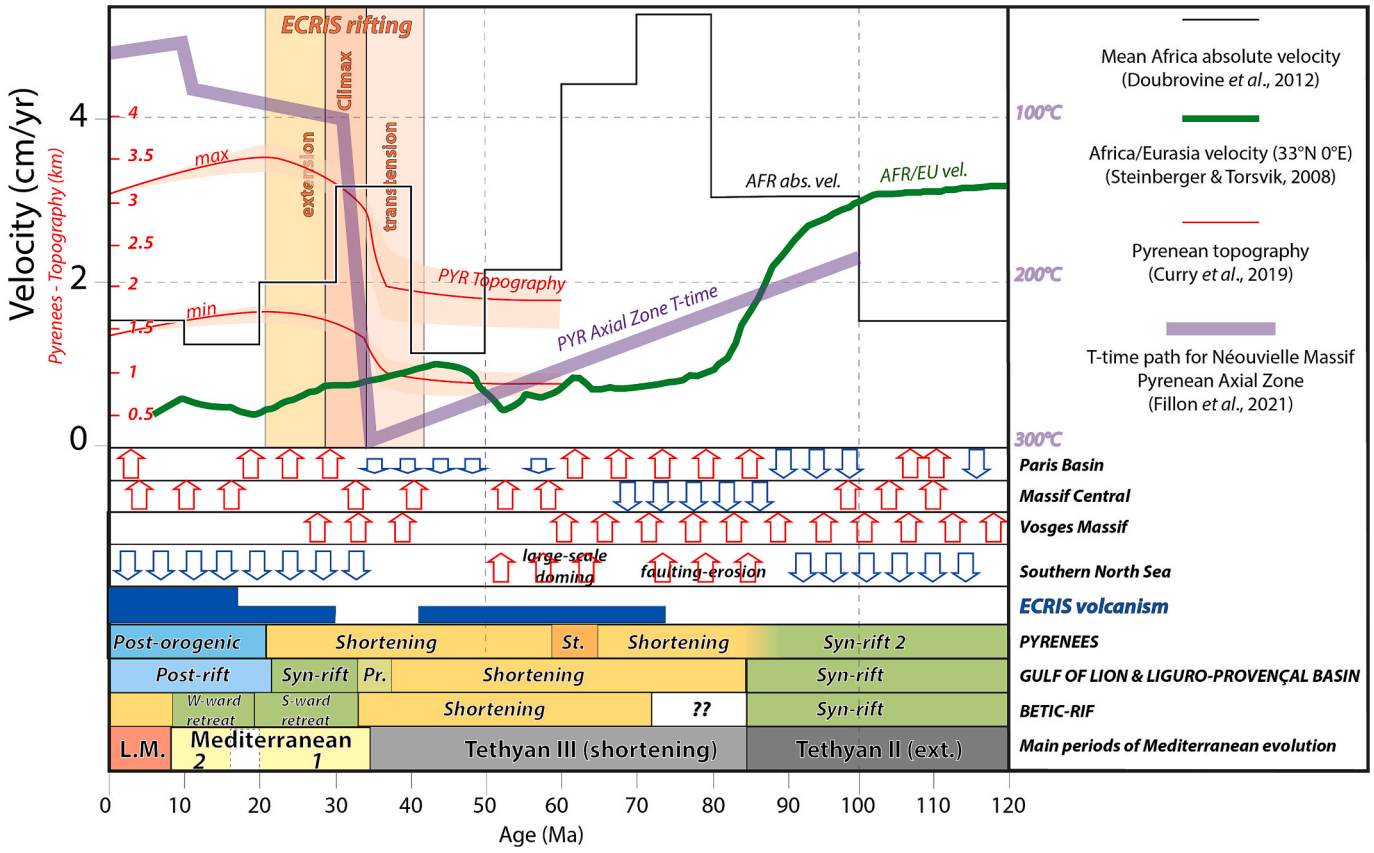

Fig. 7. Tectonic, magmatic and geodynamic timing of the Western Mediterranean region and the ECRIS: mean Africa absolute velocity (Doubrovine et al., 2012), Africa/Eurasia relative velocity (Steinberger and Torsvik, 2008), Pyrenean topography (Curry et al., 2019), Pyrenean Axial Zone topography (Fillon et al., 2020), Paris Basin subsidence vertical movements (Guillocheau et al., 2000), Massif Central (Barbarand et al., 2001, 2013; François et al., 2020), Vosges Massif (Briais et al., 2025), South North Sea (Deckers and van der Voet, 2018), ECRIS volcanism and its intensity (low vs. high) (Merle and Michon, 2001; Michon and Merle, 2001), Pyrenean tectonics (Mouthereau et al., 2014), Mediterranean tectonic evolution (Jolivet et al., 2021a).

3. Geological context of the European Cenozoic Rift System

The NNE-SSW ECRIS (Figs. 3 and 4) results from a short-lived and slow rifting event starting in the Lutetian and evolving during the Bartonian, Priabonian and part of the Rupelian (~42–32 Ma), with slower extension until the Chattian and locally the Aquitanian (Figs. 6 and 7) (Séranne, 1999; Dèzes et al., 2004; Ziegler and Dèzes, 2005; Séranne et al., 2021). The rift, set within a crust that recorded a complex Variscan and post-Variscan tectonic evolution (Ziegler et al., 2004), is geographically associated with alkaline volcanism, mostly active before and after rifting (Wilson and Bianchini, 1999; Merle and Michon, 2001; Michon and Merle, 2001; Lustrino and Wilson, 2007) (Figs. 4 and 7). The system of rifts extends from the Eger, Hessian and Lower Rhine Grabens in the north, to the Upper Rhine Graben and the Limagne and Bresse grabens, and ends in the Western Mediterranean within the Valencia Basin (Illies, 1975; Illies and Greiner, 1978; Brun et al., 1992; Lacombe et al., 1993; Sissingh, 2006; Ford et al., 2007). The finite amount of extension is small, ~17 km for the Upper Rhine Graben (Brun et al., 1991, 1992). The different sections of the rift developed within uplifted Variscan massifs, the French Massif Central, the Vosges and Black Forest Massifs, the Rhenish Massif and the Bohemian Massif. The northern part of the ECRIS, corresponding to the northern foreland of the Alps, is seismically active, as a large part of Western Europe (Cloetingh and Cornu, 2005; Cloetingh et al., 2006).

3.1. *Rifting timing and topography*

Initial rifting dates back to the Lutetian (Fig. 7) in the Limagnes and Bresse basins as well as in the Upper Rhine Graben (URG) and is younger further north in the Hessen depression (Middle Lutetian), Eger Graben (Priabonian) and Lower Rhine Graben (Priabonian) (Sissingh, 2006). The main rifting event is dated from the Bartonian and Priabonian in the Bresse, Limagnes, Upper Rhine Graben and Hessen Depression, from the Chattian in the Lower Rhine Graben and from the Rupelian in the Eger Graben (Sissingh, 2006). Rifting reached its climax in the Upper Rhine Graben, Bresse and Limagnes basins in the Rupelian (34–28 Ma in the URG, Briais et al., 2025) and it continued in the Upper Rhine Graben until the Early Miocene (~ 20 Ma) and the present-day in the Lower Rhine Graben (Sissingh, 2006).

Oligocene paleostress indicators (Fig. 6) imply a WNW-ESE extension over a wide region from southeast France to the Upper Rhine Graben and the foreland of the Swiss Alps (Bergerat, 1987). This period is preceded in the Eocene by a N-S compression compatible with shortening in the Pyrenees and the Alps at this period. The ECRIS forms parallel to the direction of the main horizontal compression in the Eocene and almost perpendicular to the direction of the Oligocene extension. A recent field study of *syn*-tectonic basins in Languedoc (Séranne et al., 2021) documents the age of the transition from Pyrenean foreland basins to transpressional deformation associated with the ECRIS rifting from the early Priabonian (~37 Ma). Before the Rupelian (34 Ma), extension in the Limagnes and Upper Rhine Graben is accommodated by small basins. From the Rupelian onward, the present-day geometry is established with pure normal faults and marine deposits (Sissingh, 2006). The transition is roughly coeval with the first evidence of back-arc extension in the Liguro-Provençal Basin (~32 Ma).

In the Upper Rhine Graben, the period of extension is limited to the Rupelian. Based on low-temperature thermochronology, Briais et al. (2025) delineate three main periods of cooling in the Vosges Massif, the

western shoulder of the Rhine Graben, Lower Cretaceous (150–100 Ma), Late Cretaceous (100–60 Ma) and from 40 Ma onward. The most recent one is attributed to uplift of the rift shoulders. The first two pre-rift events saw the erosion of the Jurassic and part of the Triassic sedimentary cover.

The Lower Cretaceous uplift or cooling ages have long been recognized in Western Europe (Ziegler, 1992a; Barbarand et al., 2020; Olivetti et al., 2020) and the Massif Central (François et al., 2020). The deposition of Upper Cretaceous deep-sea chalk in the Paris Basin is coeval with a resumption of subsidence (Guillocheau et al., 2000) and the post-chalk Late Cretaceous episode of uplift is associated with the transition from chalk deposition in the Cretaceous to terrigenous sediments in the Cenozoic. Two more uplift episodes were recognized in the Paris Basin in the Paleogene from 60 to 50 Ma (Briais et al., 2016) and after the Late Oligocene (Guillocheau et al., 2000). Uplift is also recognized in Central Europe and southern North Sea, a short wave-length uplift attributed to shortening with reverse faulting and a longer wavelength domal uplift with minor fault movements (Deckers and van der Voet, 2018; von Eynatten et al., 2021). This uplift is coeval with the inversion of basins from North Africa to the North Sea (Bosworth et al., 1999; Guiraud et al., 2005), a plate-scale compressional episode alternating with extensional periods on the same scale and attributed to switching mantle convection regimes (Jolivet et al., 2016a).

The most recent Bartonian to Miocene cooling episode recognized near the Upper Rhine Graben is interpreted as an effect of the shoulders uplift (Briais et al., 2025). In its southern half, the ECRIS interferes with the Pyrenees, the thrust front of the Alps and the Liguro-Provençal back-arc basin (Figs. 3 and 4) (Bergerat, 1987; Hippolyte et al., 1991; Hippolyte et al., 1993; Dèzes et al., 2004; Séranne et al., 2021). The Miocene uplift in the southern part of the Rift and the Rhine-Saône transfer zone shifted sedimentation toward the north (Illies, 1972) because of lithospheric folds due to the formation of the Alps (Ziegler and Dèzes, 2005; Bourgeois et al., 2007). The Alps and the Jura have overthrusted the eastern margin of the rift system in the Chattian and onward, with the westward migration of the Alpine thrust front (Lickorish and Ford, 1998; Ford et al., 2006; Kalifi et al., 2022). This episode is coeval with volcanism in Central Europe (Binder et al., 2023).

In Languedoc and Provence, two episodes of extension are recorded in the Cenozoic (Hippolyte et al., 1991, 1993). The oldest is coeval with the ECRIS, while the second one, from the Oligocene to the Early Miocene, corresponds to the formation of the Gulf of Lion passive margin in the back-arc region of the retreating Ionian subduction, which led to the opening of the Liguro-Provençal Basin and then the Tyrrhenian Sea (Séranne et al., 1995; Faccenna et al., 1997; Séranne, 1999; Jolivet et al., 2020; Séranne et al., 2021). ECRIS rifting thus started immediately after the climax of shortening in the Pyrenees and before the beginning of back-arc extension (Figs. 4 and 5). One additional noticeable point is that the main relief in the Pyrenees started to form during the post-orogenic stage, during the late stage of ECRIS rifting and the formation of the back-arc basin (Curry et al., 2019; Jolivet et al., 2020; Calvet et al., 2021). The main uplift in the Pyrenees started at around 35–32 Ma, almost coeval with the initiation of back-arc extension in the Gulf of Lion and culminated in the Early Miocene (Curry et al., 2019; Fillon et al., 2020; Curry et al., 2021). A second episode of uplift involving the

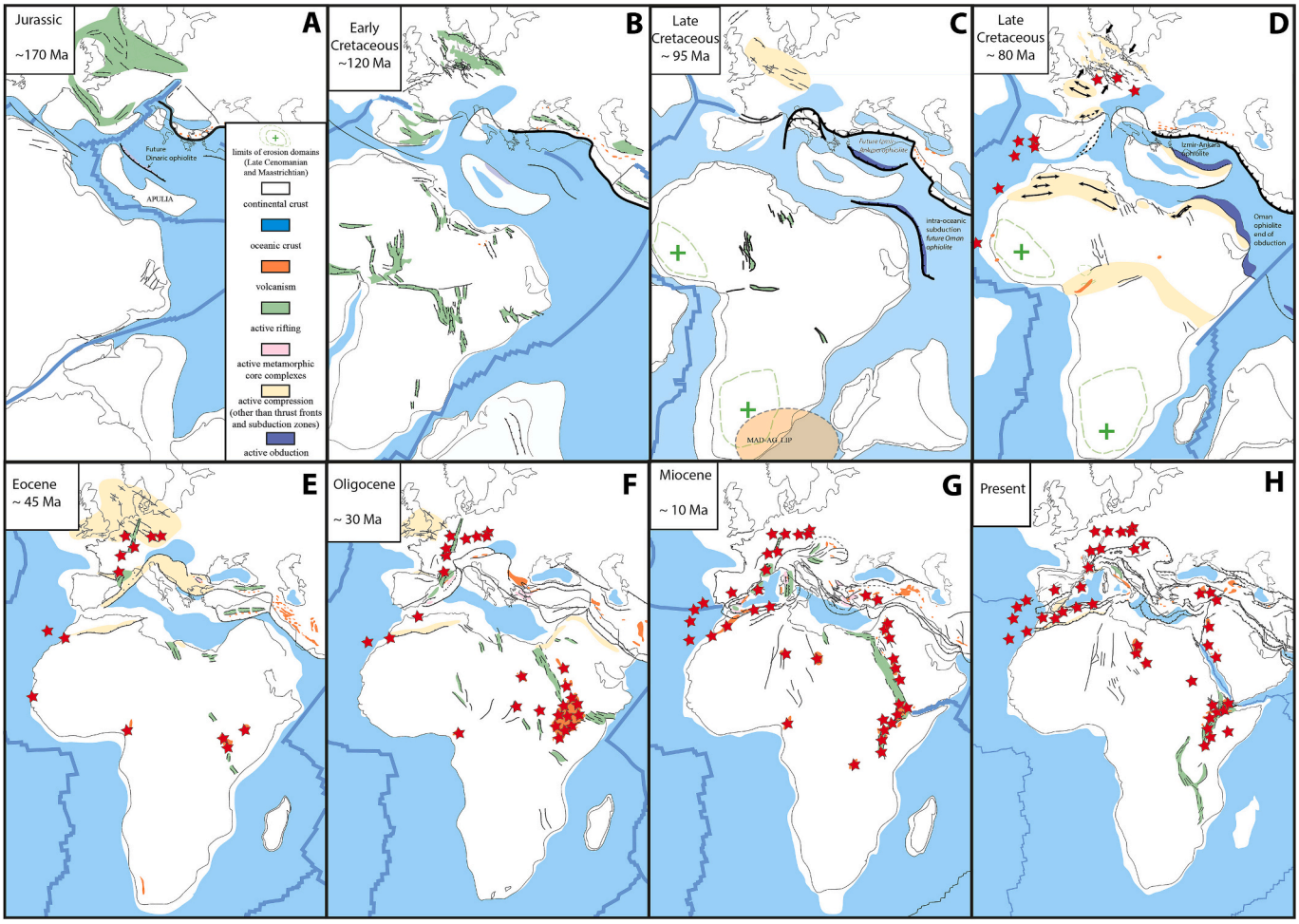

Fig. 8. Euro-Mediterranean alkaline magmatic province since 70 Ma, after Piromallo et al. (2008), Merle et al. (2018), Lebret (2014) and Marti et al. (1992). Reconstruction from Jolivet et al. (2016a, 2021a)

mountain belt and its foreland basins occurred at 11–9 Ma (Fillon et al., 2020; Calvet et al., 2021). The main period of uplift coincides with the last increments of tectonic accretion in the Pyrenean wedge, with the transition from transtension to pure extension in the ECRIS and with the beginning of slab retreat that drove back-arc extension. The Miocene uplift is clearly posterior to any compressional building of the Pyrenean wedge. Relief growth in the Massif Central and surrounding basins, as documented by low-temperature thermochronology, was sequential (Barbarand et al., 2001, 2013, 2020): a first episode of denudation recorded in the mid-Cretaceous from ~100 Ma was followed by renewed subsidence in the Late Cretaceous (Fig. 5) and a second episode of uplift happened in the northern Massif Central (Morvan) in the Paleocene.

3.2. Volcanism

Since the Late Cretaceous, the entire region has been the site of eruptions of alkaline lavas with volcanic events discontinuously recorded in the Euro-Mediterranean volcanic province (Figs. 7 and 8), from the Canaries to Cape Verde and northern Europe (Piromallo et al., 2008). According to Binder et al. (2023), volcanic activity in the Central European Volcanic Province shows two different episodes, one in the Late Cretaceous to Early Eocene (~73–47 Ma) coeval with the second uplift episode and one in the Late Oligocene and Miocene (~27–9 Ma), coeval with rifting. The source of this magmatism appears to be present almost continuously in the underlying mantle of this vast NE-SW elongated region since the Cretaceous (Fig. 8). It encompasses the Canaries and Madeira hotspots, crosses the western Mediterranean along the Mid-Alboran shear zone and then connects with the French Massif Central and the Upper Rhine Graben. In the recent period, from 10 Ma to the present, which seems the most active, all regions have recorded eruptions of alkaline volcanism, including the Valencia Basin and the Columbretes Islands in the Western Mediterranean. However, there is a temporal disjunction between the main extension and the two main episodes of magmatism, in the Massif Central and the Upper Rhine Graben where most of the magmatic activity occurred before and after the rifting episode (Fig. 7) (Merle et al., 1998; Wilson and Bianchini, 1999; Merle and Michon, 2001). ECRIS rifting was preceded by scattered magmatism from the Late Cretaceous to the Eocene (Marti et al., 1992; Goes et al., 1999; Piromallo et al., 2008; Duggen et al., 2009; Lustrino et al., 2011; Merle et al., 2018).

In the Massif Central, scattered *syn*-rift magmatism started in the north in the Late Oligocene during the last extensional and sedimentation episode and in the south with the main magmatic episode in the Upper Miocene, with a first peak between 9 Ma and 6 Ma and a second peak between 3.5 Ma and 0.5 Ma. Rifting in the northern Valencia Basin was accompanied by intense volcanism, forming a magma-rich passive margin (Maillard and Mauffret, 1999; Jolivet et al., 2020; Maillard et al., 2020; Jolivet et al., 2021b).

3.3. ECRIS, previous models

Four main models have been proposed to explain the formation of the ECRIS and its relation to the Euro-Mediterranean volcanic province; these include four viewpoints:

(1) Illies (1975) considers that the Alpine subduction induced the rise of a mantle plume beneath the foreland: "*subcrustal masses were transported under the foreland to induce mantle diapirism, volcanism and intraplate rifting*". While the plume is considered a consequence of the Alpine subduction, this model accepts the existence of a mantle diapir beneath the Upper Rhine Graben. Illies and Greiner (1978) suggested that the rift was mainly the consequence of Alpine tectonics, and the mantle rise was an "*additional factor*" controlling the rifting process. Illies (1978) separates the contribution of a mantle diapir on top of which the Upper Rhine Graben first formed, from the contribution of the maximum horizontal compression striking parallel to the rift as the result of regional tectonic conditions.

(2) Ziegler (1992b) sees the ECRIS as the result of the interactions between Africa and Eurasia with transmission of stresses within the lithosphere through the collision zone. In that respect, the ECRIS is described as a "passive" rift system with no or little effect of an underlying mantle plume. The observed rifts localized along reactivated late Variscan fractures. The origin of stress may be the Pyrenean compression and possibly also the Alpine collision.

(3) Merle and Michon (2001) proposed an alternative model where extension is mostly driven by the load of the lithospheric root of the Alps. Extension in the subducting plate is caused by the traction of the European slab subducting underneath the Alps. Here again, no mantle plume is necessary to explain the observed extension. The observed ascend of mantle material is only the consequence of lithospheric thinning and, in a later stage, of an asthenospheric return flow. In Merle and Michon's model, the ECRIS started as a passive rift and later evolved into an active rift, due to this asthenospheric return flow. One of the arguments is the temporal disconnection between extension and magmatism, and absence of doming before magmatism started.

(4) An evolution of this model (Dèzes et al., 2004; Ziegler and Dèzes, 2005; Ziegler and Dèzes, 2007) describes the interactions between the subducting slab below the Alps and the far-field stresses transmitted across the Africa/Eurasia plate boundary. Angrand and Mouthereau (2021) also consider the ECRIS as a large crack in the European lithosphere formed in the direction of the Iberia-Europe convergence direction. In these models the lithosphere is heated and weakened by small mantle plumes beneath the Massif Central and the Rhenish Massif.

In all these models, the main argument for a link with the formation of the Alps is the proximity between the rift and the Alps and an apparent parallelism between the rift and the Alpine thrust front. The last point is debatable, however, as the rift extends northward toward the Lower Rhine valley, thus significantly diverging from the Alpine front.

Evidence for one or several mantle plumes principally arises from seismic tomographic studies, geochemistry of volcanic rocks typical of HIMU-volcanic island basalts and petrology of mantle xenoliths trapped in volcanic rocks. Granet et al. (1995) proposed that active mantle upwellings, or diapirs, are of small spatial scale, and rooted within a more continuous layer below 200–250 km, and Sobolev et al. (1997) concluded that the potential temperature of this anomalous mantle is in average 150–200 °C hotter than its surroundings (see also Schaeffer and Lebedev, 2013). Local mantle diapirs were also imaged by seismic tomography beneath the Eifel and Eger rifts (Ritter et al., 2001; Plomerova et al., 2016). Such localized mantle upwellings, so-called "baby-plumes" or "secondary plumes" (Cloetingh and Ziegler, 2009; Cloetingh et al., 2022), may last for rather long periods of geological times and may trigger rifting and continental breakup (Cloetingh and Ziegler, 2009; Koptev et al., 2021). Their origin is debated and might vary, but Faccenna et al. (2010) suggested that secondary plumes may be consequences of complex flow in the upper mantle related to subduction induced return flow. Such small plumes forming above a stagnant slab were also proposed for mainland China (Tang et al., 2014) and SW Japan (Kuritani et al., 2017).

Baby plume origin and persistence is debated and likely spatially variable. The parametric study of Cloetingh et al. (2022) suggests that a secondary plume can penetrate through the entire lithospheric mantle, forming a columnar structure beneath the Moho, similar to that observed, for example, in the Eifel area (Ritter et al., 2001), under the condition that the thermal anomaly is enhanced by the density contrast due to a hydrous component. High-resolution S- and P-wave tomographic studies do not validate the presence of a sub-vertical thermal anomaly that would fit the deep baby-plume model, and the role of

preexisting discontinuities within the lithosphere that would localize the anomalous mantle is discussed (Plomerova et al., 2016). The difference in strike among the different parts of the rift system could possibly be explained by this heritage.

The localization of the rift is moreover often attributed to the reactivation of older structures, especially Variscan (Visean) strike-slip faults systems slightly oblique on the main strike of the Upper Rhine Graben) (Michon and Sokoutis, 2005; Edel et al., 2007) or the late Variscan Permo-Triassic fault systems (Ziegler et al., 1995; Schumacher, 2002). Looking for a geodynamic model for the ECRIS, we now summarize existing data for an active slow intracontinental rift, the EAR.

4. Geological context of the East African Rift

The East African Rift (EAR) is the current plate boundary between the Nubia and Somalia plates (Figs. 3 and 8) accommodating a slow divergence of ~0.5 cm/yr (Chorowicz, 2005; Kogan et al., 2012; Ebinger et al., 2017; Corti et al., 2022). The EAR formed within the African plate, progressively from the Late Eocene to the present. The first rifting happened at ~30 Ma ago, thus 15 Myr after the first hot-spot volcanism recorded in Southern Ethiopia at ~45 Ma (George et al., 1998; Ershov and Nikishin, 2004). Uplift of the Ethiopian Plateau started at ~30–25 Ma based on thermochronology studies (Pik et al., 2004). The junction with the Afar triple junction did not occur before the Miocene, at ~11 Ma (Bonini et al., 2005; Corti, 2009; Corti et al., 2019). Extension in the East African Rift is mostly perpendicular to its axis and it tends to localize spatially through time (Corti, 2009) and along strike, from the distributed deformation of Afar to the localized extension in the Main Ethiopian Rift (MERS) (Kogan et al., 2012). The localization of the rift and its fault pattern are strongly influenced by inherited structures, dating back to the Panafrican (East African Orogen) (Kogan et al., 2012). The recent localization of extension toward the center of the MERS along the Wonji fault system, with an en-échelon pattern, has been interpreted as a consequence of such a reactivation of Panafrican faults (Chorowicz et al., 1994; Corti, 2009) or to a change in the far-field direction of extension (Bonini et al., 1997). Corti (2009) described the evolution of the rift as follows. First, distributed deformation was localized on reactivated ancient faults and distributed over a wide zone, and the magmatism was diffuse. Then, the Wonji Fault system was activated in the center of the rift and feedback between deformation and magmatism ensued, extension being accommodated by both faulting and magmatism (Buck, 2004; Ebinger, 2005; Buck, 2006; Lavecchia et al., 2016).

The EAR is divided into two main branches. The eastern branch comprises the Kenyan Rift and the Main Ethiopian Rift, concentrating most of the volcanic products emitted by the large plume underlying this system (Chorowicz, 2005) and showing several phases of magmatism active since the Eocene (Rooney, 2017, 2020a). Before 20 Ma, three phases of basaltic eruptions are identified. The initial phase (45–34 Ma) was dominated by basaltic volcanism in southern Ethiopia and northern Kenya. The second phase (33.9–27 Ma) was also dominantly basaltic, with the eruption of the Ethiopian traps in the NW Ethiopian plateau and Yemen. A new surge of basaltic volcanism is also recorded in the latest Oligocene and early Miocene (26.9–22 Ma) over the entire region. Neogene to Quaternary magmatism was concentrated along the rift axis. After a pulse of basaltic magmatism at ~20 Ma, volcanic products show more evolved compositions with rhyolites and phonolites until 12 Ma, after which, until 9 Ma, a widespread surge of basaltic magmatism is observed, starting slightly later in the north, before the development of the basaltic Stratoid between 4 Ma and 1.6 Ma and finally the silicic volcanism along the rift axis. An evolution is seen toward more silicic magmatism with time during continuous thinning of the lithosphere, interpreted as an increase of melting of the convective mantle (Rooney, 2020b).

The western branch formed on the western side of the Tanzanian craton with the Albertine Rift, Edward Rift, Kivu Rift, Tanganika Rift, Rukwa Rift and Malawi Rift, from north to south. Compared to the eastern branch, faulting and volcanism have been suggested to have started later than 25 Ma (Ebinger, 1989, 2012) with a southward migration from ~20 Ma in the Lake Albert region to ~8–9 Ma in the Rukwa rift. Roberts et al. (2012) instead suggest a roughly coeval development of the two branches from ~26 Ma.

Magmatism in Afar (Stab et al., 2016; Pik et al., 2017; Rooney, 2020a) started with the emplacement of the rhyolitic and basaltic Traps formation at ~30 Ma. Between 20 Ma and 10 Ma, explosive silicic volcanism and minor basaltic highly contaminated with crustal products is recorded. From 10 Ma to 5.6 Ma, volcanism was first silicic and became dominantly basaltic while migrating toward the basin, crustal contamination being smaller than during the preceding phase. After the transitional phase of the Dahloid series, the Afar Stratoid series were emplaced between 3.9 and 1 Ma, covering a large part of the region. The Gulf series (2.8–0,3 Ma) are associated with the propagation of the Gulf of Tadjoura and the oceanic ridge of the Gulf of Aden into Afar. This was followed by the eruption of silicic and basaltic volcanoes along the rift axis from 0.7 Ma to the present. Whether all these magmatic products originate from a single (Ebinger and Sleep, 1998; Rooney, 2020a) or two mantle plumes, namely Kenya and Afar plumes (Rogers et al., 2000; Pik et al., 2006; Civiero et al., 2022), is debated. Some geochemical studies suggest that these geochemically distinct products are contributed by different parts of a thermochemically heterogeneous lithospheric mantle within the deep seated African super plume (Nelson et al., 2012; Halldórsson et al., 2014).

5. Mantle structure

The line of magmatic systems running from Ethiopia to Eastern Anatolia lies above a distinct sub-lithospheric S-wave velocity anomaly (Fig. 9, anomaly A) with a dog-leg shape as it changes strike when reaching the Red Sea and again along the western limit of the Arabian plate (Faccenna et al., 2013; Schaeffer and Lebedev, 2013; Celli et al., 2020a; Celli et al., 2020b; Hua et al., 2023). It corresponds to the upper mantle extension of a much larger velocity anomaly rising from the lower mantle toward the base of the lithosphere, and rooting in the African large, low velocity province (LLSVP) at the base of the mantle (Fig. 9, anomaly B) (Dziewonski and Woodhouse, 1987; Ritsema et al., 1999; Nyblade et al., 2000; Burke et al., 2008; Burke, 2011; Hansen et al., 2012). Together with the development and northward migration of magmatism (Ershov and Nikishin, 2004; Faccenna et al., 2013; Hua et al., 2023) from the Afar to eastern Turkey, this geometry suggests to the first order that the plume material impinged the base of the lithosphere in the Eocene, then migrated northward to reach the Tethyan subduction/collision zone in the Middle Miocene, while the Arabian plate was separated from the main body of Africa, forming the Gulf of Aden and Red Sea (Faccenna et al., 2013; Issachar et al., 2024). The dog-leg shape of the S-wave anomaly suggests that the plume material was partly channelized below the lithosphere along the Red Sea rift. Together with this northward migration of magmatic events related to the plume, a slower southward migration is also observed (Ershov and Nikishin, 2004) that was modeled by Hassan et al. (2020) with a mobile Afar plume consistent with the propagation of the rift toward the south and weakening of the plume activity.

A similar geometry is observed below the Cameroon Line (Fig. 9, anomaly E) and its offshore extension (Fitton and Dunlop, 1985; Njome and de Wit, 2014; Celli et al., 2020a, 2020b), parallel to the strike of the Walvis Ridge connecting the Tristan da Cunha hot spot with the Etendeka LIP (O'Connor and Le Roex, 1992; O'Connor et al., 2012; O'Connor and Jokat, 2015b). The Cameroon line is also parallel to the Benue Trough belonging to a series of Early Cretaceous grabens (Min and Hou, 2019). The Tibesti and Haruj volcanic regions rest on top of the same slow S-wave velocity anomaly shown by tomographic models corresponding to high-temperature mantle melting (Liégeois et al., 2005; Beccaluva et al., 2007; Ball et al., 2019). The petrology of lavas and their enclaves suggests that the hottest anomaly is located underneath Haruj

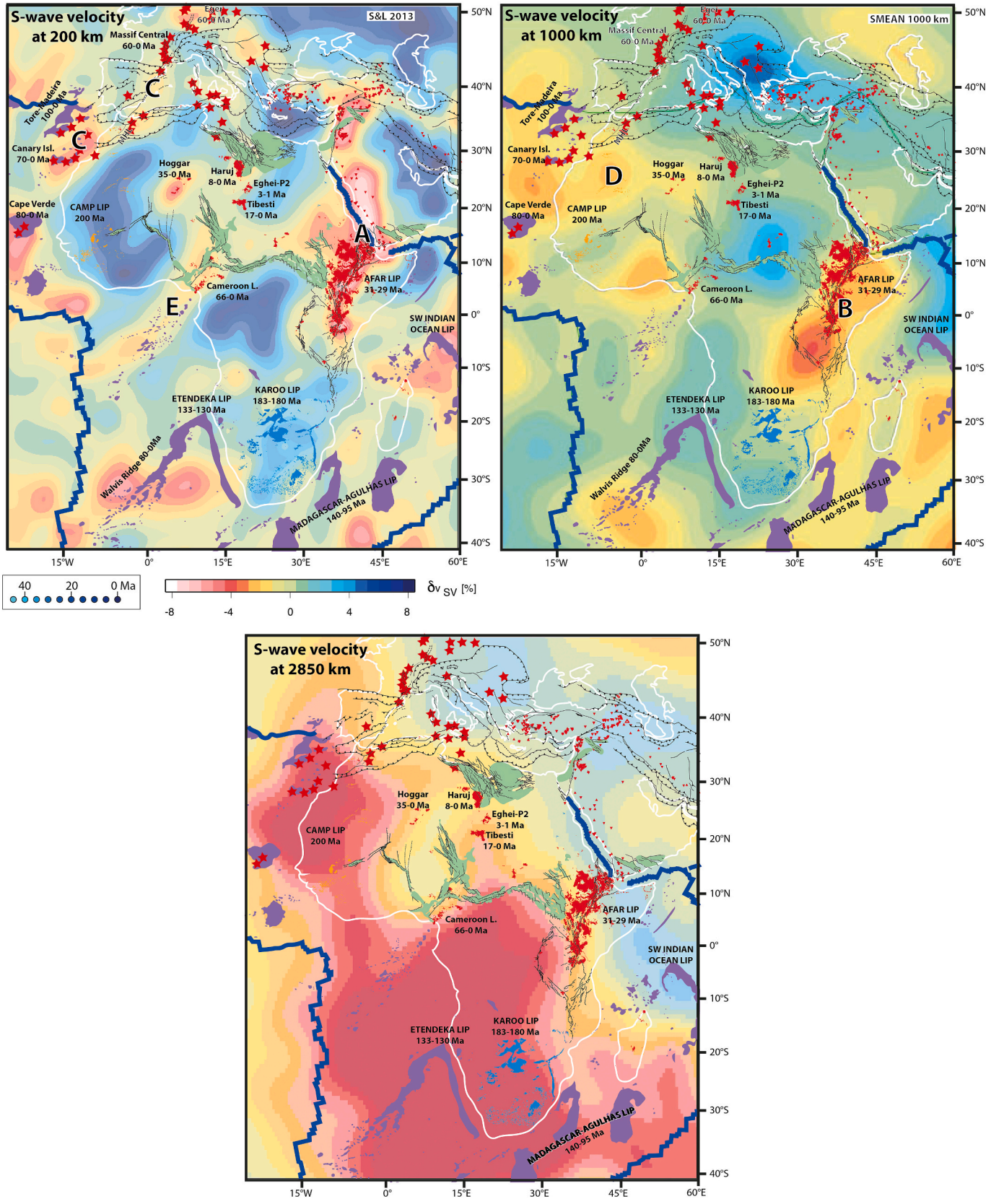

Fig. 9. LIPS and major structures on top of S-wave tomographic models. A: 200 km after Schaeffer and Lebedev (2013). B: 100 km after Becker and Boschi (2002). C: 2850 km after Torsvik and Cocks (2016).

province (Ball et al., 2019), right along the axis of the low velocity anomaly, rather than in the Tibesti slightly on the side. Further to the west, the Hoggar volcanic province also lies on top of a velocity anomaly and corresponds to the melting of mantle in two stages: first, lithospheric mantle melting and production of tholeiitic basalts and then, asthenospheric melting and production of alkali basalts (Beccaluva et al., 2007).

The West Africa and Euro-Mediterranean magmatic province is also associated to a low velocity anomaly (Fig. 9) (Goes et al., 1999; Piromallo et al., 2008). In Central Europe, the anomaly related to the Eifel hotspot is well imaged in Zhu et al. (2012) and Meier et al. (2016). The upper mantle anomaly is more or less continuous from Cape Verde to Central Europe with significant variations of its intensity along strike (Fig. 9, anomaly C). The connection of this volcanic province with lower mantle low-velocity anomalies has been challenged in a recent paper by Anguita et al. (2024) who refute the interpretation of the Canaries hotspot as related to a mantle plume. However, in contrast, a new high-resolution full waveform seismic tomography of the mantle by Munch et al. (2024) confirms the connection with deep mantle low-velocity anomalies (Fig. 9, anomaly D). The hotspots are offset from the location of the deep mantle plume by a series of low shear velocity channel or "fingers" elongated parallel to the absolute motion of the plates.

Mantle seismic tomography further reveals the shape of mantle plumes connected to the LLSVP present below West and South Africa above the core-mantle boundary (Fig. 9). The EAR rests above a horizontal low-velocity anomaly encompassing the whole upper mantle, continuous all along the EAR and reaching Arabia north of the Afar region (Hansen et al., 2012). This anomaly roots in a south-dipping anomaly connected with the African LLSVP at the base of the mantle (Courtillot et al., 2003; Boschi et al., 2007; Burke, 2011).

Recent tomographic investigation suggest that the Cameroon Line is also connected to the African low-velocity province in the lower mantle (Saeidi et al., 2023). The whole-mantle shear-wave model of French and Romanowicz, 2014; French and Romanowicz, 2015; Davaille and Romanowicz, 2020) shows the systematic connection of major hotspots with wide plumes rooting in the low-velocity anomalies at the base of the mantle (Figs. 10 and 11). It also suggests that the low-velocity anomalies are organized with finger-like horizontal domains (Low Velocity Fingers, LVF) below the lithosphere (A on Figs. 9 to 14) and below a 1000 km horizon (B on Figs. 9 to 14), pointing northeastward below Africa. Such LVFs below the lithosphere have already been identified below the Pacific plate (French et al., 2013) and more recently underneath the Atlantic Ocean where they connect with lower mantle anomalies (Munch et al., 2024).

It is well known that secondary convective anomalies can form linear features under plate shear (Richter and Parsons, 1975; Huang et al., 2003; Ballmer et al., 2007). In a plume context, low velocity channels have been explored when aligned perpendicular to the Mid-Atlantic oceanic rift around Iceland (Rickers et al., 2013) and modeled with laboratory (Schoonman et al., 2017) and numerical experiments (Koptev et al., 2017a, 2017b; François et al., 2018), for example, as well as in connection of the Canary plume to intraplate orogeny in the Atlas (Duggen et al., 2009). Such asthenospheric fingers are expected to be associated with a modulation of the topography of the lithosphere-asthenosphere boundary that can either be inherited from older tectonic events (Ebinger and Sleep, 1998) or result from the propagation of the hot anomalies. The case of the EAR is particularly clear with several LVFs from the lower to the upper mantle (Figs. 10 and 11, anomalies A and B). A similar organization of the convective mantle as that beneath Africa is also observed underneath the Canaries hotspot with one such asthenospheric finger under the lithosphere pointing toward the northeast (anomalies C and D on Figs. 9 and 11).

A comparison with other recently published S-wave tomographic models (Figs. 12 and 13) shows that this geometry is robust, with LVFs in the upper and lower mantle underneath the EAR and in the upper mantle underneath the western Europe volcanic province and ECRIS. A strong P-wave low-velocity anomaly that extends northward, associated with a step in thermal lithospheric thickness is furthermore observed underneath the Massif Central (black arrow on Fig. 13, UU-PO7 model of Amaru (Amaru, 2007). The recent study of Civiero et al. (2022) shows that the geometry of the Afar plume is more complex and may result from the coalescence of several plumes in the upper mantle, which would explain the variable intensity of the observed anomaly. One way of reconciling this last study with earlier ones is to consider that the lower and upper mantle fingers are punctually connected by vertical conduits, as suggested on Fig. 14.

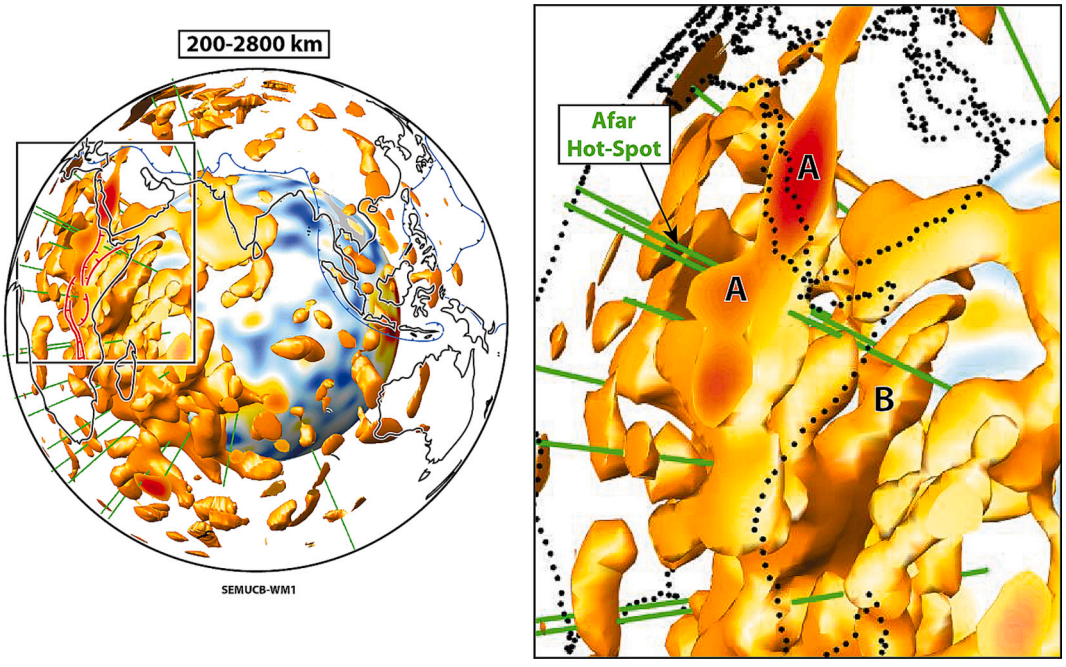

Fig. 10. 3D view of the low-velocity anomalies between 200 km and 2800 km after French and Romanowicz (2014) and Davaille and Romanowicz (2020) showing low-velocity fingers (LVF).

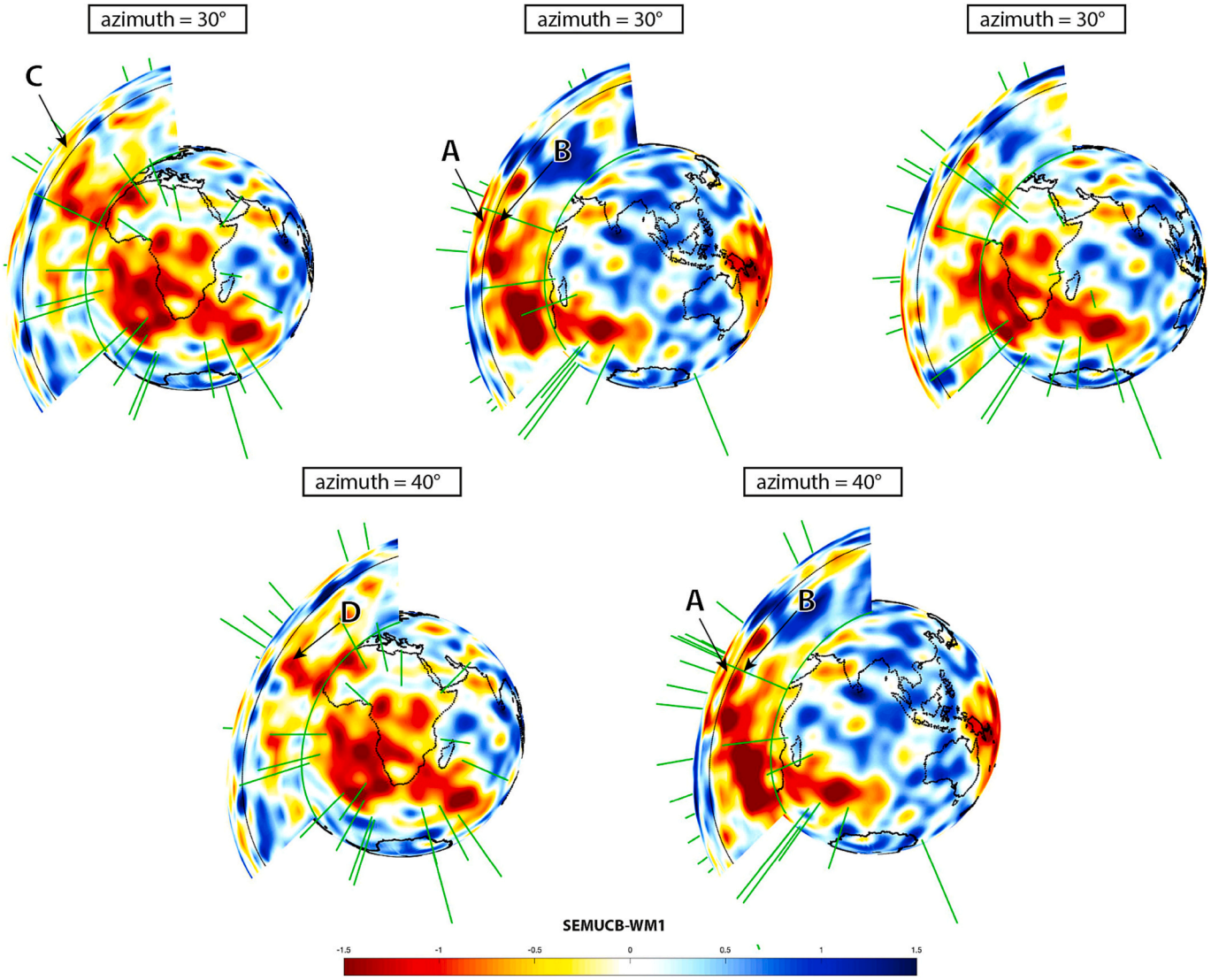

Fig. 11. Vertical sections with two different azimuths (30°E and 40°E) across low-velocity anomalies between 200 and 2800 km after French and Romanowicz (2014) and Davaille and Romanowicz (2020) showing the low-velocity fingers (LVF).

6. Mantle structure and magmatism

The ECRIS is spatially associated with alkaline magmatism in general, but some portions of the rift or periods recorded active extension without any magmatism, favoring models with no mantle plume or where the mantle plume is a consequence of extension and not the opposite (Merle and Michon, 2001; Michon and Merle, 2001).

Enlarging our vision to the scale of Africa and Europe shows that alkaline Cenozoic magmatism is widespread to the NNE of the large low-shear velocity anomalies observed in the lowermost mantle underneath south and west Africa (Fig. 9). In the east, alkaline volcanism migrated fast toward the north after the formation of the Ethiopian traps some 30 Ma ago, as far as eastern Turkey (Ershov and Nikishin, 2004), a feature interpreted by Faccenna et al. (2013) as the indication of northward migrating mantle from the Afar hotspot to eastern Turkey (Fig. 15), further explored by Hua et al. (2023) and Issachar et al. (2024). The northward migrating magmatism crossed the Red Sea and then reached eastern Turkey and Armenia some 10 Ma, crossing the western part of the Arabian plate.

Lustrino and Wilson (2007) consider that all these magmatic centers arise from diapiric instabilities in the mantle, instead of a single large plume, and small-scale convection might be expected to be more readily linked to intraplate volcanism for slowly moving plates such as Africa (Burke and Wilson, 1972). The position of the African magmatic centers can also be controlled by the reactivation of Panafrican faults or shear zones (Liégeois et al., 2005). Modelling of mafic magmatism assuming adiabatic decompression of a dry peridotite shows that among the Tibesti, Hoggar and Haruj volcanic centers, Haruj has seen the highest mantle potential temperature (Ball et al., 2019), which fits its position in the center of the S-wave low velocity anomaly, when the Tibesti is slightly aside. In the west, in the domain extending from the Canaries islands all the way to the Eifel in northern Germany, the earliest events are recorded at both ends in the Late Cretaceous (Fig. 8) and the whole system was active until recent periods, even in the north where the youngest eruptions date back to 10,900 years ago in the Eifel (Zolitschka et al., 1995; Dahm et al., 2020) and 6700 years in the Massif Central (Lac Pavin) (Nehlig et al., 2003).

On a shorter time-scale, Duggen et al. (2009), based on a compilation of geochemical characteristics and ages of volcanic products from the Canaries to the Western Mediterranean, proposed a northward propagation of a mantle finger emanating from the Canaries hot-spot during the last 15 Ma. Piromallo et al. (2008) consider that the entire region from Cape Verde to northern Europe results from an initial single plume event in the Late Cretaceous that has modified the lithosphere and

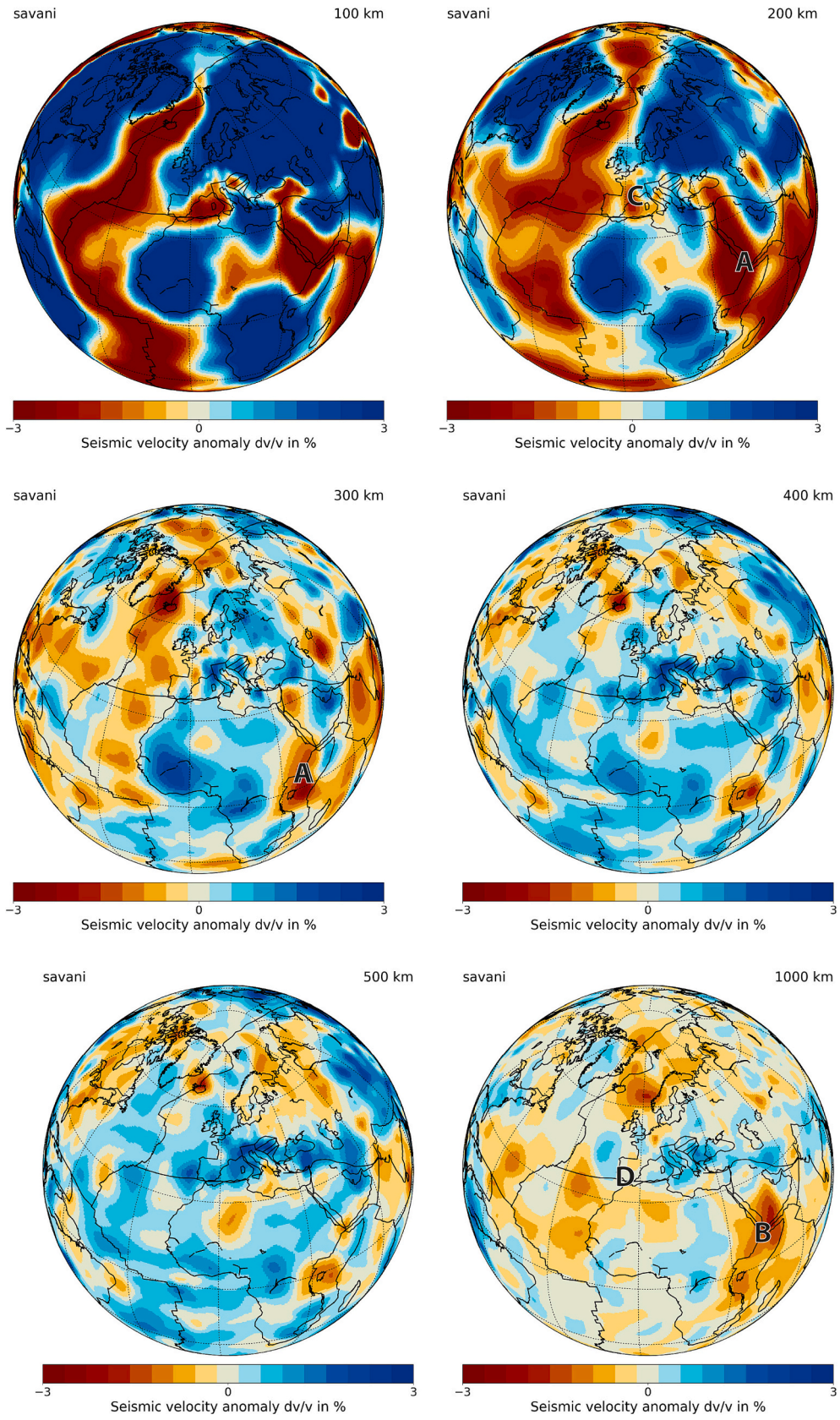

Fig. 12. Horizontal map views of the SAVANI S-wave tomographic model (Auer et al., 2014) at the indicated depths.

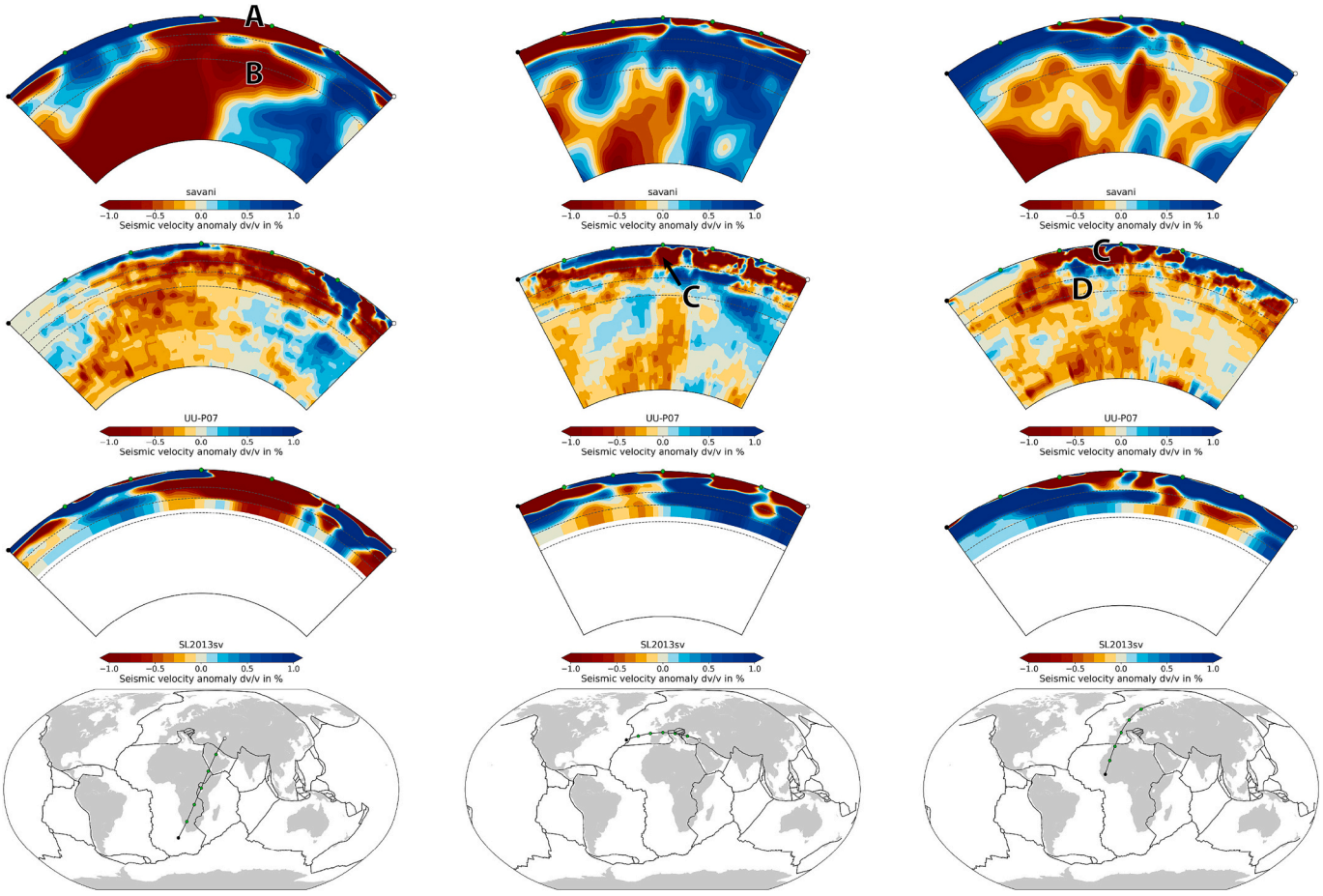

Fig. 13. vertical cross-sections through three different seismic tomography models. SAVANI (Auer et al., 2014), UU-PO7 (Amaru, 2007) and SL2013SV (Schaeffer and Lebedev, 2013).

asthenosphere underneath North Africa and Western Europe, explaining the geochemical similarities between the various sub-regions. As noticed by Piromallo et al. (2008), the southern part of the volcanic domains of western Europe were indeed located further south in the Late Cretaceous above low-velocity anomalies observed today in the lower mantle (E, F on Fig. 16), which might explain the early volcanic events along the whole system. Fig. 16 shows how these domains moved away from the high temperature anomalies after 100 Ma. The persistence of magmatism along the entire igneous province may suggest the existence of a finger of hot asthenosphere all along during a long period, with a recess of its activity during rifting and back-arc extension.

7. Mantle structure, topography and absolute motions

Figs. 16 and 17 show that these low S-wave velocity anomalies strike parallel to the absolute motion of plates, to the ECRIS and EAR rifts systems, to the grain of the non-isostatic residual topography and to volcanic provinces. Celli et al. (2020a, 2020b) show detailed 3-D S-wave tomography models of the base of the African lithosphere that delineate hot spots and cratons, due to basal erosion by mantle convection (Fig. 9). As shown by Fig. 16, these channels of hot mantle are parallel to Africa motion in a hot-spot reference frame. Anomalies below the Cameroon Line, Tibesti, Hoggar and Afar-Red Sea are located in the upper mantle and the Afar-Red Sea anomaly connects to a deep plume rooted in the lower mantle as already shown by Hansen et al. (2012) and inferred by Ritsema et al. (1999). Kinematic trajectories show that the West European magmatic province was located above a low-velocity anomaly in the lower mantle (Fig. 16) at 100 Ma, as noted by Piromallo et al. (2008).

Mantle dynamics can also be inferred from considering residual topography, i.e. the part of long-wavelength topography that does not confirm to isostasy for a given crustal and lithospheric thickness and density model. The residual topography model of Steinberger et al. (2019), for example, shows a trend parallel to the main alkaline volcanic provinces (Fig. 17a), or the absolute trajectories of Africa and Eurasia in a hotspot framework (Figs. 17b, c) (Seton et al., 2012; Zahirovic et al., 2015; Torsvik and Cocks, 2016; Müller et al., 2019) as well as the SKS-splitting derived seismic anisotropy “fast axes” over Africa and Europe. Fig. 16 shows the same trajectories on top of the S-wave tomography model of Schaeffer and Lebedev (2013). The comparison of these data sets shows that the EAR-MERS and the ECRIS, as well as associated volcanic provinces and their extension toward the SW in the Canaries and Cape Verde, appear carried by the strongest positive anomalies of residual topography. Other less intense anomalies are associated to the Cameroon Line and its offshore extension or the Walvis Ridge, also parallel to the absolute trajectories of Africa. Both alignments show a progression of ages typical of hot-spots tracks (O’Connor et al., 2012; O’Connor and Jokat, 2015a).

It thus appears that there is a first-order link between alkaline magmatic provinces, low velocity anomalies, residual topography and absolute plate motion trajectories, thus mantle dynamics. Extension in the EAR is intimately linked with large-scale topography that has developed since ~30 Ma following the first volcanic events. The East African dome, the Ethiopian dome, and the Cameroon dome further west localize the formation of these lithospheric-scale features. These basement culminations and associated volcanism are set on top of positive thermal anomalies and a thin lithosphere (Liégeois et al., 2005; Schaeffer and Lebedev, 2013; Ball et al., 2019).

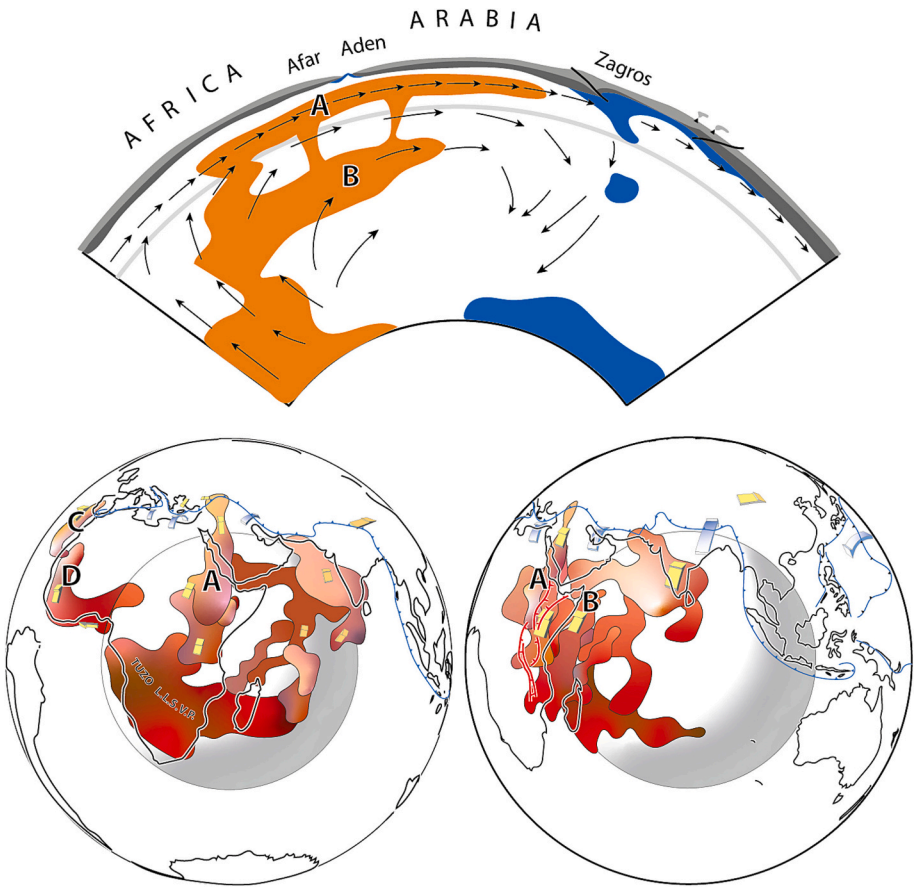

Fig. 14. simplified scheme of low-velocity fingers underneath the East African Rift and West African plate and a schematic cross-section parallel to the rift.

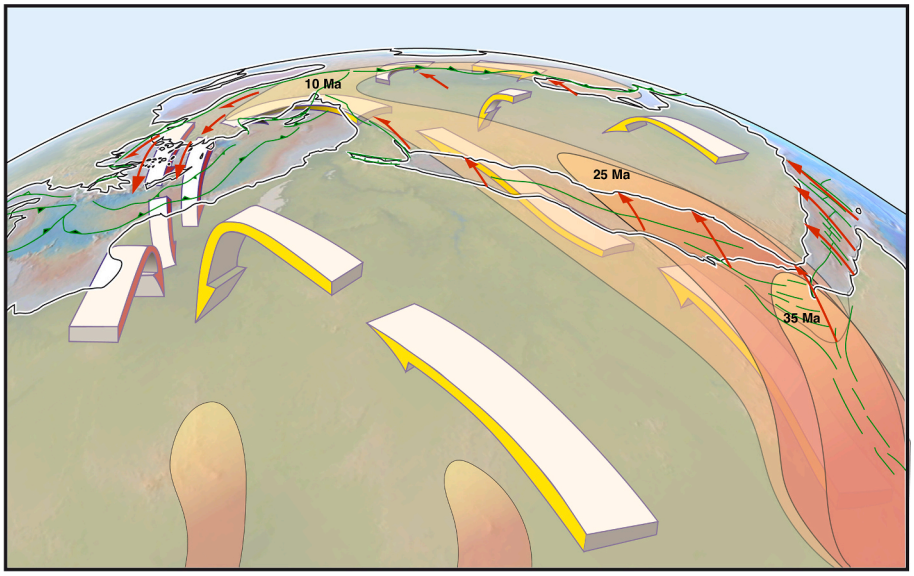

Fig. 15. Schematic representation of the LVF underneath East Africa and the Arabian plate reaching north to the Tethyan collision zone, and its relation to the fragmentation of Africa and the formation of the Arabian plate. Modified from Faccenna et al. (2013) with the addition of VLF underneath the Hoggar and Tibesti volcanic provinces.

The dynamic topography predictions of Paul et al. (2014) suggest the formation of the dome in east Africa some 15 Ma ago. More recently, a geological and geomorphological study at the scale of Africa (Guillocheau et al., 2018), based on the analysis of ancient surfaces, show that these domes first appeared after 40–30 Ma ago, coeval with the surge of alkaline volcanism in Ethiopia due to the African superplume and the beginning of volcanism in the Tibesti, Haruj and Hoggar massifs further west. The Cameroon and East African domes started to form at ~34 Ma and the Angola Mountains 15–12 Ma ago (Middle Miocene).

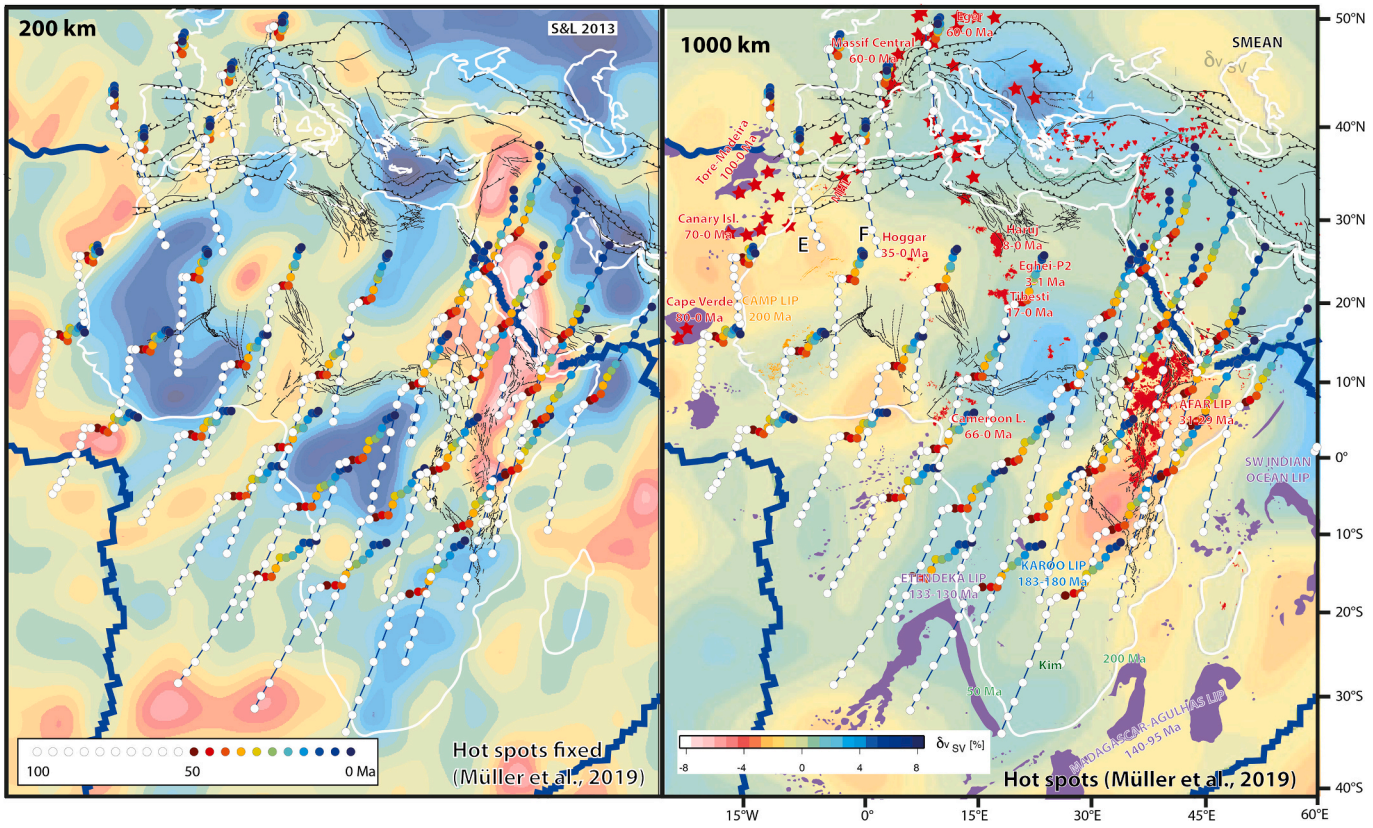

Fig. 16. Absolute kinematic plate trajectories after Müller et al. (2019) on top of S-wave tomography at 200 km after lSL2013 SV (Schaeffer and Lebedev, 2013) and SMEAN model (Becker and Boschi, 2002) at 1000 km. White dots between 100 and 50 Ma. Volcanic provinces shown with red symbols. (For interpretation of the references to colour in this figure legend, the reader is referred to the web version of this article.)

The time around 30 Ma thus appears as a turning point in the topographic and tectonic evolution of Africa. The slowdown of Africa's absolute motion was the main reason for the development of hotspots after the collision with Eurasia such as the Afar traps, the Hoggar alkaline magmatism (Burke, 1996; Burke and Gunnell, 2008). Faccenna et al. (2019) also proposed that the high temperature anomaly below the Afar region and the associated positive anomaly controlled the long-term stability of topographic gradients and the Nile River drainage system, since 30 Ma.

8. Seismic anisotropy

Figs. 17b and 18 illustrate the systematic orientation of the fast axis of SKS-wave azimuthal anisotropy from shear wave splitting, parallel to the long axis of the EAR and Main Ethiopian Rift, then slightly oblique to the Red Sea and finally parallel to the Levant Fault that marks the western boundary of the Arabian plate. Such observations have long been used to infer rift dynamics (e.g. summary in Kendall et al., 2006). Typically, the effects of partial melting are considered to at least contribute to seismic anisotropy (e.g. Holtzman and Kendall (2010), but we know that asthenospheric channeling under a thinned lithosphere can likewise align anisotropy (e.g. Faccenna et al., 2013). Assuming that the fast axes of shear wave splitting align with asthenospheric flow due to shearing in convection, that mantle flow would be (1) parallel to the rift (Andriampenomanana et al., 2021), (2) parallel to the absolute motion of the African and Arabian plate in a hot spot reference frame and (3) parallel to the positive residual topography anomalies. One can make the same observation below the Cameroon Line and Benue Rift (Fig. 17). A similar parallelism between seismic anisotropy and the absolute motion is seen below South Africa, but without a clear rift axis. Sparser data below North Africa show a similar pattern.

LVF are thus parallel to the EAR rift axis and thus to the absolute motion of Africa in a hotspot reference frame and by inference to the flow of asthenospheric mantle. The convecting mantle is organized with vertical plumes and LVFs, which while spreading on any horizon in the mantle can link to horizontal branches, including the upper mantle where the viscosity is lower and the velocity of flow faster.

9. Rifting and plume-lithosphere interactions

Burov and Gerya (2014) have studied plume-lithosphere interactions with 3-D thermo-mechanical numerical models. They show that even weak far-field extensional stresses imposed on the lithosphere control the geometry of the rift above the plume and that the plume material flows away from the plume head while rifting proceeds. Koptev et al. (2018) showed that the geometry of the rift, either wide or narrow, depends upon the rheological stratification of the impacted lithosphere. Koptev et al. also explored the interaction of a mantle plume with a heterogeneous lithosphere including a strong nucleus such as the Tanzanian craton above the plume, varying the respective sizes of the craton and the plume head and their relative positions. The results show that the craton keel deflects and channelizes the plume, which pushes the craton laterally. Additionally, the combination of the effects of the mid-ocean ridges surrounding Africa and the presence of the plume underneath the EAR was shown to lead to a direction of maximum horizontal compression parallel to the rift by Min and Hou (2018) through a spherical shell model.

The drivers of plate motion and deformation have been studied with a range of global mantle circulation models (e.g., Ricard and Vigny, 1989; Lithgow-Bertelloni and Richards, 1998; Becker and O'Connell, 2001; Conrad and Lithgow-Bertelloni, 2002). We know that the forces exerted by sinking slabs are the dominant drivers for fast plate motions

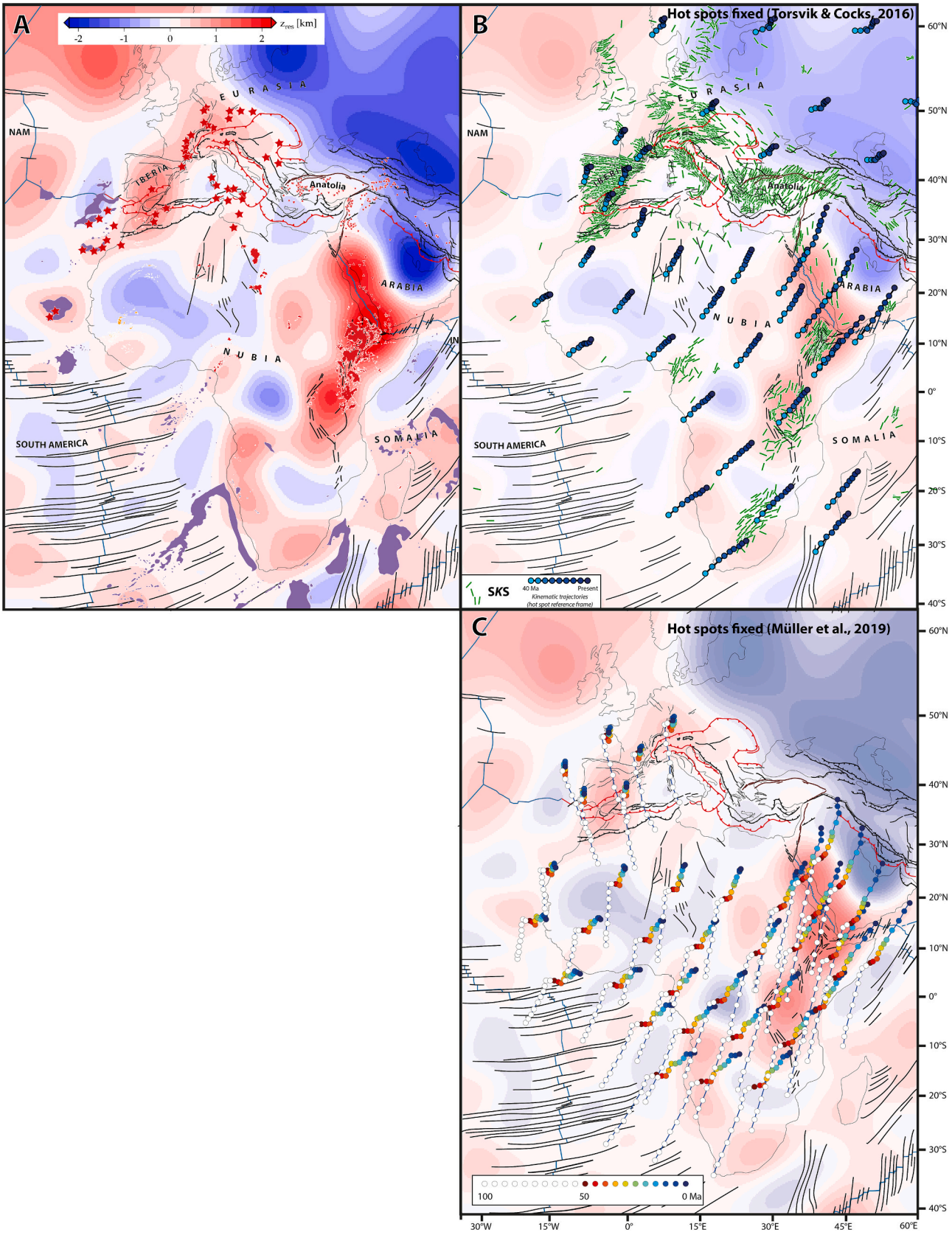

Fig. 17. LIPS related to the African LLSVP and major structures on top of (A) residual topography after Steinberger et al. (2019) and (B) with the addition of SKS-wave splitting "fast axes" (i.e. orientation of the fast axis propagation plane of inferred azimuthal anisotropy, station averaged) from the compilation of Becker et al. (2012), updated as of 10/2023, and plate motion trajectories in different kinematic frameworks (B, C) (Torsvik and Cocks, 2016; Müller et al., 2019). Background images are the same in all three panels, only dimmed in B, C and D, to better show superimposed information.

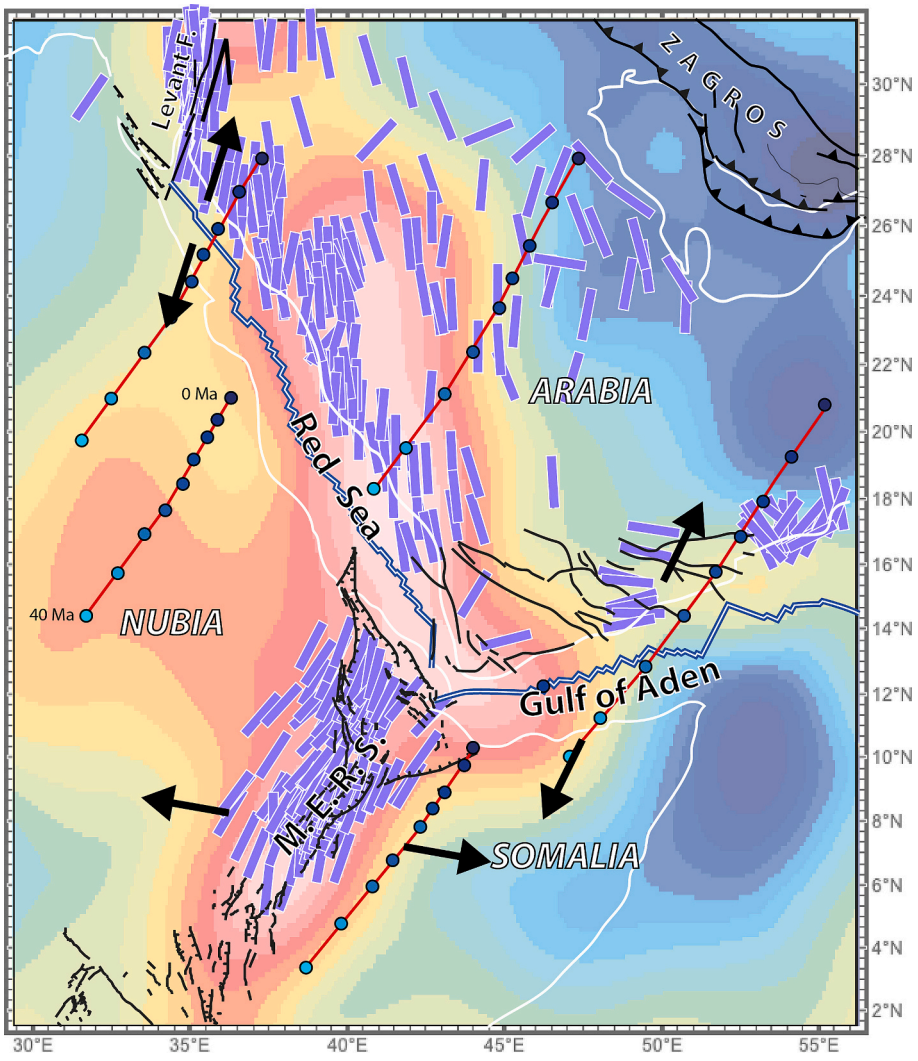

Fig. 18. Shear-wave splitting anisotropy underneath the Afar triple junction region (Qaysi et al., 2018) and S-wave tomography at 200 km depth (Schaeffer and Lebedev, 2013). The reconstructed absolute trajectories were calculated with the parameters of Torsvik and Cocks (2016).

and much of tectonic deformation. However, if local mantle flow in the asthenosphere is aligned with surface plate motions in terms of direction, and if the plate leads the mantle or vice versa, depending on plate geometry and driving density anomalies (e.g. Hager and O'Connell, 1981; Stotz et al., 2018) as well as lateral viscosity variations (e.g. Hoïnk and Lenardic, 2010; Natarov and Conrad, 2012; Becker, 2017; Semple and Lenardic, 2018), the balance between slab pull and basal drag by the flowing mantle may change. Using plate generating type convection that allow for intraplate deformation to evolve, Coltice et al. (2019) show that slab pull is a dominant force able to move plates at high rates and eventually break continents. They also show that continental plates not attached to a slab can be deformed by the faster flow of mantle underneath, for instance in back-arc regions. In their models, when a given plate is attached to a slab, it typically moves faster than the mantle underneath; alternatively, when no slab pulls the continental plate, the mantle can often flow at a higher velocity than the plate. We know that even for purely slab driven flow, the asthenosphere can locally be faster than the plate for certain geometries (e.g., Becker, 2017), and the Pacific plate likely shows extensive Poiseuille type flow (e.g., Natarov and Conrad, 2012; Becker, 2017; Stotz et al., 2018). However, taking the presence or absence of slab pull as a general indication for the effectiveness of asthenospheric motions following Coltice et al. (2019), for simplicity, the case of Africa since 30 Ma may be typical of an asthenospheric flow dominated situation with a decrease of the absolute velocity since ~30 Ma and a faster northward flow of mantle underneath because of the collision with Eurasia, which may explain the break-up forming the Red Sea and the Gulf of Aden (Jolivet and Faccenna, 2000; Bellahsen et al., 2003; Faccenna et al., 2013; Jolivet et al., 2018b).

In contrast, Stamps et al. (2014) have estimated the vertically averaged vertical stress (gravitational potential energy, GPE) and concluded that forces induced by GPE are sufficient to maintain the observed divergence across the East African Rift, and that no additional forces due to mantle flow underneath are needed. This conclusion is opposite to that of Ghosh et al. (2008) who showed that the addition of GPE and basal traction from convective mantle flow improves the fit of deformation indicators for most continental deformation zones, and an important effect of mantle tractions on crustal stress was also suggested by the modelling of Steinberger et al. (2001), for example. In the case of the East African Rift, however, the asthenospheric flow underneath is not perpendicular but parallel to the rift, as recalled above, as corroborated by the migration of magmatism from the south of Ethiopia to Caucasus and eastern Anatolia, through the east African Rift and the western part of the Arabian plate (Ershov and Nikishin, 2004) between ~45 and 10 Ma. This has prompted the proposition of the northward migration of plume material carrying on its back the Arabian plate and causing the rifting of the Red Sea and Gulf of Aden once the African plate had slowed down after the main Africa-Eurasia collision at ~30 Ma ago (Faccenna et al., 2013; Issachar et al., 2024).

One additional observation is the polarity of normal faults in the southern part of the Afar triangle. North of the main normal fault flanking the Ethiopian plateau, most normal faults indeed dip southward (Stab et al., 2016), i.e. toward the continent like in South Atlantic volcanic margins (Clerc et al., 2015; McDermott et al., 2015; Clerc et al., 2017), a geometry compatible with a top-to-the south crustal-scale shearing, induced by the northward mantle flow underneath (Jolivet et al., 2018b; Sternai et al., 2021).

The topographic expression of a plume in continental domain is complex and depends a lot upon the mechanical structure of the impacted lithosphere (Burov and Guillou-Frottier, 2005). Instead of a single dome, in case of a non-stratified lithosphere, a more complex mechanical structure will result in several domes and basins (Cloetingh et al., 2013) and this geometry can be modulated by far-field stresses leading to lithospheric folding (Burov and Cloetingh, 2009). The frequent presence of earthquakes in the lower crust of several rifts (Shudofsky et al., 1987; Deichmann, 1992) raises questions the actual rheology of the crust underneath rifts.

Topography around rifts is furthermore affected by surface processes such as erosion that changes the load and thus also the lithospheric deformation and exhumation paths underneath the rift region (Burov and Cloetingh, 1997). Another source of complexity in the topographic response of a continental lithosphere is its long tectonic and thermal history that makes it mechanically heterogeneous, especially in terms of elastic behavior (Tesauro et al., 2009; Cloetingh et al., 2010; Tesauro et al., 2012; Limberger et al., 2018). The outcome of the interactions between these different parameters can be a complex topographic signal, not a simple response to the presence of convective anomalies in the mantle. Our conclusions below must thus be taken with caution, and further studies should address the quantitative effects of the different drivers to see whether the effect of a mantle finger beneath Europe can be separated from the combined effects of other possible, second-order processes.

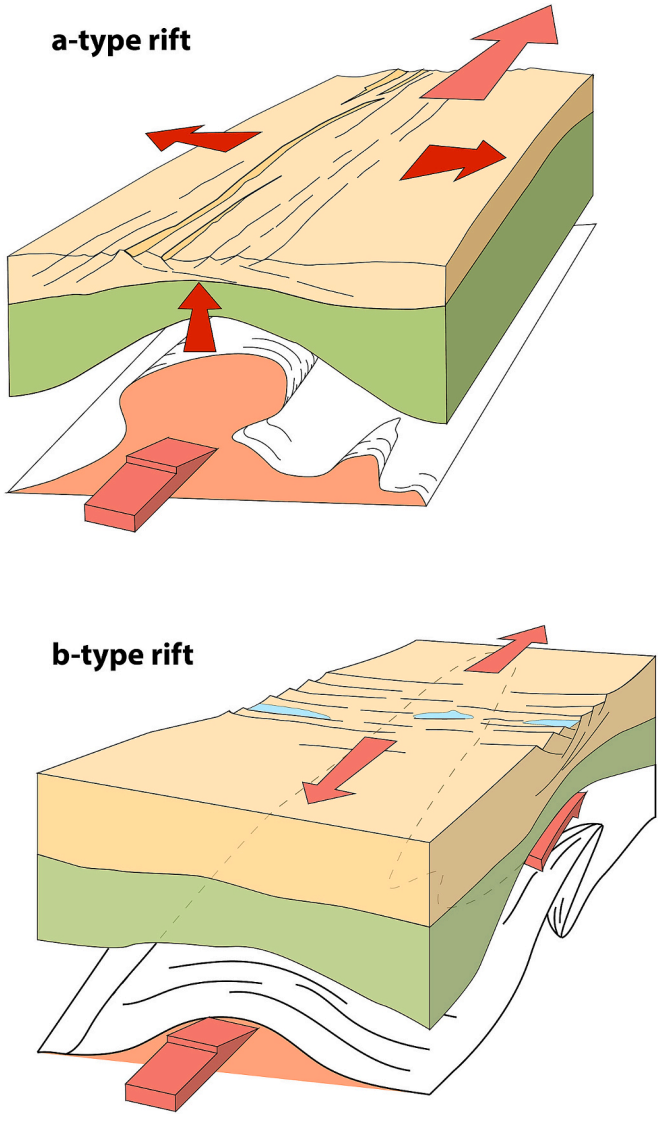

Fig. 19. Conceptual model of an *a-type* rift forming above a low-velocity finger (LVF) in the asthenospheric mantle, compared to a *b-type rift*.

10. Discussion: *a-type* vs *b-type* rifts and a scenario for the evolution of the ECRIS

10.1. Two types of rifts, a-type and b-type

Using the example of the East African Rift and the African plate, we now propose a conceptual model explaining the formation of a rift striking parallel to the absolute motion of the continental plate. The classical conception of rifts is that they strike perpendicular to the direction of mantle flow underneath, like in the original seafloor spreading hypothesis (Hess, 1962), and rifts are most often shown on 2-D sections parallel to the opening direction. The Atlantic rift belongs to this category of rifts that we then call *b-type rifts*. The East African Rift belongs to a different category. It sits on top of a non-isostatic topography anomaly supported by a low-velocity anomaly indicative of a hot mantle upwelling that has the shape of a LVF pointing north, parallel to mantle flow. We designate such rifts as *a-type rifts*. With *a-type* rifts, visualizing the inferred geometry and driving mechanism on a single sketch requires a 3-D view (Fig. 19). The LVF connects the African super plume to the Tethyan subduction zone where slab pull is active, and contributes to the break-up of Africa (Koptev et al., 2019), forming the *b-type rifts* of Aden and Red Sea, which are oriented obliquely or perpendicularly to mantle flow (Faccenna et al., 2013), and eventually evolve into oceanic seafloor. The configuration of the triple junction is controlled by the geometry and kinematics of plate boundaries as shown by analog and numerical modelling (Bellahsen et al., 2003; Koptev et al., 2018).

The Aden and Red Sea rifts formed first as *b-type* rifts and the *a-type* EAR in a second stage above and parallel to the LVF. The anomalous topography and the thin lithosphere above the convective LVF anomaly led to gravitational potential energy gradients able to maintain extension across a new *a-type* rift forming parallel to the flow once the deformation has localized in a lithosphere weakened by preexisting faults that are reactivated, and/or by the thermal anomaly and related magmatism or, along tension cracks on top of a bent continental lithosphere. Such *a-type* rifting is less likely to evolve into oceanic lithosphere than more classical *b-type* rifts, perpendicular or highly oblique to the absolute plate motion and mantle flow, controlled by stronger far-field extensional stresses and higher divergence velocities. In this conceptual model, *a-type* rifts would evolve toward seafloor spreading only after a change in the kinematic boundary conditions turning them into *b-type* rifts.

Our use of *a-type* vs *b-type* is analogous to *a-type* and *b-type* extensional metamorphic domes (Jolivet et al., 2004) that strike either parallel or perpendicular to the main direction of extension. In structural geology, the a-axis and b-axis represent respectively the transport direction (stretching lineation in non-coaxial flow) and the direction perpendicular to transport or shearing (Cloos, 1946; Sander, 1948; Kvale, 1953) in folding. For instance, in this sense, sheath-folds are *a-type* folds, their axes being parallel to the main direction of the simple shear component in non-coaxial flow in high-strain shear zones (Quinquis et al., 1978). This terminology is no longer commonly used for folds, but it is convenient for domes, and we would like to suggest its use for rifts as well.

The two large-scale rift systems reviewed in this contribution enter in

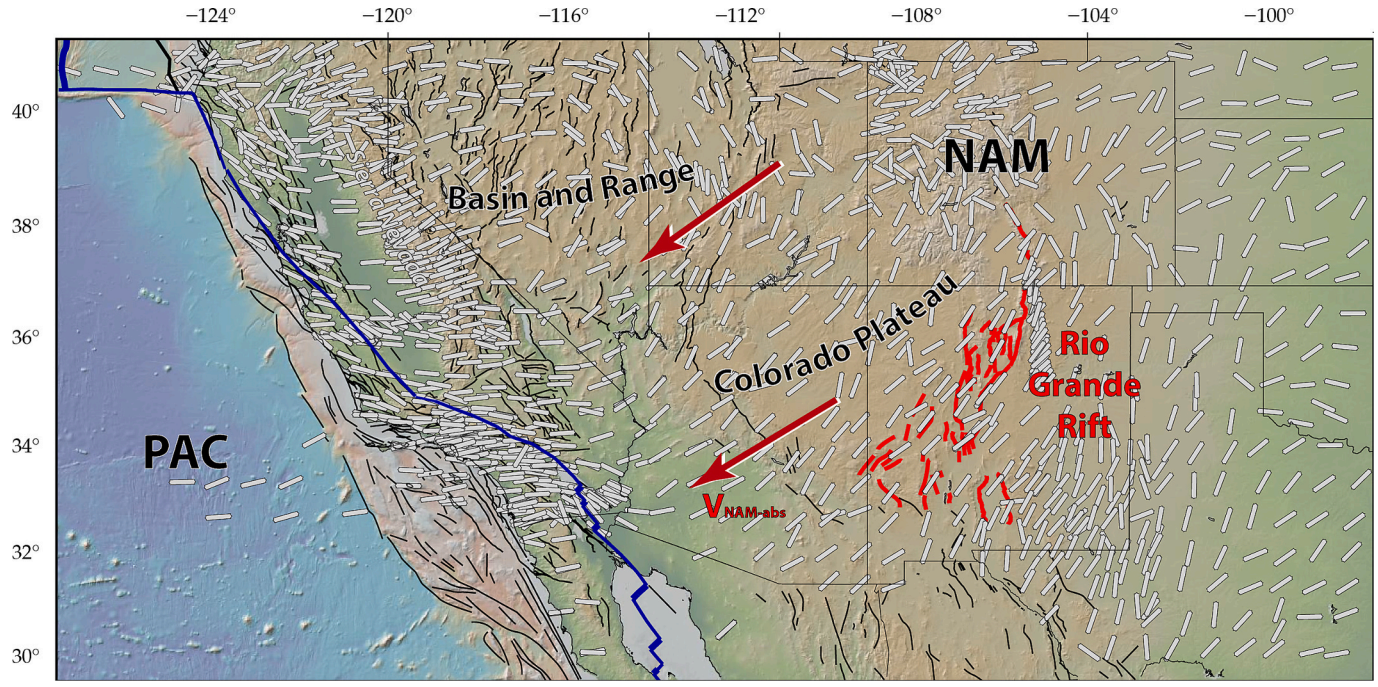

Fig. 20. Shear-wave splitting anisotropy fast orientations (light grey bars) superimposed on the topography and main faults. Rio Grande Rift fault system shown in red. Absolute plate velocities (red arrows) in the reference frame of Kreemer (2009). (For interpretation of the references to colour in this figure legend, the reader is referred to the web version of this article.)

this category, the EAR and the ECRIS (see below), which have not evolved into oceanic lithosphere and accommodate only slow extension rates. The main alkaline volcanic provinces in Western Europe and Africa are either associated with *a-type* rifts or appear isolated within the African continent but associated with S-wave low-velocity anomalies in the upper mantle that fit the general pattern of anomalies striking parallel to the absolute motion.

10.2. Comparison with the Rio Grande and other rift systems

Situated in an entirely different geodynamic setting, the Rio Grande Rift (Figs. 1 and 2) is set within a collapsed mountain belt and yet shows some similarities with the EAR and the ECRIS. Recent seismic tomographic models show a distinct low S-wave velocity anomaly parallel to the rift in the upper mantle (Figs. 20, 21 and 22). This anomaly is a robust feature seen in several tomographic models, RSAVANI (Porritt et al., 2021), SL_14 US (Schmandt and Lin, 2014) and SATONA (Hua et al., 2024). This low-velocity anomaly has the shape of a finger pointing northward and is parallel both to the absolute motion of the North American plate (here in the reference frame of Kreemer, 2009), aligned with the fast direction of SKS-wave splitting by design). The Rio Grande Rift would correspond to our definition of *a-type* rifts. The low-velocity anomaly underneath the rift is however not associated to a deeply rooted plume but seems more related to the flow of asthenosphere due to the toroidal flow underneath the Basin and Range and the behavior of the Farallon slab at depth (Zandt and Humphreys, 2008).

The Baikal Rift strikes parallel to the absolute motion of Eurasia and is associated to a low-velocity anomaly in the upper mantle, prompting the idea that it is partly an active rift (Windley and Allen, 1993). Its pull-apart configuration on the opposite allows interpreting it as a consequence of the India-Asia collision (Molnar and Tapponnier, 1975; Tapponnier et al., 1982) and thus as a passive rift. S-wave anisotropy underneath the Baikal rift shows a drastic difference in the lithosphere and the asthenosphere. The fast azimuthal anisotropy orientation is aligned perpendicular to the rift at 100 km and parallel to the rift at 200 km depth (Lebedev et al., 2006; Schaeffer and Lebedev, 2013; Jolivet et al., 2018a), indicating the passive and active characters of the rift, respectively. In contrast, the Menderes and Corinth Rifts are pure passive rifts striking perpendicular to the absolute motion of Eurasia and result from a recent localization of deformation coeval with the development of the North Anatolian Fault and the retreat of the Hellenic slab. Although the Menderes Rifts developed above a slab tear and thus above low-velocity mantle anomaly (de Boorder et al., 1998; Sternai et al., 2014; Jolivet et al., 2015), they strike perpendicular to this N-S anomaly. The Red Sea and Gulf of Aden rifts are driven both by the deep mantle anomaly and the far field stresses responsible for the separation of Arabia from the main body of Africa and they strike obliquely on the absolute motion and the direction of mantle flow (Fig. 18). They are then partly active and partly passive and thus intermediate between *a-type* and *b-type* rifts.

We then classify rifts based on two different criteria, active vs passive on the one hand (y-axis of Fig. 23) and *a-* vs. *b-type* on the other hand, based on the angle between the rift axis and the direction of mantle flow (x-axis). This diagram shows purely active rifts (EAR, ECRIS, Rio Grande), purely passive ones (Menderes, Corinth), and intermediate ones (Baikal, Red Sea, Gulf of Aden). Their position on the horizontal axis is then broadly determined based on the approximate angle between their strike and the strike of the low-velocity anomaly and/or the absolute velocity of the carrier plate. The EAR, ECRIS and Rio Grande rifts plot in the upper left corner, they are both active and *a-type* rifts. The South Atlantic Rift is oblique on the mantle flow and LVFs, it is strongly influenced by mantle plumes and led to the formation of volcanic margins, thus plotting in the center of the diagram. The Menderes rifts and the Corinth rifts plot in the lower right corner as pure passive *b-type* rifts. The non-magmatic margins of the Atlantic Ocean would result from the oceanization of a passive rift at the latitude of Western Europe would also plot in the lower right corner. Exploring further the dynamics of rifting further would necessitate a 3-D parametric study of the respective roles of far-field stresses and mantle plumes within realistic mantle convection models.

10.3. ECRIS, speculations of the evolution of an a-type rift

The southern part of the Euro-Mediterranean volcanic province,

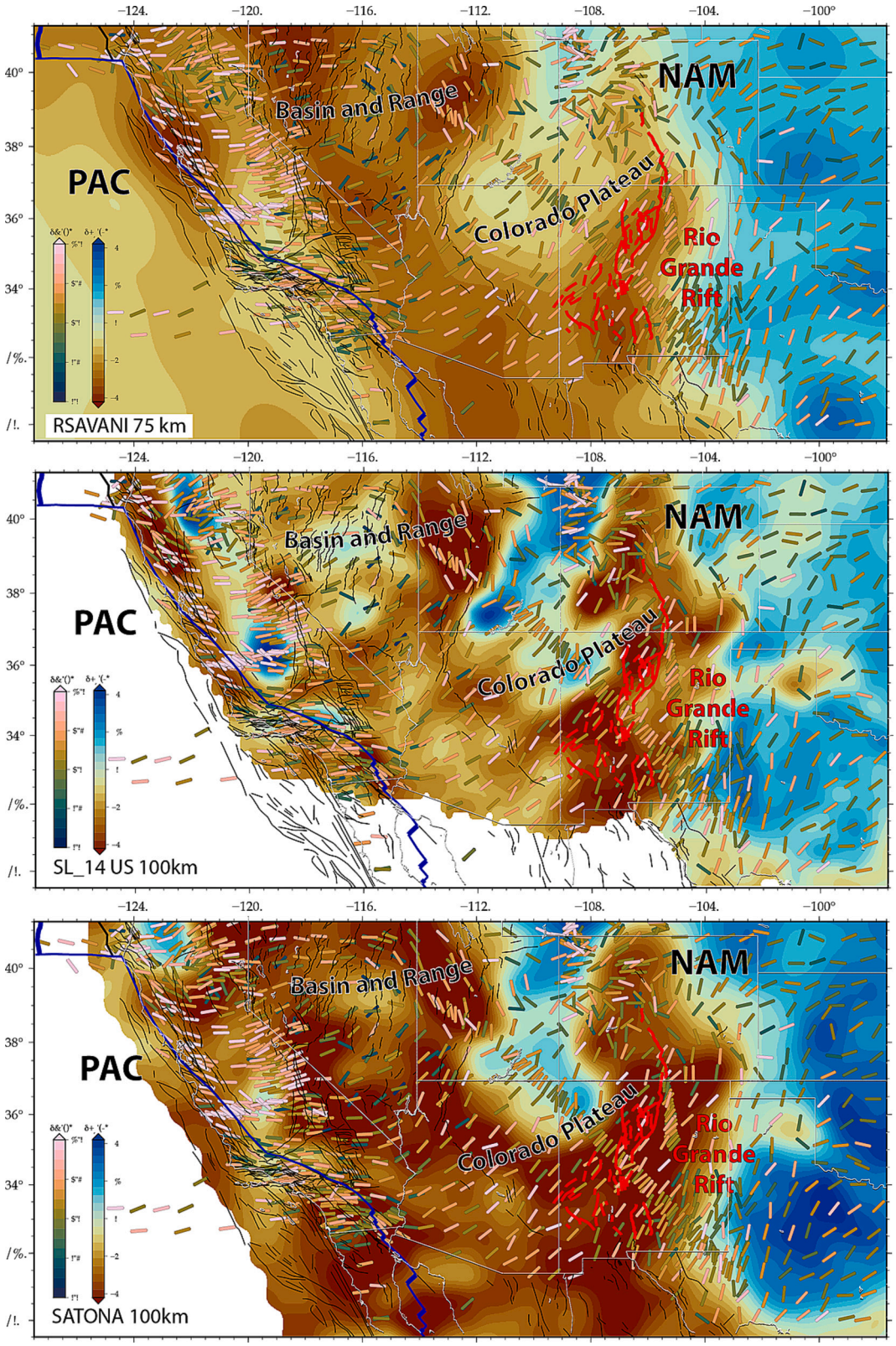

Fig. 21. Shear-wave splitting anisotropy (SKS) superposed to three different S-wave tomographic models and the Rio Grande Rift: RSAVANI (Porritt et al., 2021), SL_14 US (Schmandt and Lin, 2014) and SATONA (Hua et al., 2024).

offshore West Africa, is also associated with a LVF of convective mantle parallel to the absolute motion of Eurasia and Africa and a positive anomaly of non-isostatic topography. The entire province up to the Eger graben in the north is parallel to the absolute motion of Eurasia and is associated with a positive anomaly of residual topography. As a major difference with the East African Rift, no clear migration of magmatism is observed along the strike of this province that has been active since the Late Cretaceous, a much longer period than for East Africa. Piromallo

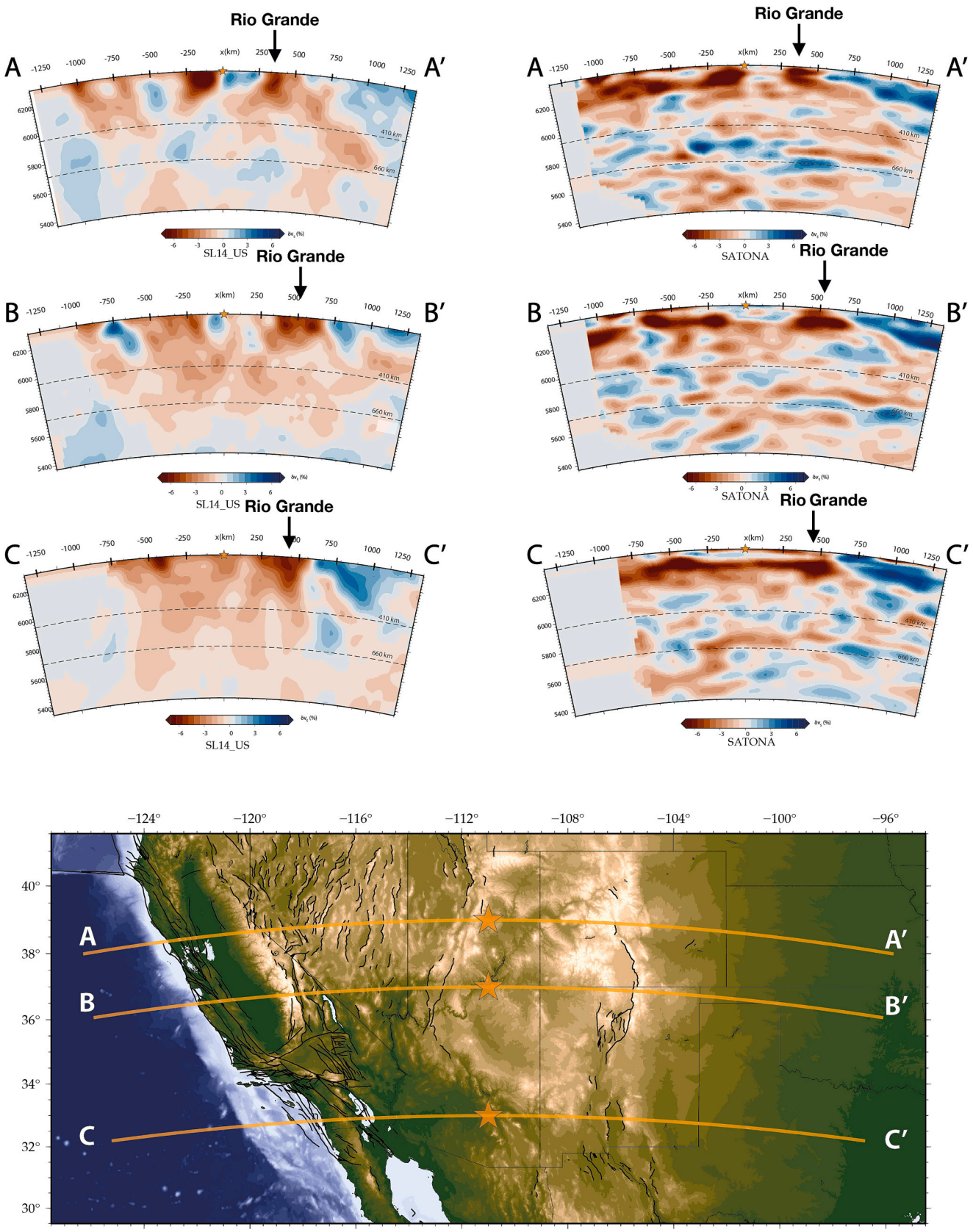

Fig. 22. Vertical cross-sections through two S-wave tomographic models and the position of the Rio Grande Rift: SL_14 US (Schmandt and Lin, 2014) and SATONA (Hua et al., 2024).

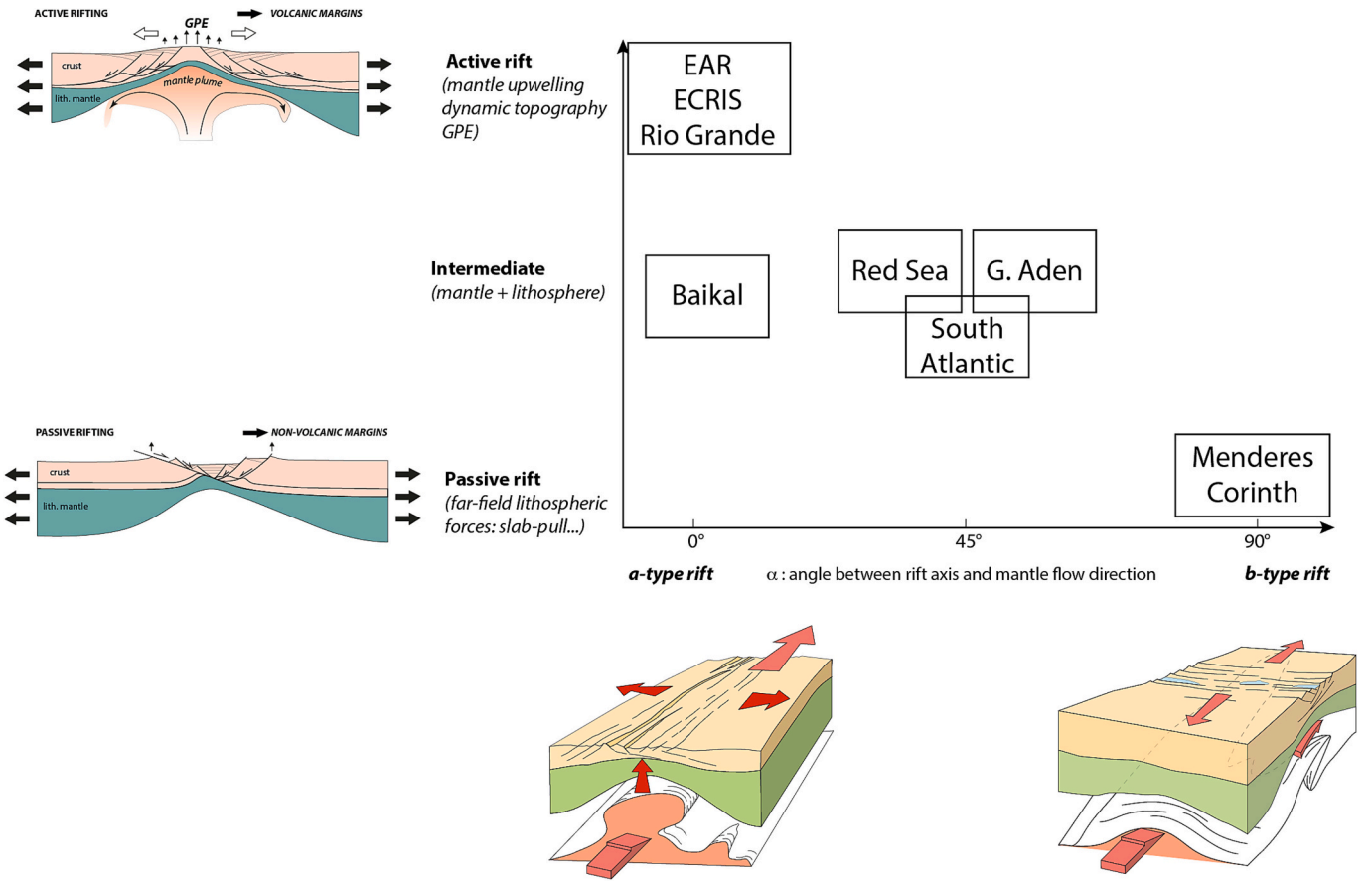

Fig. 23. Various rift systems broadly classified following two parameters (1) the angle between the rift axis and mantle flow direction (*a-type* vs *b-type* rifts) and (2) the role of the active mantle (active vs. passive rifting).

et al. (2008) have discussed the evolution of this magmatic province and proposed that it is controlled by plume material emplaced in the Cretaceous when the region was located further south, later interfering with Mediterranean subductions.

The evolution of the Mediterranean region can be divided in three main stages (Jolivet et al., 2021a) (Fig. 7). The first stage (*Tethyan period*) spans most of the Mesozoic and the beginning of the Cenozoic until ~35 Ma. It corresponds to the opening of the Tethys Ocean and its subsequent progressive closure. The second stage (*Mediterranean period*), from 35 Ma to ~8 Ma, corresponds to the development of back-arc basins above retreating slabs, the typical Mediterranean geodynamic behavior, still active in the eastern Mediterranean region. The third stage (8–0 Ma, *Late Mediterranean period*) sees the resumption of compression in the westernmost Mediterranean (Betics) and its progressive migration toward the southern margin of the Tyrrhenian Sea. This happens after the cessation of slab retreat and may indicate the return to a Tethyan dynamics.

The Euro-Mediterranean magmatic province started to form above the lower mantle low velocity anomalies situated beneath west Africa (Piromallo et al., 2008) (Fig. 16). Early Late Cretaceous subsidence in the Paris Basin may result from the northward motion of the European plate away from the mantle high temperature anomalies. In the Late Cretaceous, the region was under a compressional stress regime which induced the reactivation of the grabens formed previously during the Early Cretaceous within Africa and all the way to the North Sea (Jolivet et al., 2016b). This same period also saw the inception at ~84 Ma of the Pyrenean orogeny by closure of the North Pyrenean system of rifts, which lasted until the Late Eocene with a culmination around 37 Ma (Mouthereau et al., 2014).

We then assume that, during the last stages of the Tethyan period, a LVF of asthenospheric mantle parallel to the absolute motion of Africa and Eurasia before 35 Ma propagated northward and was active during a long period (Fig. 24). The ECRIS developed on top of the resulting non-isostatic topography anomaly with extension perpendicular to the regional compression, partly controlled by the GPE associated with the non-isostatic relief, in a way similar to the East African Rift.

The first stage of rifting, until ~32 Ma, was transtensional and the second stage, until the Early Miocene, purely extensional (Fig. 6). This transition from transtension to extension was coeval with the inception of slab retreat and rifting in the Liguro-Provençal Basin, inducing a flow of asthenosphere toward the retreating slab (Mediterranean Period), as suggested by the seismic anisotropy pattern beneath the Mediterranean region and part of Europe (Barruol and Granet, 2002; Barruol et al., 2004; Lucente et al., 2006; Jolivet et al., 2009) (Fig. 24). This mantle flow also led to the uplift of the Axial Zone of the Pyrenees, the collapse of the eastern Pyrenees and extraction of lower crust in the Valencia and Gulf of Lion rifts (Jolivet et al., 2020; Maillard et al., 2020; Jolivet et al., 2021b) and might have caused the change from transtension to pure extension in the Limagnes and Upper Rhine Graben. This mechanism could also have worked in conjunction with the retreat of the Alpine slab forced by the return flow of the Apennines slab retreat (Vignaroli et al., 2008, 2009). Our proposition here is not incompatible with Merle and Michon' model (Merle and Michon, 2001) model, and links to the role of plumes for rifting suggested by Goes et al. (1999). We thus postulate that, during the Mediterranean period, until the Late Miocene, the mantle flow induced by slab retreat was faster and dominant over the flow associated with the absolute motion of Africa and Eurasia, diverting the flow eastward and westward below the back-arc regions of the Liguro-Provençal, Tyrrhenian and Alboran basins where extension was localized, fragmenting the LVF emplaced earlier (Fig. 24).

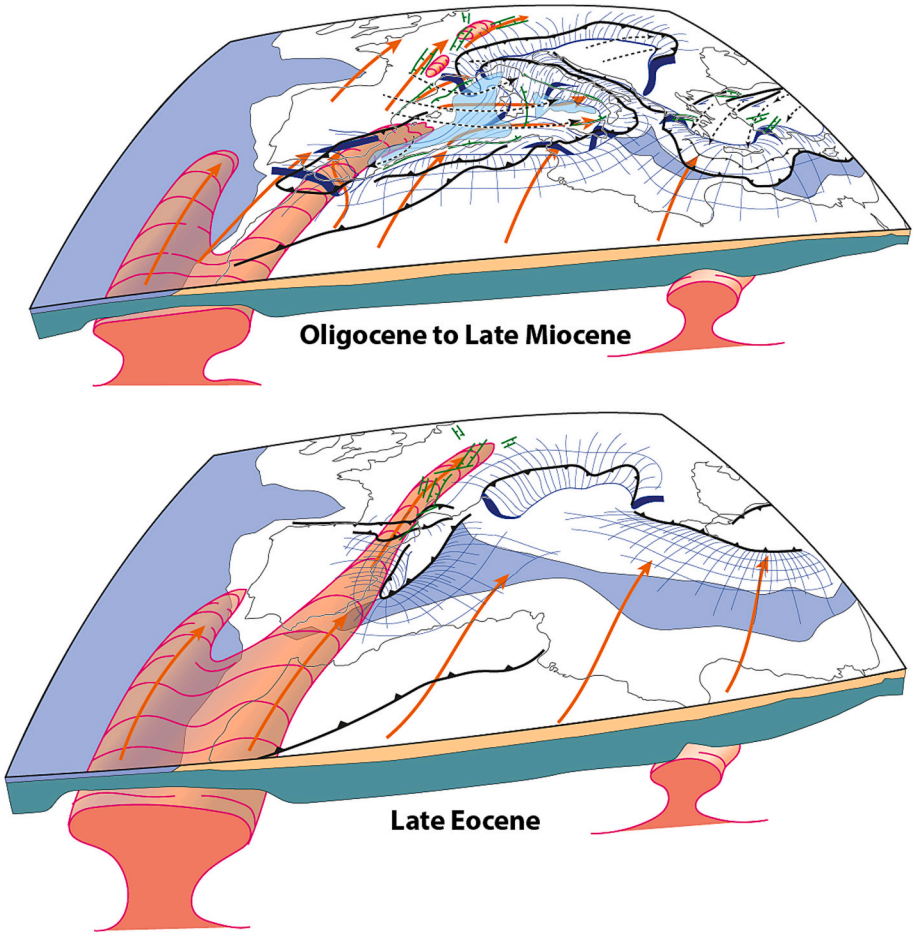

Fig. 24. Schematic mantle flow and evolution of the asthenospheric LVF, formation of the ECRIS and its demise during the Mediterranean period characterized by fast slab retreat in an absolute plate motion framework.

The transition to the Late Mediterranean Period is recorded at ~8 Ma in the Alboran region when the extensional structures of the Betics and Rif were reworked in compression (Deverchère et al., 2003; Jolivet et al., 2006; Janowski et al., 2017; d'Acremont et al., 2020; Lafosse et al., 2020; Haidar et al., 2022). It then propagated eastward until the southern Tyrrhenian Sea, north of Sicily, where it is recorded in the Quaternary (Martinez-Garcia et al., 2013; Medaouri et al., 2014; Do Couto et al., 2016; Martínez-García et al., 2017; Zitellini et al., 2019; d'Acremont et al., 2020; Lafosse et al., 2020). This period is also associated with a new period of alkaline magmatism in the Massif Central. We may then speculate that this period corresponds to the reinitiation of asthenospheric currents mostly dominated by large-scale convection with a north-pointing LVF, a resumption of the Tethyan dynamics after the end of slab retreat. Such a speculative scenario could explain the uplift of the eastern Pyrenees and the southern Massif Central in the Tortonian (Gunnell et al., 2009; Fillon et al., 2020; Calvet et al., 2021).

In this scenario, the ECRIS *a-type* rift shares some similarities with the EAR such as the orientation parallel to the absolute motion of the carrier plate, the slow divergence velocity and association with a volcanic province, formed above a low-velocity finger. Extension is slow and is not likely to give rise to evolve into seafloor spreading.

Another important difference is that volcanism has been active during a longer period, because the plume observed underneath West Africa has impacted the lithosphere earlier than underneath East Africa, and old volcanic centers were transported northward with the absolute motion of Africa and Eurasia. The persistence of magmatism through a long period except for the recess during the Mediterranean period can be due either to a single stationary large LVF or to a succession in time of smaller LVF (Goes et al., 1999), like the evolution of magmatism from North Africa to the Alboran region in the Miocene (Duggen et al., 2009) might suggest. New age data acquisition all along the volcanic province with a higher resolution would be necessary to answer this question.

In this context, the ECRIS was however short-lived, because the geodynamics of Western Europe was strongly influenced by slab retreat and formation of the Mediterranean back-arc basins since the end of the Eocene. Compared to the EAR, low-velocity anomalies beneath the ECRIS are present but patchier, rather a series of more local anomalies resulting from the dispersal of the LVF by asthenospheric flow due to slab retreat. Between 35 and 10–8 Ma, the northward flow carrying the plates was perturbed by the faster flow resulting from the retreat of Mediterranean subducting slabs, ending extension in the ECRIS. After 10 Ma, the end of slab retreat might have allowed the propagation of a new finger of mantle toward the north (Fig. 24).

One of the classical arguments against the active role of a plume during the formation of the ECRIS is the lack of evidence for a clear doming before extension started. More recent thermochronological data however indicate a period of broad uplift and exhumation of the Massif Central first in the early to mid-Cretaceous, between 100 and 150 Ma (Barbarand et al., 2001; Peyaud et al., 2005; Barbarand et al., 2020; Olivetti et al., 2020), which is before the first occurrence of alkaline volcanism in the Euro-Mediterranean region.

The early Cretaceous uplift is further corroborated by the distribution of weathered facies in the Massif Central and its periphery (Wyns et al., 2003; Thiry et al., 2006). We have seen above that the location of this region above high-temperature anomalies before 100 Ma could explain this uplift, before the subsidence during the northward

migration away from these mantle anomalies in the Late Cretaceous, before a new domal uplift at the end of the Cretaceous and Paleogene. The northern part of the Massif Central (Morvan) has also recorded a more recent exhumation in the early Paleogene (Barbarand et al., 2013) and the eastern part shows an additional post-40 Ma uplift and exhumation period attributed to a long-wavelength domal uplift supported by mantle upwelling (Olivetti et al., 2020). Although it remains to be fully documented, recent data suggest that some long-wavelength uplift has happened in the Massif Central at the time of early rifting, further strengthening the plume hypothesis. The partly different behaviors of the Massif Central and Paris Basin in the Late Cretaceous however remain to be explained.

The scenario described above fits many characteristics of the ECRIS, but the near absence of magmatism in the Massif Central during a large part of the rifting event, i.e. between 35 and 25 Ma, and until the Late Miocene in the South Massif Central, must be studied more in depth. However, we may further speculate that the asthenospheric flow induced by slab retreat, which is also recorded underneath the Massif Central by azimuthal seismic anisotropy, has sheared the asthenosphere and the base of the lithosphere viscously and shifted regions of partial melting toward the SE, away from the zone of crustal thinning. The end of slab retreat in the Late Miocene shut down this component of mantle flow and the volcanism could resume its course toward the surface while the Oligocene and Miocene fabric was frozen in the mantle. Such a process would require either that a LVF had persisted in the lower mantle during slab retreat and was then able to feed upper mantle plumes as soon as slab retreat had stopped, or that a new LVF had propagated fast northward as suggested above.

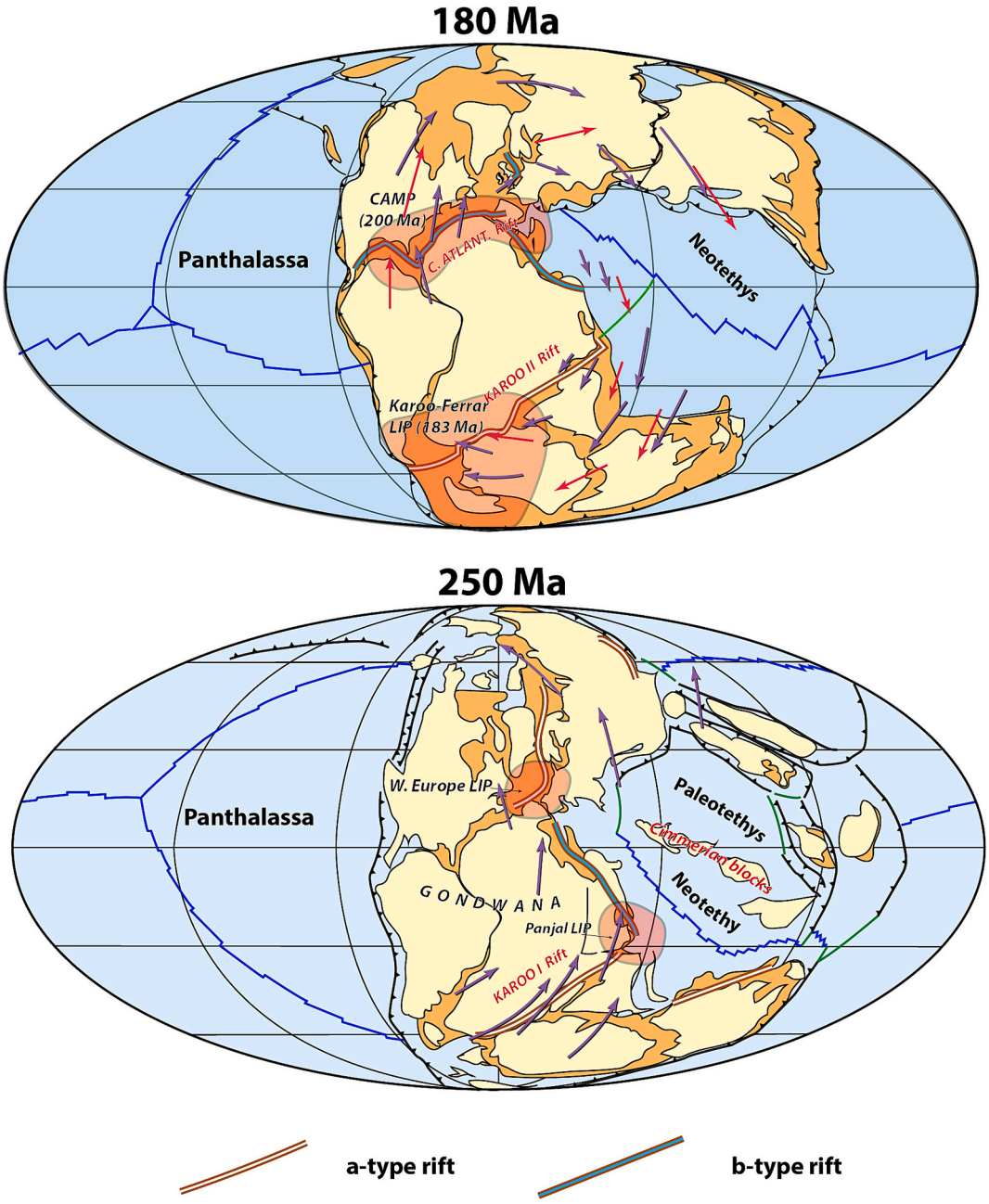

Fig. 25. Two reconstructions at 250 and 180 Ma redrawn from Torsvik and Cocks (2016) and Frizon de Lamotte et al. (2015) showing the *a-type* and *b-type* rifts systems responsible for the break-up of Pangea in the Mesozoic. Absolute motion at the time of reconstructions after Torsvik et al. (2012) (violet) and Müller et al. (2016) (red). (For interpretation of the references to colour in this figure legend, the reader is referred to the web version of this article.)

The concomitance of the initiation of slab retreat and the change of extensional regime in the rift at 32 Ma is also an important question. At the scale of the Mediterranean, the drastic change of the subduction regime toward a strong component of slab retreat is attributed to the hard collision of Africa and Eurasia in the east and possibly also in the west, resulting in the slowing of the absolute motion of the African plate, leaving the Mediterranean region as a land-locked basin where the consequence was slab retreat, sustaining a high rate of subduction (Jolivet and Faccenna, 2000; Bellahsen et al., 2003). For slab retreat to be active, a significant length of oceanic lithosphere must have already sunk in the asthenosphere to provide strong slab pull. The presence of a volcanic arc as soon as the Late Eocene in Provence and Sardinia shows indeed that the slab had already reached 120–150 km before slab retreat started, implying that subduction started at least 12–15 Myr before the first arc volcanism, assuming a slow subduction at 1 cm/yr, thus at 50 Ma or earlier. If the formation of the rift was the consequence of a finger of hot asthenospheric mantle, as we suggest here, then the asthenospheric finger formed while subduction was already active. The question of the interactions between the formation of the finger and the initiation of slab retreat is worth exploring, especially whether the LVF has split the slab in two parts retreating in opposite directions, southeastward and southwestward, which would explain the observed respective timing of ECRIS rifting, back-arc extension and formation of the relief of the Pyrenees.

10.4. A-type, b-type rifts and the fragmentation of Pangea

Considering the fragmentation of Pangea (Fig. 25) suggests that similar processes were already active in the Early Mesozoic. Two reconstructions based on the works of Torsvik and Cocks (2016) and Frizon de Lamotte et al. (2015) show that the opening of the Neotethys was accompanied by the formation of perpendicular rifts. Absolute motions at the time of reconstructions, shown with violet and red arrows on Fig. 25 based on Torsvik et al. (2012) and Müller et al. (2016) suggest that rifts perpendicular to the main Neotethys ocean might be classified as *a-type* rifts. 250 Ma ago, the Neotethys was forming by the separation of the Cimmerian blocks drifting away from the Gondwana margin. A similar process had previously formed the Paleotethys and would then form the Mesogean Ocean in the Late Jurassic with Apulia, or Adria, rifting away from Africa (Jolivet et al., 2016a). The most recent block separating from Africa was the Arabian plate. The rifts formed during these periods evolving into oceanic tracts are *b-type* rifts oblique on the absolute motion, like the present-day Red Sea and Gulf of Aden. Similarly to the formation of the EAR since the Miocene, the North Sea rift system was formed parallel to the absolute motion at the time of reconstruction. The Karoo I rift formed with a low obliquity on the absolute motion and did not lead to oceanisation, and the formation of the India Ocean occurred only some 100 Ma later after a plate reorganization (Roche et al., 2021; Roche and Ringenbach, 2021; Roche et al., 2022). One can then propose that the Karoo I rift system was an *a-type* rift striking parallel to the flow of mantle underneath. The Karoo-Ferrar LIPS then formed at around 180 Ma at a period of slow African plate motion and the Karoo II rift system was at that time an *a-type* rift, before the opening of the Indian Ocean after an acceleration of plate motion (Ruhl et al., 2022). The Central Atlantic would mostly be a *b-type* rift. The Siberian Rift might have formed at the Permian to Triassic transition as an *a-type* rift before it aborted. If these hypotheses were confirmed by further studies, it would suggest that the fragmentation of Pangea was achieved both by *a-type* and *b-type* rifts, *b-type* rifts evolving into oceanic seafloor and *a-type* rifts preparing the lithosphere for later oceanisation. This process, entirely due to the interactions between the convecting mantle and the lithosphere of Pangea, would be an additional process organizing the geometry of fragmentation, beside the reactivation of ancient sutures zones as discussed by Argand (1924) or Buiter and Torsvik (2014), keeping in mind that topographic irregularities of the base of the lithosphere could also interfere with the direction of asthenospheric flow underneath. This conceptual model gives a major role to mantle convection in eroding the base of the lithosphere (Schaeffer and Lebedev, 2013; Celli et al., 2020a), forming corridors oriented parallel to the absolute motion and causing surface uplift, alkaline magmatism, and extension.

11. Conclusions

Based on a compilation of geological constraints, seismic tomographic models, seismic anisotropy measurements and non-isostatic topographic models, we discuss the tectonic evolution of the ECRIS compared to the EAR and we then generalize to other rift systems. Some first order similarities and differences between ECRIS and EAR are noted. The main similarities are the strike of the rifts, both parallel to the direction of absolute motion of their carrier plate, and to the strike of positive anomalies of residual topography. We further characterize the geometry of the rifts by defining two end-member types of situations: *a-type rifts* forming parallel to the mantle flow and absolute motion of the plate versus *b-type rifts*, perpendicular or highly oblique. We then attempt to describe the different rift systems based on two criteria: (1) active vs passive rifting and (2) *a-type* vs. *b-type* rifting. The EAR, ECRIS and Rio Grande rifts are a-type active rifts while the Menderes and Corinth rifts are b-type passive rifts, the Red Sea, Gulf of Aden and Baikal rifts being intermediate for both criteria. *A-type* rifts are less likely to evolve into seafloor spreading than b-type.

We then propose a conceptual model of the tectonic history of the ECRIS involving the propagation toward the north of a low-velocity finger (LVF) of asthenospheric mantle emanating from the deep mantle anomalies underneath Africa. In this conceptual model, the ECRIS is described as an *a-type rift* similar to the East African Rift. It started to form at the end of a period of overall compression in Western Europe parallel to the absolute motion of Africa and Eurasia, and extension was controlled by the GPE caused by the large-scale uplift due to the asthenospheric LVF. It was then perturbed by the vigorous slab retreat in the Mediterranean realm after 35–30 Ma during the Mediterranean period, which induced the formation of *b-type* rifts in the back-arc domain, the recent period being associated to a return to pre-Mediterranean (Tethyan) conditions.

We finally discuss the type of rifts formed during the fragmentation of Pangea based on published reconstructions and we conclude that the continent was broken by a series of successive *b-type* rifts leading to the drifting of continental blocks off the northern margin of Gondwana during the formation of the Neotethys and then the Mesogean Ocean, a process still active today with the separation of Arabia from Africa, while *a-type* rifts formed perpendicular to the main ocean, progressively dislocating Gondwana. These *a-type* rifts later evolved into *b-type* ones, forming the Central Atlantic and Indian Oceans.

This study opens new research pathways on (1) the detailed timing of magmatism in the European-Mediterranean volcanic province to further test the LVF hypothesis, (2) the interactions between the northward propagation of a LVF and its interactions with the Mediterranean subduction in the Eocene, possibly leading to the separation of the slab in two halves retreating in opposite directions, and (3) the geometry of convection underneath Pangea and the distribution of *a-type* and *b-type* rifts leading to the puzzle of present-day plates.

Declaration of competing interest

The authors declare the following financial interests/personal relationships which may be considered as potential competing interests:

Laurent JOLIVET reports financial support was provided by French National Research Agency. Alexander KOPTEV reports financial support was provided by Research Grant Hungary. Thorsten BECKER reports financial support was provided by National Science Foundation. Reports a relationship with that includes:. Has patent pending to. If there are other authors, they declare that they have no known competing financial

interests or personal relationships that could have appeared to influence the work reported in this paper.

Acknowledgments

Several figures have been drawn with base maps extracted from GeoMapApp (Ryan et al., 2009), and we thank seismologists sharing their tomographic models and anisotropy observations. Many of the tomographic cross-sections were plotted with Submachine (Hosseini et al., 2018). Research was funded by the GERESFAULT ANR Project ANR-19-C05-0043. A.K. acknowledge funding and support from the Research Grant Hungary (RGH_L 151351) and the International Lithosphere Program. TWB was partially supported by NSF EAR 192593 and 2045292.

Data availability

No data was used for the research described in the article.

References

Aktug, B., Nocquet, J.M., Cingöz, A., Parsons, B., Erkan, Y., England, P., Lenk, O., Gürdal, M.A., Kilicoglu, A., Akdeniz, H., Tekgül, A., 2009. Deformation of western Turkey from a combination of permanent and campaign GPS data: Limits to block-like behavior. J. Geophys. Res. 114. https://doi.org/10.1029/2008JB006000.

Alvarez, W., 2010. Protracted continental collisions argue for continental plates driven by basal traction. Earth Planet. Sci. Lett. 296, 434–442 doi:410.1016/j.epsl.2010.1005.1030.

Amaru, M., 2007. Global Travel Time Tomography with 3-D Reference Models. Utrecht University, p. 174.

Andriampenomanana, F., Nyblade, A., Durrheim, R., Tugume, F., Nyago, J., 2021. Shear wave splitting measurements in northeastern Uganda and southeastern Tanzania: corroborating evidence for sublithospheric mantle flow beneath East Africa. Geophys. J. Int. 226, 1696–1704 doi: doi: 1610.1093/gji/ggab1167.

Angrand, P., Mouthereau, F., 2021. Evolution of the Alpine orogenic belts in the Western Mediterranean region as resolved by the kinematics of the Europe-Africa diffuse plate boundary. BSGF - Earth Sci. Bull. 192, 42. https://doi.org/10.1051/bsgf/2021031.

Anguita, F., Fernández, C., Márquez, A., León, R., Casillas, R., 2024. The Canary hotspot revisited: Refutation of the Hawaii paradigm and an alternative, plate-based hypothesis. Earth Sci. Rev. https://doi.org/10.1016/j.earscirev.2024.105038.

Argand, E., 1924. La tectonique de l'Asie. In: Proc. 13th Int. Geol. Congr. Brussels 1924, pp. 171–372.

Armijo, R., Meyer, B., King, G.C.P., Rigo, A., Papanastassiou, D., 1996. Quaternary evolution of the Corinth Rift and its implications for the late Cenozoic evolution of the Aegean. Geophys. J. Int. 126, 11–53.

Auer, L., Boschi, L., Becker, T.W., Nissen-Meyer, T., Giardini, D., 2014. Savani: a variable resolution whole-mantle model of anisotropic shear velocity variations based on multiple data sets. J. Geophys. Res. Solid Earth 119, 3006–3034 doi:3010.1002/2013JB010773.

Augustin, N., van der Zwan, F.M., Devey, C.W., Brandsdóttir, B., 2021. 13 million years of seafloor spreading throughout the Red Sea Basin. Nat. Commun. 12, 2427 doi:2410.1038/s41467-41021-22586-41462.

Avallone, A., Briole, P., Agatza-Balodimou, A.M., Billiris, H., Charade, O., Mitsakaki, C., Nercessian, A., Papazissi, K., Paradissis, D., Veis, G., 2004. Analysis of eleven years of deformation measured by GPS in the Corinth Rift Laboratory area. C. R. Geosci. 336, 301–311 doi:310.1016/j.crte.2003.1012.1007.

Bagley, B., Nyblade, A.A., 2013. Seismic anisotropy in eastern Africa, mantle flow, and the African superplume. Geophys. Res. Lett. 40, 1500–1505 doi:1510.1002/grl.50315.

Ball, P.W., White, N.J., Masoud, A., Nixon, S., Hoggard, M.J., Maclennan, J., 2019. Quantifying asthenospheric and lithospheric controls on mafic magmatism across North Africa. Geochem. Geophys. Geosyst. 20. https://doi.org/10.1029/2019GC008303.

Ballmer, M.D., van Hunen, J., Ito, G., Tackley, P.J., Bianco, T.A., 2007. Non-hotspot volcano chains originating from small-scale sublithospheric convection. Geophys. Res. Lett. 34, L23310 doi:23310.21029/22007GL031636.

Barbarand, J., Lucazeau, F., Pagel, M., Séranne, M., 2001. Burial and exhumation history of the south-eastern Massif Central. Tectonophysics 335, 275–290.

Barbarand, J., Quesnel, F., Pagel, M., 2013. Lower Paleogene denudation of Upper cretaceous cover of the Morvan Massif and southeastern Paris Basin (France) revealed by AFT thermochronology and constrained by stratigraphy and paleosurfaces. Tectonophysics 608, 1310–1327 https://doi.org/1310.1016/j.tecto.2013.1306.1011.

Barbarand, J., Préhaud, P., Baudin, F., Missenard, Y., Matray, J.M., François, T., Blaise, T., Pinna-Jamme, R., Gautheron, C., 2020. Where are the limits of Mesozoic intracontinental sedimentary basins of southern France? Mar. Pet. Geol. 121, 104589.

Barruol, G., Granet, M., 2002. A Tertiary asthenospheric flow beneath the southern French Massif Central indicated by upper mantle seismic anisotropy and related to the West Mediterranean extension. Earth Planet. Sci. Lett. 202, 31–47.

Barruol, G., Deschamps, A., Coutant, O., 2004. Mapping Upper mantle anisotropy beneath SE France by SKS splitting: evidence for a Neogene asthenospheric flow induced by the Apulian slab rollback and deflected by the deep Alpine roots. Tectonophysics 394, 125–138.

Bastow, I.D., Pilidou, S., Kendall, J.M., Stuart, G.W., 2010. Melt-induced seismic anisotropy and magma assisted rifting in Ethiopia: evidence from surface waves. Geochem. Geophys. Geosyst. 11, Q0AB05. https://doi.org/10.1029/2010GC003036.

Beccaluva, L., Azzouni-Sekkal, A., Benhallou, A., Bianchini, G., Ellam, R.M., Marzola, M., Siena, F., Stuart, F.M., 2007. Intracratonic asthenosphere upwelling and lithosphere rejuvenation beneath the Hoggar swell (Algeria): evidence from HIMU metasomatised lherzolite mantle xenoliths. Earth Planet. Sci. Lett. 260, 482–494 doi:410.1016/j.epsl.2007.1005.1047.

Becker, T.W., 2017. Superweak asthenosphere in light of upper mantle seismic anisotropy. Geochem. Geophys. Geosyst. 18, 1986–2003 doi:1910.1002/2017GC006886.

Becker, T.W., Boschi, L., 2002. A comparison of tomographic and geodynamic mantle models. Geochem. Geophys. Geosyst. 3, 10.129/2001GC000168.

Becker, T.W., O'Connell, R.J., 2001. Predicting plate velocities with mantle circulation models. Geochem. Geophys. Geosyst. 2. https://doi.org/10.1029/2001GC000171.

Becker, T.W., Lebedev, S., Long, M.D., 2012. On the relationship between azimuthal anisotropy from shear wave splitting and surface wave tomography. J. Geophys. Res. 117, B01306 doi:01310.01029/02011JB008705.

Bellahsen, N., Faccenna, C., Funiciello, F., Daniel, J.M., Jolivet, L., 2003. Why did Arabia separate from Africa, insights from 3-D laboratory experiments. Earth Planet. Sci. Lett. 216, 365–381.

Beniest, A., Koptev, A., Burov, E., 2017. Numerical models for continental break-up: Implications for the South Atlantic. Earth Planet. Sci. Lett. 461, 176–189 https://doi.org/110.1016/j.epsl.2016.1012.1034.

Bergerat, F., 1987. Stress field in the European platform at the time of Africa-Eurasia collision. Tectonics 6, 99–132.

Binder, T., Marks, M.A.W., Gerdes, A., Walter, B.F., Grimmer, J., Beranoaguirre, A., Wenzel, T., Markl, G., 2023. Two distinct age groups of melilitites, foidites, and basanites from the southern central European Volcanic Province reflect lithospheric heterogeneity. Int. J. Earth Sci. 112 (112), 881–905 doi: 110.1007/s00531-00022-02278-y.

Bird, P., 1998. Testing hypotheses on plate-driving mechanisms with global lithosphere models including topography, thermal structure and faults. J. Geophys. Res. 103, 10115–10129.

Bonini, M., Souriot, T., Bocaletti, M., Brun, J.P., 1997. Successive rthogonal and oblique extension episodes in a rift zone: Laboratory experiments with application to the Ethiopian Rift. Tectonics 16, 347–362.

Bonini, M., Corti, G., Innocenti, F., Manetti, P., Mazzarini, F., Abebe, T., Pecskay, Z., 2005. Evolution of the Main Ethiopian Rift in the frame of Afar and Kenya rifts propagation. Tectonics 24, TC1007 doi:1010.1029/2004TC001680.

Boschi, L., Becker, T.W., Steinberger, B., 2007. Mantle plumes: Dynamic models and seismic images. Geochem. Geophys. Geosyst 8, Q10006, 10010.11029/12007GC001733.

Bosworth, W., Guiraud, R., Kessler, L.G., 1999. Late cretaceous (ca. 84 Ma) compressive deformation of the stable platform of Northeast Africa (Egypt): Far-field stress effects of the "Santonian event" and origin of the Syrian arc deformation belt. Geology 27, 633–636.

Bosworth, W., Huchon, P., McClay, K., 2005. The Red Sea and Gulf of Aden Basins. J. Afr. Earth Sci. 43, 334–378 doi:310.1016/j.jafrearsci.2005.1007.1020.

Bourgeois, O., Ford, M., Diraison, M., Carlier, Le, de Veslud, C., Gerbault, M., Pik, R., Ruby, N., Bonnet, S., 2007. Separation of rifting and lithospheric folding signatures in the NW-Alpine foreland. Int. J. Earth Sci. (Geol Rundsch) 96, 1003–1031. DOI 1010.1007/s00531-00007-00202-00532.

Bozkurt, E., 2001. Neotectonics of Turkey - a synthesis. Geodin. Acta 14, 3–30.

Bozkurt, E., Sözbilir, H., 2004. Tectonic evolution of the Gediz Graben: field evidence for an episodic, two-stage extension in western Turkey. Geol. Mag. 141, 63–79.

Bozkurt, E., Satır, M., Bugdaycıoglu, C., 2011. Surprisingly young Rb/Sr ages from the Simav extensional detachment fault zone, northern Menderes Massif, Turkey. J. Geodyn. 52, 406–431.

Briais, J., Guillocheau, F., Lasseur, E., Robin, C., Châteauneuf, J.J., Serrano, O., 2016. Response of a low-subsiding intracratonic basin to long wavelength deformations: the Palaeocene–early Eocene period in the Paris Basin. Solid Earth 7, 205–228 doi:210.5194/se-5197-5205-2016.

Briais, J., Barbarand, J., Lasseur, E., Homberg, C., Allanic, C., Bellahsen, N., Carter, A., Chateauneuf, J.J., Beccaletto, L., Jolivet, L., Ourliac, C., 2025. Tectono-sedimentary evolution of the Upper Rhine Graben (Cretaceous to Oligocene): Large scale deformation to oblique rifting. Tectonophysics submitted.

Briole, P., Rigo, A., Lyon-Caen, H., Ruegg, J.C., Papazissi, K., Mitsataki, C., Badolimou, A., Veis, G., Hatzfeld, D., Deschamps, A., 2000. Active deformation of the Corinth rift, Greece: results from repeated Global Positionning System surveys between 1990 and 1995. J. Geophys. Res. 105, 25605–25626.

Brun, J.P., Wenzel, F., team, E.-D, 1991. Crustal-scale structure of the southern Rhine graben from ECORS-DEKORP seismic reflection data. Geology 19, 758–762.

Brun, J.P., Gutscher, M.A., DEKORP-ECORS teams, 1992. Deep crustal structure of the Rhine Graben from DEKORP-ECORS seismic reflection data: a summary. Tectonophysics 208, 139–147.

Bryan, S.E., Ernst, R.E., 2008. Revised definition of large igneous provinces (LIPs). Earth Sci. Rev. 86, 175–202 https://doi.org/110.1016/j.earscirev.2007.1008.1008.

Bryan, S.E., Ferrari, L., 2013. Large igneous provinces and silicic large igneous provinces: Progress in our understanding over the last 25 years. GSA Bull. 125, 1053–1078 https://doi.org/1010.1130/B30820.30821.
Buck, W.R., 1991. Modes of continental lithospheric extension. J. Geophys. Res. 96, 20,161-120,178.
Buck, W.R., 2004. Consequences of asthenospheric variability on continental rifting. In: Karner, G.D., Taylor, B., Driscoll, N.W., Kholstedt, D.L. (Eds.), Rheology and Deformation of the Lithosphere at Continental Margins. Columbia University Press, pp. 1–31.
Buck, W.R., 2006. The role of magma in the development of the Afro-Arabian system. In: Yirgu, G., Ebinger, C.J., Maguire, P.K.H. (Eds.), The Afar Volcanic Province within the East African Rift System. Special Publications, 259 Geological Society, London, pp. 43–54.
Buiter, S.J.H., Torsvik, T.H., 2014. A review of Wilson Cycle plate margins: a role for mantle plumes in continental break-up along sutures? Gondwana Res. 26 (2014), 627–653 https://doi.org/610.1016/j.gr.2014.1002.1007.
Burke, K., 1996. The African Plate. S. Afr. J. Geol. 99, 341–409.
Burke, K., 2011. Plate Tectonics, the Wilson Cycle, and Mantle Plumes: Geodynamics from the Top. Annu. Rev. Earth Planet. Sci. 39, 1–29. https://doi.org/10.1146/annurev-earth-040809-152521.
Burke, K., Gunnell, Y., 2008. The African erosion surface: a continental-scale synthesis of geomorphology, tectonics and environmental changes over the past 180 million years. AMemoirs Geol. Soc. Am. 201, 66.
Burke, K., Wilson, J.T., 1972. Is the African Plate stationary ? Nature 239, 387–390.
Burke, K., Steinberger, B., Torsvik, T.H., Smethurst, M.A., 2008. Plume Generation zones at the margins of large Low Shear Velocity Provinces on the core–mantle boundary. Earth Planet. Sci. Lett. 265, 49–60. https://doi.org/10.1016/j.epsl.2007.1009.1042.
Burov, E.B., Cloetingh, S., 1997. Erosion and rift dynamics: new thermomechanical aspects of post-rift evolution of extensional basins. Earth Planet. Sci. Lett. 150, 7–27.
Burov, E., Cloetingh, S., 2009. Controls of mantle plumes and lithospheric folding on modes of intraplate continental tectonics: differences and similarities. Geophys. J. Int. 178, 1691–1722 doi: 1610.1111/j.1365-1246X.2009.04238.x.
Burov, E., Gerya, T., 2014. Asymmetric three-dimensional topography over mantle plumes. Nature 513, 85–89. https://doi.org/10.1038/nature13703.
Burov, E., Guillou-Frottier, L., 2005. The plume head–continental lithosphere interaction using a tectonically realistic formulation for the lithosphere. Geophys. J. Int. 161, 469–490.
Calais, E., Lesne, O., Deverchère, J., 1998. Crustal deformation in the Baikal rift from GPS measurements. Geophys. Res. Lett. 25, 4003–4006.
Calais, E., Vergnolle, M., San'kov, V., Lukhnev, A., Miroshnitchenko, A., Amarjargal, S., Déverchère, J., 2003. GPS measurements of crustal deformation in the Baikal-Mongolia area (1994–2002): Implications for current kinematics of Asia. J. Geophys. Res. 108, 2501 doi:2510.1029/2002JB002373.
Calvet, M., Gunnell, Y., Laumonier, B., 2021. Denudation history and palaeogeography of the Pyrenees and their peripheral basins: an 84-million-year geomorphological perspective. Earth Sci. Rev. 215 (2021), 103436 doi: 103410.101016/j.earscirev.102020.103436.
Celli, N.L., Lebedev, S., Schaeffer, A.J., Gaina, C., 2020a. African cratonic lithosphere carved by mantle plumes. Nat. Commun. 11, 92. https://doi.org/10.1038/s41467-41019-13871-41462.
Celli, N.L., Lebedev, S., Schaeffer, A.J., Ravenna, M., Gaina, C., 2020b. The upper mantle beneath the South Atlantic Ocean, South America and Africa from waveform tomography with massive data sets. Geophys. J. Int. 221, 178–204 doi: 110.1093/gji/ggz1574.
Chorowicz, J., 2005. The East African rift system. J. Afr. Earth Sci. 43, 379–410 doi: 310.1016/j.jafrearsci.2005.1007.1019.
Chorowicz, J., Collet, B., Bonavia, F.F., Korme, T., 1994. Northwest to north-northwest extension direction in the Ethiopian rift deduced from the orientation of extension structures and fault-slip analysis. Geol. Soc. Am. Bull. 105, 1560–1570.
Civiero, C., Lebedev, S., Celli, N.L., 2022. A complex mantle plume head below East Africa-Arabia shaped by the lithosphere-asthenosphere boundary topography. Geochem. Geophys. Geosyst. 23, e2022GC010610 https:// doi.org/010610.011029/012022GC010610.
Clerc, C., Jolivet, L., Ringenbach, J.C., 2015. Ductile extension shear zones on the lower crust of a passive margin. Earth Planet. Sci. Lett. 431, 1–7. https://doi.org/10.1016/j.epsl.2015.1008.1038.
Clerc, C., Ringenbach, J.C., Jolivet, L., Ballard, J.F., 2017. Rifted margins: ductile deformation, boudinage, continentward-dipping normal faults and the role of the weak lower crust. Gondwana Res. 53, 20–40. https://doi.org/10.1016/j.gr.2017.1004.1030.
Cloetingh, S.A.P.L., Cornu, T., 2005. Surveys on environmental tectonics. Quat. Sci. Rev. 24, 235–240 doi:210.1016/j.quascirev.2004.1007.1012.
Cloetingh, S.A.P.L., Ziegler, P.A., 2009. TOPO-EUROPE: coupled deep earth – surface processes in Europe. Eur. Rev. 17, 517–540 doi:510.1017/S1062798709000933.
Cloetingh, S., Burov, E.B., Poliakov, A., 1999. Lithosphere folding: primary response to compression ? (from Central Asia to Paris Basin). Tectonics 18, 1064–1083.
Cloetingh, S., Cornua, T., Ziegler, P.A., Beekman, F., Group, a.t.E.T.E.W, 2006. Neotectonics and intraplate continental topography of the northern Alpine Foreland. Earth Sci. Rev. 74, 127–196 doi:110.1016/j.earscirev.2005.1006.1001.
Cloetingh, S., van Wees, J.D., Ziegler, P.A., Lenkey, L., Beekman, F., Tesauro, M., Förster, A., Norden, B., Kaban, M., Hardebol, N., Bonté, D., Genter, A., Guillou-Frottier, L., Ter Voorde, M., Sokoutis, D., Willingshofer, E., Cornu, T., Worum, G., 2010. Lithosphere tectonics and thermo-mechanical properties: an integrated modelling approach for Enhanced Geothermal Systems exploration in Europe. Earth Sci. Rev. 102, 159–206 doi:110.1016/j.earscirev.2010.1005.1003.
Cloetingh, S., Burov, E., Francois, T., 2013. Thermo-mechanical controls on intra-plate deformation and the role of plume-folding interactions in continental topography. Gondwana Res. 24, 815–837 https://doi.org/810.1016/j.gr.2012.1011.1012.
Cloetingh, S., Koptev, A., Lavecchia, A., Kovács, E.J., Beekman, F., 2022. Fingerprinting secondary mantle plumes. Earth Planet. Sci. Lett. 597, 117819 doi: 117810.111016/j.epsl.112022.117819.
Cloos, E., 1946. Lineation, a critical reveiw and annotated bibliography. Geological Society of America Memoir 18.
Colletta, B., Quellec, P.L., Letouzey, J., Moretti, I., 1987. Longitudinal evolution of the Suez rift (Egypt). Tectonophysics 153, 221–233.
Coltice, N., Husson, L., Faccenna, C., Arnould, M., 2019. What drives tectonic plates? Sci. Adv. 5, eaax4295.
Conrad, C.P., Lithgow-Bertelloni, C., 2002. How mantle slabs drive plate tectonics. Science 298.
Corti, G., 2009. Continental rift evolution: from rift initiation to incipient break-up in the Main Ethiopian Rift, East Africa. Earth Sci. Rev. 96, 1–53. https://doi.org/10.1016/j.earscirev.2009.1006.1005.
Corti, G., Cioni, R., Franceschini, Z., Sani, F., Scaillet, S., Molin, P., Isola, I., Mazzarini, F., Brune, S., Keir, D., Erbello, A., Muluneh, A., Illsley-Kemp, F., Glerum, A., 2019. Aborted propagation of the Ethiopian rift caused by linkage with the Kenyan rift. Nat. Commun. 10, 1309 doi: 1310.1038/s41467-41019-09335-41462.
Corti, G., Maestrelli, D., Sani, F., 2022. Large-to local-scale control of pre- existing structures on continental rifting: examples from the Main Ethiopian Rift, East Africa. Front. Earth Sci. 10, 808503 doi: 808510.803389/feart.802022.808503.
Courtillot, V., Jaupart, C., Manighetti, I., Tapponnier, P., Besse, J., 1999. On causal links between flood basalts and continental breakup. Earth Planet. Sci. Lett. 166, 177–195.
Courtillot, V., Davaille, A., Besse, J., Stock, J., 2003. Three distinct types of hotspots in the Earth's mantle. Earth Planet. Sci. Lett. 205, 295–308.
Curry, M.E., van der Beek, P., Huismans, R.S., Wolf, S.G., Muñoz, J.P., 2019. Evolving paleotopography and lithospheric flexure of the Pyrenean Orogen from 3D flexural modeling and basin analysis. Earth Planet. Sci. Lett. 515, 26–37. https://doi.org/10.1016/j.epsl.2019.1003.1009.
Curry, M.E., van der Beek, P., Huismans, R.S., Wolf, S.G., Fillon, C., Muñoz, J.A., 2021. Spatio-temporal patterns of Pyrenean exhumation revealed by inverse thermo-kinematic modeling of a large thermochronologic data set. Geology 49, 738–742 doi: 710.1130/G48687.48681.
d'Acremont, E., Lafosse, M., Rabaute, A., Teurquety, G., Do Couto, D., Ercilla, G., Juan, C., Mercier de Lépinay, B., Lafuerza, S., Galindo-Zaldivar, J., Estrada, F., Vazquez, J.T., Leroy, S., Poort, J., Ammar, A., Gorini, C., 2020. Polyphase tectonic evolution of fore-arc basin related to STEP fault as revealed by seismic reflection data from the Alboran Sea (W- Mediterranean). Tectonics 39, e2019TC005885 doi: 005810.001029/002019TC005885.
Dahm, T., Stiller, M., Mechie, J., Heimann, S., Hensch, M., Woith, H., 2020. Seismological and geophysical signatures of the deep crustal magma systems of the Cenozoic volcanic fields beneath the Eifel, Germany. Geochem. Geophys. Geosyst. 21, e2020GC009062 doi: 009010.001029/002020GC009062.
Davaille, A., Romanowicz, B., 2020. Deflating the LLSVPs: Bundles of mantle thermochemical plumes rather than thick stagnant "piles". Tectonics 39, e2020TC006265 https:// doi.org/006210.001029/002020TC006265.
de Boorder, H., Spakman, W., White, S.H., Wortel, M.J.R., 1998. Late Cenozoic mineralization, orogenic collapse and slab detachment in the European Alpine Belt. Earth Pl. Sc. Lett. 164, 569–575.
Deckers, J., van der Voet, E., 2018. A review on the structural styles of deformation during late cretaceous and Paleocene tectonic phases in the southern North Sea area. J. Geodyn. 115, 1–9. https://doi.org/10.1016/j.jog.2018.1001.1005.
Deichmann, N., 1992. Structural and rheological implications of lower-crustal earthquakes below northern Switzerland. Phys. Earth Planet. Inter. 69, 270–280.
Deverchère, J., Yelles, K., Calais, E., 2003. Active deformation along the Algerian margin (MARADJA cruise): framework of the May 21 2003 Mw-6.8 Boumerdes earthquke. Eos. Trans. AGU 84, S42E–0216.
Dewey, J.F., 1988. Extensional collapse of orogens. Tectonics 7, 1123–1139.
Dèzes, P., Schmid, S.M., Ziegler, P.A., 2004. Evolution of the European Cenozoic Rift System: interaction of the Alpine and Pyrenean orogens with their foreland lithosphere. Tectonophysics 389, 1–33.
Do Couto, D., Gorini, C., Jolivet, L., Lebret, N., Augier, R., Gumiaux, C., d'Acremont, E., Ammar, A., Jabour, H., Auxietre, J.L., 2016. Tectonic and stratigraphic evolution of the Western Alboran Sea Basin in the last 25 Myrs. Tectonophysics. https://doi.org/10.1016/j.tecto.2016.1003.1020.
Doubrovine, P., Steinberger, B., Torsvik, T.H., 2012. Absolute plate motions in a reference frame defined by moving hotspots in the Pacific, Atlantic and Indian oceans. J. Geophys. Res. 117, B09101 doi:09110.01029/02011JB009072.
Duggen, S., Hoernle, K.A., Hauff, F., Klügel, A., Bouabdellah, M., Thirlwall, M.F., 2009. Flow of Canary mantle plume material through a subcontinental lithospheric corridor beneath Africa to the Mediterranean. Geology 37, 283–286 doi:210.1130/G25426A.25421.
Dziewonski, A.M., Woodhouse, J.H., 1987. Global images of the Earth's interior. Science 236, 37–48.
Ebinger, C.J., 1989. Tectonic development of the western branch of the East African rift system. Geol. Soc. Am. Bull. 101, 885–903.
Ebinger, C., 2005. The Bullerwell Lecture: continental break-up, the East African perspective. Astron. Geophys. 46, 16–12.
Ebinger, C., 2012. Evolution of the Cenozoic East African rift system: Cratons, plumes, and continental breakup. In: Roberts, D.G., Bally, A.W. (Eds.), Regional Geology and Tectonics: Phanerozoic Rift Systems and Sedimentary Basins. Elsevier, Amsterdam, pp. 133–162.

Ebinger, C.J., Sleep, N.H., 1998. Cenozoic magmatism throughout East Africa resulting from impact of a single plume. Nature 395, 788–791.
Ebinger, C.J., Keir, D., Bastow, I.D., Whaler, K., Hammond, J.O.S., Ayele, A., Miller, M.S., Tiberi, C., Hautot, S., 2017. Crustal structure of active deformation zones in Africa: Implications for global crustal processes. Tectonics 36. https://doi.org/10.1002/2017TC004526.
Ebinger, C.J., Reiss, M.C., Bastow, I., Karanja, M.M., 2024. Shallow sources of upper mantle seismic anisotropy in East Africa. Earth Planet. Sci. Lett. 625, 118488 doi: 118410.111016/j.epsl.112023.118488.
Edel, J.B., Schulmann, K., Rotstein, Y., 2007. The Variscan tectonic inheritance of the Upper Rhine Graben: evidence of reactivations in the Lias, Late Eocene–Oligocene up to the recent. Int. J. Earth Sci. (Geol Rundsch) 96, 305–325. DOI 310.1007/s00531-00006-00092-00538.
Ershov, A.V., Nikishin, A.M., 2004. Recent geodynamics of the Caucasus–Arabia–East Africa Region. Geotectonics. Eng. Trans. 38, 123–136.
Faccenna, C., Mattei, M., Funiciello, R., Jolivet, L., 1997. Styles of back-arc extension in the Central Mediterranean. Terra Nova 9, 126–130.
Faccenna, C., Becker, T.W., Lallemand, S., Lagabrielle, Y., Funiciello, F., Piromallo, C., 2010. Subduction-triggered magmatic pulses: a new class of plumes? Earth Planet. Sci. Lett. 299, 54–68. https://doi.org/10.1016/j.epsl.2010.1008.1012.
Faccenna, C., Becker, T.W., Jolivet, L., Keskin, M., 2013. Mantle convection in the Middle East: Reconciling Afar upwelling, Arabia indentation and Aegean trench rollback. Earth Planet. Sci. Lett. 375, 254–269 dx.doi.org/210.1016/j.epsl.2013.1005.1043.
Faccenna, C., Glišović, P., Forte, A., Becker, T.W., Garzanti, E., Sembroni, A., Gvirtzman, Z., 2019. Role of dynamic topography in sustaining the Nile River over 30 million years. Nat. Geosci. 12, 1012–1017 doi: 1010.1038/s41561-41019-40472-x.
Fillon, C., Mouthereau, F., Calassou, S., Pik, R., Bellahsen, R., Gautheron, C., Stockli, D., Brichau, S., Daril, N., Mouchené, M., van der Beek, P., 2020. Post-orogenic exhumation in the western Pyrenees: evidence for extension driven by pre-orogenic inheritance. J. Geol. Soc. Lond. 178 jsg2020-2079. doi: 2010.1144/jgs2020-2079.
Fitton, J.G., Dunlop, H.M., 1985. The Cameroon line, West Africa, and its bearing on the origin of oceanic and continental alkali basalt. Earth Planet. Sci. Lett. 72, 23–38.
Ford, M., Duchêne, S., Gasquet, D., Vanderhaeghe, O., 2006. Two-phase orogenic convergence in the external and internal SW Alps. J. Geol. Soc. Lond. 163, 815–826.
Ford, M., Carlier, Le, de Veslud, C., Bourgeois, O., 2007. Kinematic and geometric analysis of fault-related folds in a rift setting: the Dannemarie basin, Upper Rhine Graben, France. J. Struct. Geol. 29, 1811–1830 doi:1810.1016/j.jsg.2007.1808.1001.
François, T., Koptev, A., Cloetingh, S., Burov, E., Gerya, T., 2018. Plume-lithosphere interactions in rifted margin tectonic settings: Inferences from thermo-mechanical modelling. Tectononophysics 746, 138–154. https://doi.org/10.1016/j.tecto.2017.11.027.
François, T., Barbarand, J., Wyns, R., 2020. Lower cretaceous inversion of the European Variscan basement: record from the Vendée and Limousin (France). Int. J. Earth Sci. 109, 1837–1852.
Franke, D., 2013. Rifting, lithosphere breakup and volcanism: Comparison of magma-poor and volcanic rifted margins. Mar. Pet. Geol. 43, 63–87. https://doi.org/10.1016/j.marpetgeo.2012.1011.1003.
French, S.W., Romanowicz, B.A., 2014. Whole-mantle radially anisotropic shear velocity structure from spectral-element waveform tomography. Geophys. J. Int. 199, 1303–1327 doi: 1310.1093/gji/ggu1334.
French, S.W., Romanowicz, B., 2015. Broad plumes rooted at the base of the Earth's mantle beneath major hotspots. Nature 525, 95–101 doi:110.1038/nature14876.
French, S., Lekic, V., Romanowicz, B., 2013. Waveform Tomography reveals Channeled Flow at the Base of the Oceanic Asthenosphere. Science 342, 227–230. DOI: 210.1126/science.1241514.
Frizon de Lamotte, D., Fourdan, B., Leleu, S., Leparmentier, F., de Clarens, P., 2015. Style of rifting and the stages of Pangea breakup. Tectonics 34, 1009–1029 doi: 1010.1002/2014TC003760.
Fullea, J., Lebedev, S., Agius, M.R., Jones, A.G., Afonso, J.C., 2012. Lithospheric structure in the Baikal–central Mongolia region from integrated geophysical-petrological inversion of surface-wave data and topographic elevation. Geochem. Geophys. Geosyst. 13, Q0AK09. https://doi.org/10.1029/2012GC004138.
Geoffroy, L., Burov, E.B., Werner, P., 2015. Volcanic passive margins: another way to break up continents. Sci. Rep. 5, 14828 |. DOI: 14810.11038/srep14828.
George, R., Rogers, N., Kelley, S., 1998. Earliest magmatism in Ethiopia: evidence for two mantle plumes in one flood basalt province. Geology 26, 923–926 https://doi.org/910.1130/00917613(1998)1026<0923:EMIEEF>1132.1133.CO;1132.
Gessner, K., Markwitz, V., Güngör, T., 2018. Crustal fluid flow in hot continental extension: tectonic framework of geothermal areas and mineral deposits in western Anatolia. Geol. Soc. Lond. Spec. Publ. 453, 289–311.
Ghosh, A., Holt, W.E., Wen, L., Haines, A.J., Flesch, L.M., 2008. Joint modeling of lithosphere and mantle dynamics elucidating lithosphere-mantle coupling. Geophys. Res. Lett. 35, L16309 doi:16310.11029/12008GL034365.
Goes, S., Spakman, W., Bijwaard, H., 1999. A lower mantle source for central European Volcanism. Science 286, 1928–1931.
Granet, M., Wilson, M., Achauer, U., 1995. Imaging a mantle plume beneath the French Massif Central. Earth Planet. Sci. Lett. 136, 281–296.
Guillocheau, F., Robin, C., Allemand, P., Bourquin, S., Brault, N., Dromart, G., Freidenberg, R., Garci, J.P., Gaulier, J.M., Gaumet, F., Grosdoy, B., Hanot, F., Le Strat, P., Mettraux, M., Nalpas, T., Prijac, C., Rigollet, C., Serrano, O., Grandjean, G., 2000. Meso-cenozoic geodynamic evolution of the Paris basin, stratigraphic constraints. Geodynam. Acta 13, 189–246.
Guillocheau, F., Simon, B., Baby, G., Bessin, P., Robin, C., Dauteuil, O., 2018. Planation surfaces as a record of mantle dynamics: the case example of Africa. Gondwana Res. 53, 82–98. https://doi.org/10.1016/j.gr.2017.1005.1015.
Guiraud, R., Bosworth, W., Thierry, J., Delplanque, A., 2005. Phanerozoic geological evolution of Northern and Central Africa: an overview. J. Afr. Earth Sci. 43, 83–143.
Gunnell, Y., Calvet, M., Brichau, S., Carter, A., Aguilar, J.P., Zeyen, H., 2009. Low long-term erosion rates in high-energy mountain belts: Insights from thermo- and biochronology in the Eastern Pyrenees. Earth Planet. Sci. Lett. 278, 208–218 doi: 210.1016/j.epsl.2008.1012.1004.
Hager, B.H., O'Connell, R.J., 1981. A simple global model of plate dynamics and mantle convection. J. Geophys. Res. 86, 4843–4867.
Haidar, S., Déverchère, J., Graindorge, D., Arab, M., Medaouri, M., Klingelhoefer, F., 2022. Back-arc dynamics controlled by slab rollback and tearing: a reappraisal of seafloor spreading and kinematic evolution of the Eastern Algero-Balearic basin (western Mediterranean) in;the Middle-late Miocene. Tectonics 41, e2021TC006877 doi: 006810.001029/002021TC006877.
Halldórsson, S.A., Hilton, D.R., Scarsi, P., Abebe, T., Hopp, J., 2014. A common mantle plume source beneath the entire East African Rift System revealed by coupled helium-neon systematics. Geophys. Res. Lett. 41, 2304–2311 doi:2310.1002/2014GL059424.
Hansen, S.E., Nyblade, A.A., Benoit, M.H., 2012. Mantle structure beneath Africa and Arabia from adaptively parameterized P-wave tomography: Implications for the origin of Cenozoic Afro-Arabian tectonism. Earth Planet. Sci. Lett. 319-320, 23–34. https://doi.org/10.1016/j.epsl.2011.1012.1023.
Hassan, R., Williams, S.E., Gurnis, M., Müller, D., 2020. East African topography and volcanism explained by a single, migrating plume. Geosci. Front. 11 (2020), 1669–1680 doi: 1610.1016/j.gsf.2020.1601.1003.
Hess, H.H., 1962. History of ocean basins, Petrologic Studies: a volume in honor of A. F. Buddington. Geol. Soc. Am. 599–620.
Hippolyte, J.C., Nury, D., Angelier, J., Bergerat, F., 1991. Relations entre tectonique extensive et sédimentation continentale: exemple des bassins oligocènes de Marseille et de Basse-Provence. Bull. Soc. géol. France 162, 1083–1094.
Hippolyte, J.C., Angelier, J., Bergerat, F., Nury, D., Guieu, G., 1993. Tectonic-stratigraphic record of paleostress time changes in the Oligocene basins of the Provence, southern France. Tectonophysics 226, 15–35.
Hoïnk, T., Lenardic, A., 2010. Long wavelength convection, Poiseuille–Couette flow in the low-viscosity asthenosphere and the strength of plate margins. Geophys. J. Int. 180, 23–33. https://doi.org/10.1111/j.1365-1246X.2009.04404.x.
Hoïnk, T., Jellinek, A.M., Lenardic, A., 2011. Viscous coupling at the lithosphere-asthenosphere boundary. Geochem. Geophys. Geosyst. 12, Q0AK02. https://doi.org/10.1029/2011GC003698.
Holtzman, B.K., Kendall, J.M., 2010. Organized melt, seismic anisotropy, and plate boundary lubrication. Geochem. Geophys. Geosyst. 11, Q0AB06. https://doi.org/10.1029/2010GC003296.
Hosseini, K., Matthews, K.J., Sigloch, K., Shephard, G.E., Domeier, M., Tsekhmistrenko, M., 2018. SubMachine: Web-based tools for exploring seismic tomography and other models of Earth's deep interior. Geochem. Geophys. Geosyst. 19, 1464–1483 doi: 1410. 1029/2018GC007431.
Hoyer, P.A., Haase, K.M., Regelous, M., O'Coonor, J.M., Homrighausen, S., Geissler, W. H., Jokat, W., 2022. Mantle plume and rift-related volcanism during the evolution of the Rio Grande Rise. Commun. Earth Environ. 3, 18. https://doi.org/10.1038/s43247-43022-00349-43241.
Hua, J., Fischer, K.M., Gazel, E., Parmentier, E.M., Hirth, G., 2023. Long-distance asthenospheric transport of plume-influenced mantle from Afar to Anatolia. Geochem. Geophys. Geosyst. 24, e2022GC010605 https:// doi.org/010610.011029/012022GC010605.
Hua, J., Grand, S., Becker, T., Janiszewski, H., Liu, C., journal., T.i.a.p.i.h.n.b.p.r.b.a, 2024. Mobilization and thinning of cratonic lithosphere by a lower mantle slab. preprint, not reviewed. https://doi.org/10.21203/rs.21203.rs-3254038/v3254031.
Huang, J., Zhong, S., van Hunen, J., 2003. Controls on sublithospheric small-scale convection. J. Geophys. Res. Solid Earth 108 (B8), 2405 doi:2410.1029/2003JB002456.
Huismans, R.S., Podladchikov, Y.Y., Cloetingh, S., 2001. Transition from passive to active rifting: relative importance of asthenospheric doming and passive extension of the lithosphere. J. Geophys. Res. 106, 11271–11291.
Humphreys, E.D., Coblentz, D.D., 2007. North American dynamics and western US tectonics. Rev. Geophys. 45, RG3001 doi:3010.1029/2005RG000181.
Illies, J.H., 1972. The Rhine graben rift system-plate tectonics and transform faulting. Geophys. Surv. 1, 27–60.
Illies, H., 1975. Intraplate tectonics in stable Europe as related to plate tectonics in the Alpine system. Geol. Rundsch. 64, 677–699.
Illies, J.H., 1978. Two stages Rhinegraben rifting. In: Ramberg, I.B., Neumann, E.R. (Eds.), Tectonics and Geophysics of Continental riftsReidel Publishing Company. Holland, Dordrecht, pp. 63–71.
Illies, J.H., Greiner, G., 1978. Rhine Graben and the Alpine system. Geol. Soc. Am. Bull. 89, 770–782.
Issachar, R., Haas, P., Augustin, N., Ebbing, J., 2024. Rift and plume: a discussion on active and passive rifting mechanisms in the Afro-Arabian rift based on synthesis of geophysical data. Solid Earth 15, 807–826 doi: 810.5194/se-5115-5807-2024.
Ivanov, A.V., Demonterova, E.I., He, H., Perepelov, A.B., Travin, A.V., Lebedev, V.A., 2015. Volcanism in the Baikal rift: 40 years of active-versus-passive model discussion. Earth Sci. Rev. 148, 18–43. https://doi.org/10.1016/j.earscirev.2015.1005.1011.
Janowski, M., Loget, N., Gautheron, C., Barbarand, J., Bellahsen, N., Van Den Driessche, J., Babault, J., Meyer, B., 2017. Neogene exhumation and relief evolution

in the eastern Betics (SE Spain): Insights from the Sierra de Gador. Terra Nova 1-7. https://doi.org/10.1111/ter.12252.
Janssen, M.E., Stephenson, R.A., Cloetingh, S., 1995. Temporal and spatial correlations between changes in plate motions and the evolution of rifted basins in Africa. GSA Bull. 107, 1317–1332 doi: https://doi.org/1310.1130/0016-7606(1995)1107<1317:TASCBC>1312.1313.CO;1312.
Jolivet, L., Brun, J.P., 2010. Cenozoic geodynamic evolution of the Aegean region. Int. J. Earth Sci. 99, 109–138. DOI: 110.1007/s00531-00008-00366-00534.
Jolivet, L., Faccenna, C., 2000. Mediterranean extension and the Africa-Eurasia collision. Tectonics 19, 1095–1106 doi:1010.1029/2000TC900018.
Jolivet, L., Famin, V., Mehl, C., Parra, T., Aubourg, C., Hébert, R., Philippot, P., 2004. Strain localization during crustal-scale boudinage to form extensional metamorphic domes in the Aegean Sea. In: Whitney, D.L., Teyssier, C., Siddoway, C.S. (Eds.), Gneiss Domes in Orogeny.Geological Society of America Special Paper 380. Geological Society of America, Boulder, Colorado, pp. 185–210.
Jolivet, L., Augier, R., Robin, C., Suc, J.P., Rouchy, J.M., 2006. The geodynamic context of the Messinian salinity crisis. Sediment. Geol. 188-189, 9–33.
Jolivet, L., Faccenna, C., Piromallo, C., 2009. From Mantle to crust: stretching the Mediterranean. Earth Planet. Sci. Lett. 285, 198–209 doi:110.1016/j.epsl.2009.1006.1017.
Jolivet, L., Lecomte, E., Huet, B., Denèle, Y., Lacombe, O., Labrousse, L., Le Pourhiet, L., Mehl, C., 2010. The North cycladic detachment system. Earth Planet. Sci. Lett. 289, 87–104 doi:110.1016/j.epsl.2009.1010.1032.
Jolivet, L., Faccenna, C., Huet, B., Labrousse, L., Le Pourhiet, L., Lacombe, O., Lecomte, E., Burov, E., Denèle, Y., Brun, J.P., Philippon, M., Paul, A., Salaün, G., Karabulut, H., Piromallo, C., Monié, P., Gueydan, F., Okay, A.I., Oberhänsli, R., Pourteau, A., Augier, R., Gadenne, L., Driussi, O., 2013. Aegean tectonics: Strain localisation, slab tearing and trench retreat. Tectonophysics 597–598, 1–33. https://doi.org/10.1016/j.tecto.2012.06.011.
Jolivet, L., Menant, A., Sternai, P., Rabillard, A., Arbaret, L., Augier, R., Laurent, V., Beaudoin, A., Grasemann, B., Huet, B., Labrousse, L., Le Pourhiet, L., 2015. The geological signature of a slab tear below the Aegean. Tectonophysics 659 (166–182), 166–182 doi:110.1016/j.tecto.2015.1008.1004.
Jolivet, L., Faccenna, C., Agard, P., Frizon de Lamotte, D., Menant, A., Sternai, P., Guillocheau, F., 2016a. Neo-Tethys geodynamics and mantle convection: from extension to compression in Africa and a conceptual model for obduction. Can. J. Earth Sci. 53, 1190–1204.
Jolivet, L., Faccenna, C., Becker, T.W., 2016b. Mantle Flow and Deforming Continents, the Tethys Realm. AGU Fall Meeting, San Francisco, pp. T53B–07.
Jolivet, L., Faccenna, C., Tesauro, M., Sternai, P., Bouilhol, P., 2018a. Mantle flow and deforming continents: From India-Asia convergence to Pacific subduction. Tectonics 37. https://doi.org/10.1029/2018TC005036.
Jolivet, L., Menant, A., Clerc, C., Sternai, P., Bellahsen, N., Leroy, S., Pik, R., Stab, M., Faccenna, C., Gorini, C., 2018b. Extensional crustal tectonics and crust-mantle coupling, a view from the geological record. Earth Sci. Rev. 185, 1187–1209 doi:1110.1016/j.earscirev.2018.1109.1010.
Jolivet, L., Romagny, A., Gorini, C., Maillard, A., Thinon, I., Couëffé, R., Ducoux, M., Séranne, M., 2020. Fast dismantling of a mountain belt by mantle flow: late-orogenic evolution of Pyrenees and Liguro-Provençal rifting. Tectonophysics 776, 228312 doi.org/228310.221016/j.tecto.222019.228312.
Jolivet, L., Baudin, T., Calassou, S., Chevrot, S., Ford, M., Issautier, B., Lasseur, E., Masini, E., Manatschal, G., Mouthereau, F., Thinon, I., Vidal, O., 2021a. Geodynamic evolution of a wide plate boundary in the Western Mediterranean, near-field versus far-field interactions. BSGF - Earth Sci. Bull. 192, 48. https://doi.org/10.1051/bsgf/2021043.
Jolivet, L., Menant, A., Roche, V., Le Pourhiet, L., Maillard, A., Augier, R., Do Couto, D., Gorini, C., Thinon, I., Canva, A., 2021b. Transfer zones in Mediterranean back-arc regions and tear faults. BSGF - Earth Sci. Bull. 192, 11. https://doi.org/10.1051/bsgf/2021006.
Jourdon, A., Le Pourhiet, L., Mouthereau, F., May, D., 2020. Modes of propagation of continental breakup and associated oblique rift structures. J. Geophys. Res. Solid Earth 125, e2020JB019906.
Kalifi, A., Sorrel, P., Leloup, P.H., Galy, A., Spina, V., Huet, B., Russo, S., Pittet, B., Rubino, J.L., 2022. Tectonic control on the palaeogeographical evolution of the Miocene Seaway along the Western Alpine foreland basin. In: Rossi, V.M., Longhitano, S., Olariu, C., Chiocci, F. (Eds.), Straits and Seaways: Controls, Processes and Implications in Modern and Ancient Systems523 Geological Society, London doi: 10.1144/SP1523-2021-1178.
Keen, C.E., 1985. The dynamics of rifting: deformation of the lithosphere by active and passive driving forces. Geophys. J. R. Astron. Soc. 80, 95–120.
Kendall, J.M., Pilidou, S., Keir, D., Bastow, I.D., Stuart, G.W., Ayele, A., 2006. Mantle upwellings, melt migration and the rifting of Africa: insights from seismic anisotropy. In: Yirgu, G., Ebinger, C.J., Maguire, P.K.H. (Eds.), The Afar Volcanic Province within the East African Rift System.Special Publications, 259 Geological Society, London, pp. 55–72.
King, G., Ouyang, Z., Papadimitriou, P., Deschamps, A., Gagnepain, A., Houseman, G., Jackson, J., Soufleris, C., Virieux, J., 1985. The evolution of the Gulf of Corinth (Greece) an aftershock study of the 1981 earthquake. Geophys. J. R. Astron. Soc. 80, 677–693.
Kogan, L., Fisseha, S., Bendick, R., Reilinger, R., McClusky, S., King, R., Solomon, T., 2012. Lithospheric strength and strain localization in continental extension from observations of the East African Rift. J. Geophys. Res. 117, B03402 doi: 03410.01029/02011JB008516.
Kooi, H., Cloetingh, S., 1992. Lithospheric necking and regional isostasy at extensional basins 2. Stress-induced vertical motions and relative sea level changes. J. Geophys. Res. 97, 17,573-517,591.
Kooi, H., Cloetingh, S., Burrus, J., 1992. Lithospheric necking and regional isostasy at extensional basins, I, Subsidence and gravity modeling with an application to the Gulf of Lions Margin (SE France). J. Geophys. Res. 97, 17,553-517,571.
Koptev, A., Cloetingh, S., 2024. Role of large Igneous Provinces in continental break-up varying from "Shirker" to "Producer". Commun. Earth Environ. 5, 27. https://doi.org/10.1038/s43247-43023-01191-43249.
Koptev, A.I., Ershov, A.V., 2010. The role of the gravitational potential of the lithosphere in the formation of a global stress field. Izv. Phys. Solid Earth 46, 1080–1094.
Koptev, A., Burov, E., Gerya, T., Le Pourhiet, L., Leroy, S., Calais, E., Jolivet, L., 2017a. Plume-induced continental rifting and break-up in ultra-slow extension context: Insights from 3D numerical modeling. Tectonophysics. https://doi.org/10.1016/j.tecto.2017.1003.1025.
Koptev, A., Cloetingh, S., Burov, E., François, T., Gerya, T., 2017b. Long-distance impact of Iceland plume on Norway's rifted margin. Sci. Rep. 7, 10408. DOI:10410.11038/s41598-10017-07523-y.
Koptev, A., Burov, E., Gerya, T., Le Pourhiet, L., Leroy, S., Calais, E., Jolivet, L., 2018. Plume-induced continental rifting and break-up in ultra-slow extension context: Insights from 3D numerical modeling. Tectonophysics 746, 121–137 https://doi.org/110.1016/j.tecto.2017.1003.1025.
Koptev, A., Beniest, A., Gerya, T., Ehlers, T.A., Jolivet, L., Leroy, S., 2019. Plume-induced breakup of a subducting plate: Microcontinent formation without cessation of the subduction process. Geophys. Res. Lett. 46. https://doi.org/10.1029/2018GL081295.
Koptev, A., Cloetingh, S., Ehlers, T.A., 2021. Longevity of small-scale ('baby') plumes and their role in lithospheric break-up. Geophys. J. Int. 227, 439–471 doi: 410.1093/gji/ggab1223.
Kreemer, C., 2009. Absolute plate motions constrained by shear wave splitting orientations with implications for hot spot motions and mantle flow. J. Geophys. Res. 114, B10405 doi:10410.11029/12009JB006416.
Kuritani, T., Sakuyama, T., Kamada, N., Yokoyama, T., Nakagawa, M., 2017. Fluid-fluxed melting of mantle versus decompression melting of hydrous mantle plume as the cause of intraplate magmatism over a stagnant slab: Implications from Fukue Volcano Group, SW Japan. Lithos 282–283, 98–110.
Kvale, A., 1953. Linear structures and their relation to movement in the Caledonides of Scandinavia and Scotland. Q. J. Geol. Soc. 109, 51–73. https://doi.org/10.1144/GSL.JGS.1953.1109.1101-1104.1104.
Lacombe, O., Angelier, J., Byrne, D., Dupin, J.M., 1993. Eocene-Oligocene tectonics and kinematics of the Rhine-Saone continental transform zone (eastern France). Tectonics 12, 874–888.
Lafosse, M., d'Acremont, E., Rabaute, A., Estrada, F., Jollivet-Castelot, M., Vazquez, J.T., Galindo-Zaldivar, J., Ercilla, G., Alonso, B., Smit, J., Ammar, A., Gorini, C., 2020. Plio-Quaternary tectonic evolution of the southern margin of the Alboran Basin (Western Mediterranean). Solid Earth 11, 741–765 doi: 710.5194/se-5111-5741-2020.
Larvet, T., Le Pourhiet, L., Agard, P., 2022. Cimmerian block detachment from Gondwana: A slab pull origin? Earth and Planetary Science Letters 596, 117790.
Lavecchia, A., Beekman, F., Clark, S.R., Cloetingh, S.A.P.L., 2016. Thermo-rheological aspects of crustal evolution during continental breakup and melt intrusion: the Main Ethiopian Rift, East Africa. Tectonophysics 686, 51–62. https://doi.org/10.1016/j.tecto.2016.1007.1018.
Lavier, L., Manatschal, G., 2006. A mechanism to thin the continental lithosphere at magma-poor margins. Nature 440, 324–328, 310.1038/nature04608.
Le Pourhiet, L., Huet, B., May, D.A., Labrousse, L., Jolivet, L., 2012. Kinematic interpretation of the 3D shapes of metamorphic core complex. Geochem. Geophys. Geosyst. 13, Q09002 doi:09010.01029/02012GC004271.
Le Pourhiet, L., May, D.A., Huille, L., Watremez, L., Leroy, S., 2017. A genetic link between transform and hyper-extended margins. Earth Planet. Sci. Lett. 465, 184–192 https://doi.org/110.1016/j.epsl.2017.1002.1043.
Lebedev, S., Meier, T., van der Hilst, R.D., 2006. Asthenospheric flow and origin of volcanism in the Baikal Rift area. Earth Planet. Sci. Lett. 249, 415–424 doi: 410.1016/j.epsl.2006.1007.1007.
Lebret, N., 2014. Contexte structural et métallogénique des skarns à magnétite des Beni Bou Ifrour (Rif oriental, Maroc). Apports à l'évolution géodynamique de la Méditerranée occidentale, Institut des Sciences de la Terre d'Orléans. Université d'Orléans 477.
Leroy, S., Razin, P., Autin, J., Bache, F., d'Acremont, E., Watremez, L., Robinet, J., Baurion, C., Denèle, Y., Bellahsen, N., Lucazeau, F., Rolandone, F., Rouzo, S., Kiel, J. S., Robin, C., Guillocheau, F., Tiberi, C., Basuyau, C., Beslier, M.O., Ebinger, C., Stuart, G., Ahmed, A., Khanbari, K., Al Ganad, I., de Clarens, P., Unternehr, P., Al Toubi, K., Al Lazki, A., 2012. From rifting to oceanic spreading in the Gulf of Aden: a synthesi. Arab. J. Geosci. 5, 859–901.
Leroy, S., Razin, P., Autin, J., Bache, F., d'Acremont, E., Watremez, L., Robinet, J., Baurion, C., Denèle, Y., Bellahsen, N., 2013. From Rifting to Oceanic Spreading in the Gulf of Aden: A Synthesis. The Arabian Plate and AnaloguesSpringer, Berlin, Heidelberg, Lithosphere Dynamics and Sedimentary Basins, pp. 385–427.
Lickorish, W.H., Ford, M., 1998. Sequential restoration of the external Alpine Digne thrust system, SE France, constrained by kinematic data and synorogenic sediments. Geol. Soc. Lond. Spec. Publ. 134, 189–211.
Liégeois, J.P., Benhallou, A., Azzouni-Sekkal, A., Yahiaoui, R., Bonin, B., 2005. The Hoggar swell and volcanism: Reactivation of the Precambrian Tuareg shield during Alpine convergence and West African Cenozoic volcanism. In: Foulger, G.R., Natland, J.H., Presnall, D.C., Anderson, D.L. (Eds.), Plates, plumes, and paradigms, Geological Society of America Special Paper, 388. Geological Society of America, pp. 379–400.
Limberger, J., van Wees, J.D., Tesauro, M., Smit, J., Bonté, D., Békési, E., Pluymaekers, M., Struijk, M., Vrijlandt, M., Beekman, F., Cloetingh, S., 2018.

Refining the thermal structure of the European lithosphere by inversion of subsurface temperature data. Glob. Planet. Chang. 171, 18–47. https://doi.org/10.1016/j.gloplacha.2018.1007.1009.
Lister, G.S., Banga, G., Feenstra, A., 1984. Metamorphic core complexes of cordilleran type in the Cyclades, Aegean Sea, Greece. Geology 12, 221–225 doi:210.1130/0091-7613(1984)1112<1221:MC COCT>1132.1130.CO;1132.
Lithgow-Bertelloni, C., Richards, M.A., 1998. The dynamics of Cenozoic and Mesozoic plate motions. Rev. Geophys. 36, 27–78.
Lucente, F.P., Margheriti, L., Piromallo, C., Barruol, G., 2006. Seismic anisotropy reveals the long route of the slab through the western-Central Mediterranean mantle. Earth Pl. Sc. Lett. 241, 517–529.
Lustrino, M., Wilson, M., 2007. The circum-Mediterranean anorogenic Cenozoic igneous province. Earth Sci. Rev. 81, 1–65. https://doi.org/10.1016/j.earscirev.2006.1009.1002.
Lustrino, M., Duggen, S., Rosenberg, C.L., 2011. The Central-Western Mediterranean: Anomalous igneous activity in an anomalous collisional tectonic setting. Earth Sci. Rev. 104, 1–40.
Maillard, A., Mauffret, A., 1999. Crustal structure and riftogenesis of the Valencia Trough (North-Western Mediterranean Sea). Basin Res. 11, 357–379.
Maillard, A., Jolivet, L., Lofi, J., Couëffé, R., Thinon, I., 2020. Transfer Faults and associated volcanic province in the transition zone between the Valencia Basin and the Gulf of Lion: consequences on crustal thinning. Mar. Pet. Geol. 119. https://doi.org/10.1016/j.marpetgeo.2020.104419, 104419.
Manatschal, G., 2004. New models for evolution of magma-poor rifted margins based on a review of data and concepts from West Iberia and the Alps. Int. J. Earth Sci. (Geol Rundsch) 93, 432–466. DOI 410.1007/s00531-00004-00394-00537.
Manatschal, G., Chenin, P., Lescoutre, R., Miró, J., Cadenas, P., Saspiturry, N., Masini, E., Chevrot, S., Ford, M., Jolivet, L., Mouthereau, F., Thinon, I., Issautier, B., Calassou, S., 2021. The role of inheritance in forming rifts and rifted margins and building collisional orogens: a Biscay-Pyrenean perspective. BSGF - Earth Sci. Bull. 192, 55. https://doi.org/10.1051/bsgf/2021042.
Marti, J., Mitjavila, J., Roca, E., Aparicio, A., 1992. Cenozoic magmatism of the Valencia trough (western Mediterranean) : relationship between structural evolution and volcanism. Tectonophysics 203, 145–165.
Martinez-Garcia, P., Comas, M., Soto, J.I., Lonergan, L., Watts, A.B., 2013. Strike-slip tectonics and basin inversion in the Western Mediterranean: the Post-Messinian evolution of the Alboran Sea. Basin Res. 25, 361–387 doi: 310.1111/bre.12005.
Martínez-García, P., Comas, M., Lonergan, L., Watts, A.B., 2017. From extension to shortening: Tectonic inversion distributed in time and space in the Alboran Sea, western Mediterranean. Tectonics 36, 2777–2805 doi: 2710.1002/ 2017TC004489.
McClusky, S., Balassanian, S., Barka, A., Demir, C., Ergintav, S., Georgiev, I., Gurkan, O., Hamburger, M., Hurst, K., Kahle, H., Kastens, K., Kekelidze, G., King, R., Kotzev, V., Lenk, O., Mahmoud, S., Mishin, A., Nadariya, M., Ouzonis, A., Paradissis, D., Peter, Y., Prilepin, M., Reilinger, R., Sanli, I., Seeger, H., Tealeb, A., Toksöz, M.N., Veis, G., 2000. Global Positioning System constraints on plate kinematics and dynamics in the eastern Mediterranean and Caucasus. J. Geophys. Res. 105, 5695–5720.
McDermott, K., Gillbard, E., Clarke, N., 2015. From Basalt to Skeletons – the 200 million-year history of the Namibian margin uncovered by new seismic data. First Break 33, 77–85.
Medaouri, M., Déverchère, J., Graindorge, D., Bracene, R., Badjia, R., Ouabadic, A., Yelles-Chaouched, K., Bendiab, F., 2014. The transition from Alboran to Algerian basins (Western Mediterranean Sea): Chronostratigraphy, deep crustal structure and tectonic evolution at the rear of a narrow slab rollback system. J. Geodyn. 77, 186–205 https://doi.org/110.1016/j.jog.2014.1001.1003.
Meier, T., Soomro, R.A., Viereck, L., Lebedev, S., Behrmann, J.H., Weidle, C., Cristiano, L., Hanemann, R., 2016. Mesozoic and Cenozoic evolution of the central European lithosphere. Tectonophysics 692, 58–73. https://doi.org/10.1016/j.tecto.2016.1009.1016.
Menant, A., Jolivet, L., Vrielynck, B., 2016a. Kinematic reconstructions and magmatic evolution illuminating crustal and mantle dynamics of the eastern Mediterranean region since the late cretaceous. Tectonophysics 675, 103–140 doi: 110.1016/j.tecto.2016.1003.1007.
Menant, A., Sternai, P., Jolivet, L., Guillou-Frottier, L., Gerya, T., 2016b. 3D numerical modeling of mantle flow, crustal dynamics and magma genesis associated with slab roll-back and tearing: the eastern Mediterranean case. Earth Planet. Sci. Lett. 442, 93–107.
Merle, O., Michon, L., 2001. The formation of the West European Rift: a new model as exemplified by the Massif Central Area. Bull. Soc. Géol. France 172, 213–221.
Merle, O., Michon, L., Camus, G., De Goër, A., 1998. L'extension oligocène sur la transversale septentrionale du rift du Massif Central. Bull. Soc. Géol. France 169, 615–626.
Merle, R., Jourdan, F., Girardeau, J., 2018. Geochronology of the Tore- Madeira rise seamounts and surrounding areas: a review. Aust. J. Earth Sci. 65, 591–605. DOI: 510.1080/08120099.08122018.01471005.
Michon, L., Merle, O., 2001. The evolution of the Massif Central Rift: spatio-temporal distribution of the volcanism. Bull. Soc. Géol. France 172, 201–211.
Michon, L., Sokoutis, D., 2005. Interaction between structural inheritance and extension direction during graben and depocentre formation: an experimental approach. Tectonophysics 409, 125–146 doi:110.1016/j.tecto.2005.1008.1020.
Min, G., Hou, G., 2018. Geodynamics of the East African Rift System ~30 Ma ago: a stress field model. J. Geodyn. 117, 1–11. https://doi.org/10.1016/j.jog.2018.1002.1004.
Min, G., Hou, G., 2019. Mechanism of the Mesozoic African rift system: Paleostress field modeling. J. Geodyn. 132, 101655 https://doi.org/101610.101016/j.jog.102019.101655.
Molnar, P., Tapponnier, P., 1975. Cenozoic tectonics of Asia: Effects of a continental collision. Science 189, 419–426.
Moretti, I., Colletta, B., 1987. Spatial and temporal evolution of the Suez rift subsidence. J. Geodyn. 7, 151–168.
Morgan, W.J., 1971. Convection plume in the lower mantle. Nature 230, 42–43.
Mouthereau, F., Filleaudeau, P.Y., Vacherat, A., Pik, R., Lacombe, O., Fellin, M.G., Castelltort, S., Christophoul, F., Masini, E., 2014. Placing limits to shortening evolution in the Pyrenees: Role of margin architecture and implications for the Iberia/Europe convergence. Tectonics 33, 2283–2314 doi:2210.1002/2014TC003663.
Mouthereau, F., Angrand, P., Jourdon, A., Ternois, S., Fillon, C., Calassou, S., Chevrot, S., Ford, M., Jolivet, L., Manatschal, G., Masini, E., Thinon, I., Vidal, O., Baudin, T., 2021. Cenozoic mountain building and topographic evolution in Western Europe: impact of billion years lithosphere evolution and plate tectonics. BSGF-Earth Sci. Bull. 192, 56. https://doi.org/10.1051/bsgf/2021040.
Müller, R.D., Seton, M., Zahirovic, S., Williams, S.E., Matthews, K.J., Wright, N.M., Shephard, G.E., Maloney, K.T., Barnett-Moore, N., Hosseinpour, M., Bower, D., Cannon, J., 2016. Ocean Basin evolution and global-scale plate reorganization events since pangea breakup. Annu. Rev. Earth Planet. Sci. 44 (107–138), 110.1146/annurev-earth-060115-012211.
Müller, R.D., Zahirovic, S., Williams, S.E., Cannon, J., Seton, M., Bower, D.J., Tetley, M.G., Heine, C., Le Breton, E., Liu, S., Russell, S.H.J., Yang, T., Leonard, J., Gurnis, M., 2019. A global plate model including lithospheric deformation along major rifts and orogens since the Triassic. Tectonics 38, 1884–1907 doi: 1810.1029/2018TC005462.
Munch, F.D., Romanowicz, B., Mukhopadhyay, S., Rudolphd, M.L., 2024. Deep mantle plumes feeding periodic alignments of asthenospheric fingers beneath the central and southern Atlantic Ocean. PNAS 121, e2407543121 doi: 2407543110.2407541073/pnas.2407543121.
Naliboff, J.B., Lithgow-Bertelloni, C., Ruff, L.J., Koker, N., 2012. The effects of lithospheric thickness and density structure on Earth' s stress field. Geophys. J. Int. 188, 1–17.
Natarov, S.I., Conrad, C.P., 2012. The role of Poiseuille flow in creating depth-variation of asthenospheric shear. Geophys. J. Int. 190, 1297–1310 doi: 1210.1111/j.1365-1246X.2012.05562.x.
Nehlig, P., Boivin, P., de Goër, A., Mergoil, J., Prouteau, G., Sustrac, G., Thiéblemont, D., 2003. Les volcans du Massif Central. Géologues 130-131, 1–41.
Nelson, W.R., Furman, T., van Keken, P.E., Shirey, S.B., Hanan, B.B., 2012. Os\Hf isotopic insight into mantle plume dynamics beneath the East African Rift System. Chem. Geol. 320-321, 66–79. https://doi.org/10.1016/j.chemgeo.2012.1005.1020.
Njome, M.S., de Wit, M.J., 2014. The Cameroon Line: Analysis of an intraplate magmatic province transecting both oceanic and continental lithospheres: Constraints, controversies and models. Earth Sci. Rev. 139, 168–194.
Nyblade, A.A., Owens, T.J., Gurrola, H., Ritsema, J., Langston, C.A., 2000. Seismic evidence for a deep upper mantle thermal anomaly beneath East Africa. Geology 28, 599–602.
O'Connor, J.M., Jokat, W., 2015a. Tracking the Tristan-Gough mantle plume using discrete chains of intraplate volcanic centers buried in the Walvis Ridge, 43, 715–718 doi:710.1130/G36767.36761.
O'Connor, J.M., Jokat, W., 2015b. Tracking the Tristan-Gough mantle plume using discrete chains of intraplate volcanic centers buried in the Walvis Ridge. Geology 43, 715–718 doi:710.1130/G36767.36761.
O'Connor, J.M., Le Roex, A.P., 1992. South Atlantic hot spot-plume systems: 1. Distribution of volcanism in time and space. Earth Planet. Sci. Lett. 113, 343–364.
O'Connor, J.M., Jokat, W., le Roex, A.P., Class, C., Wijbrans, J.R., Keßling, S., Kuiper, K.F., Nebel, O., 2012. Hotspot trails in the South Atlantic controlled by plume and plate tectonic processes. Nat. Geosci. 5, 735–738. DOI: 710.1038/NGEO1583.
Olivetti, V., Balestrieri, M.L., Godard, V., Gautheron, O.B., Valla, P.G., Zattin, M., Faccenna, C., Pinna-Jamme, R., Manchuel, K., 2020. Cretaceous and late Cenozoic uplift of a Variscan Massif: the case of the French Massif Central studied through low-temperature thermochronometry. Lithosphere 12.
Olsen, K.H., Baldridge, W.S., Callender, J.F., 1987. Rio Grande rift: an overview. Tectonophysics 143, 119–139.
Paul, J.D., Roberts, G.G., White, N., 2014. The African landscape through space and time. Tectonics 33, 898–935 doi:810.1002/2013TC003479.
Pérouse, E., Vernant, P., Chéry, J., Reilinger, R., McClusky, S., 2010. Active surface deformation and sub-lithospheric processes in the western Mediterranean constrained by numerical models. Geology 38, 823–826 doi: 810.1130/G30963.30961.
Pérouse, E., Chamot-Rooke, N., Rabaute, A., Briole, P., Jouanne, F., Georgiev, I., Dimitrov, D., 2012. Bridging onshore and offshore present-day kinematics of central and eastern Mediterranean: implications for crustal dynamics and mantle flow. Geochem. Geophys. Geosyst. 13, Q09013 doi:09010.01029/02012GC004289.
Petit, C., Deverchère, J., 2006. Structure and evolution of the Baikal rift: a synthesis. Geochem. Geophys. Geosyst. 7, Q11016 doi:11010.11029/12006GC001265.
Peyaud, J.B., Barbarand, J., Carter, A., Pagel, M., 2005. Mid-cretaceous uplift and erosion on the northern margin of the Ligurian Tethys deduced from thermal history reconstruction. Int. J. Earth Sci. (Geol Rundsch) 94, 462–474. DOI 410.1007/s00531-00005-00486-z.
Pik, R., Marty, B., Carignan, J., Lave, J., 2004. Stability of the Upper Nile drainage network (Ethio- pia) deduced from (U-Th)/He thermochronometry: implications for uplift and erosion of the Afar plume dome. Earth Planet. Sci. Lett. 215, 73–88.
Pik, R., Marty, B., Hilton, D.R., 2006. How many mantle plumes in Africa? The geochemical point of view. Chem. Geol. 226, 100–114 doi:110.1016/j.chemgeo.2005.1009.1016.

Pik, R., Stab, M., Ancellin, M., Medinsky, S., Cloquet, Y., Ayalew, D., Yirgu, G., Chazot, G., Vye-Brown, C., Bellahsen, N., Leroy, S., Le Gall, B., 2017. Development of the Central-Afar volcanic margin, mantle upwelling and break-up processes. EGU Vienna pp. EGU Vienna, EGU2017-13702.

Piromallo, C., Gasperini, D., Macera, P., Faccenna, C., 2008. A late Cretaceous contamination episode of the European–Mediterranean mantle. Earth Planet. Sci. Lett. 268, 15–27. https://doi.org/10.1016/j.epsl.2007.1012.1019.

Plomerova, J., Munzarova, H., Vecsey, L., Kissling, E., Achauer, U., Babuska, V., 2016. Cenozoic volcanism in the Bohemian Massif in the context of P- and S-velocity high-resolution teleseismic tomography of the upper mantle. Geochem. Geophys. Geosyst. 17, 3326–3349 doi:3310.1002/ 2016GC006318.

Porritt, R., Becker, T.W., Boschi, L., Auer, L., 2021. Multi-scale, radially anisotropic shear wave imaging of the mantle underneath the contiguous United States through joint inversion of USArray and global datasets. Geophys. J. Int. 265, 1730–1746.

Qaysi, S., Liu, K.H., Gao, S.S., 2018. A database of shear-wave splitting measurements for the arabian plate. Seismol. Res. Lett. 89, 2294–2298 doi: 2210.1785/0220180144.

Quinquis, H., Audren, C., Brun, J.P., Cobbold, P.R., 1978. Intense progressive shear in Ile de Groix blueschists and compatibility with subduction or obduction. Nature 273, 43–45.

Reilinger, R.E., McClusky, S.C., Oral, M.B., King, R.W., Tokzoz, M.N., Barka, A.A., Kinik, I., Lenk, O., Sanli, I., 1997. Global positionning system measurements of present-day crustal movements in the Arabia-Africa-Eurasia plate collision zone. J. Geophys. Res. 102, 9983–9999.

Reilinger, R., McClusky, S., Paradissis, D., Ergintav, S., Vernant, P., 2010. Geodetic constraints on the tectonic evolution of the Aegean region and strain accumulation along the Hellenic subduction zone. Tectonophysics 488, 22–30.

Ribot, M., Klinger, Y., Jónsson, S., Avsar, U., Pons-Branchu, E., Matrau, R., Mallon, F.L., 2021. Active faults' geometry in the Gulf of Aqaba, southern Dead Sea fault, illuminated by multibeam bathymetric data. Tectonics 40, e2020TC006443 doi: 006410.001029/002020TC006443.

Ricard, Y., Vigny, C., 1989. Mantle dynamics with induced plate tectonics. J. Geophys. Res. 94, 17543–17559.

Richter, F.M., Parsons, B., 1975. On the interaction of two scales of convection in the mantle. J. Geophys. Res. 80, 2529–2541.

Rickers, F., Fichtner, A., Trampert, J., 2013. The Iceland–Jan Mayen plume system and its impact on mantle dynamics in the North Atlantic region: evidence from full-waveform inversion. Earth Planet. Sci. Lett. 367, 39–51.

Ring, U., Glodny, J., Will, T., Thomson, S., 2010. The Hellenic Subduction System: High-pressure Metamorphism, Exhumation, Normal Faulting, and Large-Scale Extension. Annu. Rev. Earth Planet. Sci. 38, 45–76. https://doi.org/10.1146/annurev.earth.050708.170910.

Ritsema, H.J., van Heijst, J.H., Woodhouse, J.H., 1999. Complex shear velocity structure beneath Africa and Iceland. Science 286, 1925–1928.

Ritter, J.R.R., Jordan, M., Christensen, U.R., Achauer, U., 2001. A mantle plume below the Eifel volcanic fields, Germany. Earth Planet. Sci. Lett. 186, 7–14.

Roberts, E.M., Stevens, N.J., O'Connor, P.M., Dirks, P.H.G.M., Gottfried, M.D., Clyde, W. C., Armstrong, R.A., Kemp, A.I., Hemming, S., 2012. Initiation of the western branch of the East African Rift coeval with the eastern branch. Nat. Geosci. 5, 289–294 https://doi.org/210.1038/NGEO1432.

Roche, V., Ringenbach, J.C., 2021. The Davie Fracture Zone: a recorder of continents drifts and kinematic changes. Tectonophysics 823, 229188 doi: 229110.221016/j.tecto.222021.229188.

Roche, V., Bouchot, V., Beccaletto, L., Jolivet, L., Guillou-Frottier, L., Tuduri, J., Bozkurt, E., Oguz, K., Tokay, B., 2018. Structural, lithological and geodynamic controls on geothermal activity in the Menderes geothermal Province (Western Anatolia, Turkey). Int. J. Earth Sci. (Geol Rundsch). https://doi.org/10.1007/s00531-00018-01655-00531.

Roche, V., Leroy, S., Guillocheau, F., Revillon, S., Ruffet, G., Watremez, L., d'Acremont, E., Nonn, C., Vetel, W., Despinois, F., 2021. The Limpopo magma-rich transform margin, South Mozambique– 2: Implications for the Gondwana breakup. Tectonics 40, e2021TC006914 doi: 006910.001029/002021TC006914.

Roche, V., Leroy, S., Revillon, S., Guillocheau, F., Ruffet, G., Vétel, W., 2022. Gondwana break-up controlled by tectonic inheritance and mantle plume activity: Insights from Natal rift development (South Mozambique, Africa). Terra Nova 34, 290–304 https://doi. org/210.1111/ter.12590.

Rogers, N., Macdonald, R., Fitton, J.G., George, R., Smith, M., Barreiro, B., 2000. Two mantle plumes beneath the East African rift system: Sr, Nd and Pb isotope evidence from Kenya Rift basalts. Earth Planet. Sci. Lett. 176, 387–400.

Romagny, A., Jolivet, L., Menant, A., Bessière, E., Maillard, A., Canva, A., Thinon, I., 2020. Detailed tectonic reconstructions of the Western Mediterranean region for the last 35 Ma, insights on driving mechanisms. BSGF-Earth Sci. Bull. 191, 37. https://doi.org/10.1051/bsgf/2020040.

Rooney, T.O., 2017. The Cenozoic magmatism of East-Africa: part I — Flood basalts and pulsed magmatism. Lithos 286–287, 264–301 https://doi.org/210.1016/j.lithos.2017.1005.1014.

Rooney, T.O., 2020a. The Cenozoic magmatism of East Africa: Part II – Rifting of the mobile belt. Lithos 360–361, 105291 doi: 105210.101016/j.lithos.102019.105291.

Rooney, T.O., 2020b. The Cenozoic magmatism of East Africa: Part IV – the terminal stages of rifting preserved in the Northern East African Rift System. Lithos 360–361, 105381 doi: 105310.101016/j.lithos.102020.105381.

Royden, L.H., Papanikolaou, D.J., 2011. Slab segmentation and late Cenozoic disruption of the Hellenic arc. Geochem. Geophys. Geosyst. 12, Q03010 doi:03010.01029/02010GC003280.

Ruhl, M., Hesselbo, S.P., Jenkyns, H.C., Xu, W., Silva, R.L., Matthews, K.J., Mather, T.A., Mac Niocaill, C., Riding, J.B., 2022. Reduced plate motion controlled timing of early Jurassic Karoo-Ferrar large igneous province volcanism. Sci. Adv. 8, eabo0866.

Ryan, W.B.F., Carbotte, S.M., Coplan, J.O., O'Hara, S., Melkonian, A., Arko, R., Weissel, R.A., Ferrini, V., Goodwillie, A., Nitsche, F., Bonczkowski, J., Zemsky, R., 2009. Global Multi-Resolution Topography synthesis. Geochem. Geophys. Geosyst. 10, Q01005 doi:01010.01029/02003GC000614.

Saeidi, H., Hansen, S.E., Nyblade, A.A., 2023. Deep mantle influence on the Cameroon Volcanic Line. Geochem. Geophys. Geosyst. 24, e2022GC010621 https://doi. org/010610.011029/012022GC010621.

Sander, B., 1948. Einftihrung in die Gefiigekunde der geologischen Körper, Vienna.

Schaeffer, A.J., Lebedev, S., 2013. Global shear-speed structure of the upper mantle and transition zone. Geophys. J. Int. 194, 417–449 doi:410.1093/gji/ggt1095.

Schmandt, B., Lin, F.C., 2014. P and S wave tomography of the mantle beneath the United State. Geophys. Res. Lett. 41, 6342–6349 doi:6310.1002/2014GL061231.

Schoonman, C.M., White, N.J., Pritchard, D., 2017. Radial viscous fingering of hot asthenosphere within the Icelandic plume beneath the North Atlantic Ocean. Earth Planet. Sci. Lett. 468, 51–61. https://doi.org/10.1016/j.epsl.2017.1003.1036.

Schumacher, M.E., 2002. Upper Rhine Graben: Role of preexisting structures during rift evolution. Tectonics 21 (1006), 1010.1029/2001TC900022.

Semple, A.G., Lenardic, A., 2018. Plug flow in the Earth's asthenosphere. Earth Planet. Sci. Lett. 496, 29–36. https://doi.org/10.1016/j.epsl.2018.1005.1030.

Sengör, A.M.C., Burke, K., 1978. Relative timing of rifting and volcanism on Earth and its tectonic implications. Geophys. Res. Lett. 5, 419–421.

Séranne, M., 1999. The Gulf of Lions continental margin (NW Mediterranean) revisited by IBS: An overview. In: Durand, B., Jolivet, L., Horvàth, F., Séranne, M. (Eds.), The Mediterranean Basins: Tertiary Extension within the Alpine Orogen156 Geological Society, London, pp. 15–36.

Séranne, M., Benedicto, A., Truffert, C., Pascal, G., Labaume, P., 1995. Structural style and evolution of the Gulf of Lion Oligo-Miocene rifting: Role of the Pyrenean orogeny. Mar. Pet. Geol. 12, 809–820.

Séranne, M., Couëffé, R., Husson, E., Villard, J., 2021. The transition from Pyrenean shortening to Gulf of Lion rifting in Languedoc (South France) – a tectonic-sedimentation analysis. BSGF - Earth Sci. Bull. 192, 27. https://doi.org/10.1051/bsgf/2021017.

Serpelloni, E., Vannucci, G., Pondrelli, S., Argnani, A., Casula, G., Anzidei, M., Baldi, P., Gasperini, P., 2007. Kinematics of the Western Africa-Eurasia plate boundary from focal mechanisms and GPS data. Geophys. J. Int. 169, 1180–1200, 1110.1111/j.1365-1246X.2007.03367.x.

Seton, M., Müller, R.D., Zahirovic, S., Gaina, C., Torsvik, T., Shephard, G., Talsma, A., Gurnis, M., Turner, M., Maus, S., Chandler, M., 2012. Global continental and ocean basin reconstructions since 200 Ma. Earth Sci. Rev. 113, 212–270 doi:210.1016/j.earscirev.2012.1003.1002.

Shudofsky, G.N., Cloetingh, S., Stein, S., Wortel, R., 1987. Unusually deep earthquakes in East Africa: constraints ofthe thermo-mechanical structure of a continental rift system. Geophys. Res. Lett. 14, 741–744.

Sissingh, W., 2006. Kinematic sequence stratigraphy of the European Cenozoic Rift System and Alpine Foreland Basin: correlation with Mediterranean and Atlantic plate-boundary events. Netherlands Journal of Geosciences —. Geol. Mijnb. 85, 77–129.

Sobolev, S.V., Zeyen, H., Granet, M., Achauer, U., Bauer, C., Werling, F., Altherr, R., Fuchs, K., 1997. Upper mantle temperatures and lithosphere-asthenosphere system beneath the French Massif Central constrained by seismic, gravity, petrologic and thermal observations. Tectonophysics 275, 143–164.

Stab, M., Bellahsen, N., Pik, R., Quidelleur, X., Ayalew, D., Leroy, S., 2016. Modes of rifting in magma-rich settings: Tectono-magmatic evolution of Central Afar. Tectonics 35, 2–38. https://doi.org/10.1002/2015TC003893.

Stamps, D.S., Flesch, L.M., Calais, E., Ghosh, A., 2014. Current kinematics and dynamics of Africa and the East African Rift System. J. Geophys. Res. Solid Earth 119, 5161–5186 doi:5110.1002/2013JB010717.

Steinberger, B., Torsvik, T.H., 2008. Absolute plate motions and true polar wander in the absence of hotspot tracks. Nature 452, 620–623.

Steinberger, B., Schmeling, H., Marquart, G., 2001. Large-scale lithospheric stress field and topography induced by global mantle circulation. Earth Planet. Sci. Lett. 186, 75–91.

Steinberger, B., Conradb, C.P., Tutu, A.O., Hoggard, M.J., 2019. On the amplitude of dynamic topography at spherical harmonic degree two. Tectonophysics 760, 221–228 doi: 210.1016/j.tecto.2017.1011.1032.

Sternai, P., Jolivet, L., Menant, A., Gerya, T., 2014. Subduction and mantle flow driving surface deformation in the Aegean-Anatolian system. Earth Planet. Sci. Lett. 405, 110–118 doi.org/110.1016/j.epsl.2014.1008.1023.

Sternai, P., Avouac, J.P., Jolivet, L., Faccenna, C., Gerya, T., Becker, T.W., Menant, A., 2016. On the influence of the asthenospheric flow on the tectonics and topography at a collision-subduction transition zones: comparison with the eastern Tibetan margin. J. Geodyn. 100, 184–197 doi: 110.1016/j.jog.2016.1002.1009.

Sternai, P., Muller, V.A.P., Jolivet, L., Garzanti, E., Corti, G., Pasquero, C., Sembroni, A., Faccenna, C., 2021. Effects of asthenospheric flow and orographic precipitation on continental rifting. Tectonophysics 820, 229120 doi: 229110.221016/j.tecto.222021.229120.

Stotz, I.L., Iaffaldano, G., Davies, D.R., 2018. Pressure-driven Poiseuille flow: a major component of the torque-balance governing Pacific Plate motion. Geophys. Res. Lett. 45, 117–125 doi: 110.1002/2017GL075697.

Tang, Y., Obayashi, M., Niu, F., Grand, S.P., Chen, Y.J., Kawakatsu, H., Tanaka, S., Ning, J., Ni, J.F., 2014. Changbaishan volcanism in Northeast China linked to subduction-induced mantle upwelling. Nat. Geosci. 7, 470–475. DOI: 410.1038/NGEO2166.

Tapponnier, P., 1977. Evolution du système alpin en Méditerranée: poinçonnement et écrasement rigide-plastique. Bull. Soc. Geol. Fr. 7 (19), 437–460.

Tapponnier, P., Molnar, P., 1977. Active faulting and tectonics in China. J. Geophys. Res. 82, 2905–2930.
Tapponnier, P., Peltzer, G., Dain, A.Y.L., Armijo, R., Cobbold, P., 1982. Propagating extrusion tectonics in Asia: new insights from simple experiments with plasticine. Geology 10, 611–616.
Tesauro, M., Kaban, M.K., Cloetingh, S.A.P.L., 2009. How rigid is Europe's lithosphere? Geophys. Res. Lett. 36, L16303 doi:16310.11029/12009GL039229.
Tesauro, M., Audet, P., Kaban, M.K., Bürgmann, R., Cloetingh, S., 2012. The effective elastic thickness of the continental lithosphere: Comparison between rheological and inverse approaches. Geochem. Geophys. Geosyst. 13, Q09001 doi:09010.01029/02012GC004162.
Thiry, M., Quesnel, F., Yans, J., Wyns, R., Vergari, A., Théveniaut, H., Simon-Coinçon, R., Ricordel, C., Moreau, M.G., Giot, D., Dupuis, C., Bruxelles, L., Barbarand, J., Baele, J. M., 2006. Continental France and Belgium during the early cretaceous: paleoweatherings and paleolandforms. Bull. Soc. géol. Fr. 177, 155–175.
Tikoff, B., Russo, R., Teyssier, C., Tommasi, A., 2004. Mantle-driven deformation of orogenic zone and clutch tectonics. In: Grocott, J., McCaffrey, K.J.W., Taylor, G., Tikoff, B. (Eds.), Vertical Coupling and Decoupling in the Lithosphere.Special Publications, 227 Geological Society, London, pp. 41–64.
Torsvik, T.H., Cocks, L.R.M., 2016. Earth History and Palaeogeography. Cambridge University Press.
Torsvik, T.H., Van der Voo, R., Preeden, U., Mac Niocaill, C., Steinberger, B., Doubrovine, P.V., van Hinsbergen, D.J.J., Domeier, M., Gaina, C., Tohver, E., Meert, J.G., McCausland, P.J.A., Cocks, R.M., 2012. Phanerozoic polar wander, palaeogeography and dynamics. Earth Sci. Rev. 114, 325–368 doi:310.1016/j.earscirev.2012.1006.1007.
Turcotte, D.L., Emerman, S.H., 1983. Mechanisms of active and passive rifting. Tectonophysics 94, 39–50. https://doi.org/10.1016/B1978-1010-1444-42198-42192.50010-42199.
van Hinsbergen, D.J.J., Langereis, C.G., Meulenkamp, J.E., 2005. Revision of the timing, magnitude and distribution of Neogene rotations in the western Aegean region. Tectonophysics 396, 1–34.
Vignaroli, G., Faccenna, C., Jolivet, L., Piromallo, C., Rossetti, F., 2008. Orogen-parallel extension and arc bending forced by slab tearing and toroidal flow at the junction between Alps and Apennines. Tectonophysics 450, 34–50. https://doi.org/10.1016/j.tecto.2007.1012.1012.
Vignaroli, G., Faccenna, C., Rossetti, F., Jolivet, L., 2009. Insights from the apennines metamorphic complexes and their bearing on the kinematics evolution of the orogen. In: Van Hinsbergen, D.J.J., Edwards, M.A., Govers, R. (Eds.), Collision and collapse at the Africa-Arabia-Eurasia subduction zone.Special Publications, 311 The Geological Society, London, pp. 235–256.
von Eynatten, H., Kley, J., Dunkl, I., Hoffmann, V.E., Simon, A., 2021. Late cretaceous to Paleogene exhumation in Central Europe–localized inversion vs. large-scale domal uplift. Solid Earth 12, 935–958.
Wilson, J.T., 1963. Evidence from islands on the spreading of ocean floor. Nature 197, 536–538.
Wilson, J.T., 1966. Did the Atlantic close and then re-open? Nature 211, 676–681.
Wilson, J.T., 1973. Mantle plume and plate motions. Tectonophysics 19, 149–164.
Wilson, M., Bianchini, G., 1999. Tertiary-Quaternary magmatism within the Mediterranean and surrounding regions. In: Durand, B., Jolivet, L., Horvath, F., Seranne, M. (Eds.), The Mediterranean Basins: Tertiary extension within the Alpine Orogen.Geol. Soc. London, Special Publication, 156, pp. 141–168.
Windley, B.F., Allen, M.B., 1993. Mongolian Plateau: evidence for a Late Cenozoic mantle plume under central Asia. Geology 21, 295–298.
Wyns, R., Quesnel, F., Simon-Coinçon, R., Guillocheau, F., Lacquement, F., 2003. Major weathering in France related to lithospheric deformation. Géol. Fr. 1, 79–87.
Zahirovic, S., Müller, R.D., Seton, M., Flament, N., 2015. Tectonic speed limits from plate kinematic reconstructions. Earth Planet. Sci. Lett. 418, 40–52. https://doi.org/10.1016/j.epsl.2015.1002.1037.
Zandt, G., Humphreys, E., 2008. Toroidal mantle flow through the western US slab window. Geology 36, 295–298.
Zhu, H., Bozdağ, E., Peter, D., Tromp, J., 2012. Structure of the European upper mantle revealed by adjoint tomography. Nat. Geosci. 5, 493–497. DOI: 410.1038/NGEO1501.
Ziegler, P.A., 1992a. European Cenozoic rift system. Tectonophysics 208, 91–111.
Ziegler, P.A., 1992b. Plate tectonics, plate moving mechanisms and rifting. Tectonophysics 215, 9–34.
Ziegler, P.A., Cloetingh, S., 2004. Dynamic processes controlling evolution of rifted basins. Earth Sci. Rev. 64, 1–50. https://doi.org/10.1016/S0012-8252(1003)00041-00042.
Ziegler, P.A., Dèzes, P., 2005. Evolution of the lithosphere in the area of the Rhine Rift System. Int. J. Earth Sci. (Geol Rundsch) 94, 594–614. DOI 510.1007/s00531-00005-00474-00533.
Ziegler, P.A., Dèzes, P., 2007. Cenozoic uplift of Variscan Massifs in the Alpine foreland: timing and controlling mechanisms. Glob. Planet. Chang. 58, 237–269 doi:210.1016/j.gloplacha.2006.1012.1004.
Ziegler, P.A., Cloetingh, S., van Wees, J.D., 1995. Dynamics of intra-plate compressional deformation: the Alpine foreland and other examples. Tectonophysics 252, 7–59.
Ziegler, P.A., Schumacher, M.E., Dèzes, P., van Wees, J.D., Cloetingh, S., 2004. Post-Variscan evolution of the lithosphere in the Rhine Graben area: Constraints from subsidence modelling. Geol. Soc. Lond. Spec. Publ. 223, 289–317. DOI: 210.1144/GSL.SP.2004.1223.1101.1113.
Zitellini, N., Ranero, C.R., Loreto, M.F., Ligi, M., Pastore, M., D'Oriano, P., Sallares, V., Grevemeyer, I., Moeller, S., Prada, M., 2019. Recent inversion of the Tyrrhenian Basin. Geology 48, 123–127 doi: 110.1130/G46774.46771.
Zolitschka, B., Negendank, J.F., Lottermoser, B.G., 1995. Sedimentological proof and dating of the early Holocene volcanic eruption of Ulmener Maar (Vulkaneifel, Germany). Geol. Rundsch. 84, 213–219.